INVESTIGATING THE MOLECULAR MECHANISM OF SHROOM-ROCK INTERACTION AND ITS ROLE IN CELLULAR AND TISSUE MORPHOGENESIS

by

Debamitra Das

Bachelor of Science, Presidency College, University of Calcutta, 2005

Master of Science, Presidency College, University of Calcutta, 2007

Submitted to the Graduate Faculty of the Kenneth P.

Dietrich School of Arts and Sciences in partial fulfillment

of the requirements for the degree of

Doctor of Philosophy

University of Pittsburgh

2014

UNIVERSITY OF PITTSBURGH

KENNETH P. DIETRICH SCHOOL OF ARTS AND SCIENCES

This dissertation was presented

by

Debamitra Das

It was defended on

March 19, 2014

and approved by

Jeffrey Brodsky, Ph.D., Professor, Biological Sciences

Anthony Schwacha, Ph.D., Associate Professor, Biological Sciences

Andrew VanDemark, Ph.D., Assistant Professor, Biological Sciences

Beth Stronach, Ph.D., Associate Professor, Microbiology and Molecular Genetics

Dissertation Advisor: Jeffrey Hildebrand, Ph.D., Associate Professor, Biological Sciences

INVESTIGATING THE MOLECULAR MECHANISM OF SHROOM-ROCK INTERACTION AND ITS ROLE IN CELLULAR AND TISSUE MORPHOGENESIS

Debamitra Das, PhD

University of Pittsburgh, 2014

During development cells undergo highly synchronized, dynamic morphogenetic movements to pattern the complex 3D architecture of tissues and organs involving processes like cell adhesion, migration, shape and polarity. This cellular remodeling is brought about by proteins that can spatially and temporally modulate the dynamics and organization of the cytoskeleton. Shroom is a class of actin-associated proteins that has been implicated in regulating cell and tissue architecture. Shroom3 along with another cytoskeleton regulator protein Rock, a kinase, locally activates non-muscle myosin II and facilitates assembly of a contractile actomyosin network at the apical surface of cells which subsequently alters cell shape and behavior. In order to elucidate the molecular mechanism and dynamics of Shroom-Rock interaction it becomes important to map the residues mediating this interaction. My project aims to dissect the molecular nature of Shroom-Rock interaction using a variety of biochemical and cell based assays, guided by structural studies and novel Shroom3 mutants. Shroom SD2 is known to form a three segmented antiparallel coiled-coil dimer. We have identified a highly conserved patch of surface exposed residues in Shroom SD2 that are important for Rock binding and interiorly buried residues required for Shroom dimerization. I have shown that the SD2 mutants that fail to bind Rock or dimerize also fail to cause apical constriction in MDCK cells. I have also shown specifically an Arginine residue in Shroom SD2 to be essential for Rock binding, apical constriction and neural tube morphogenesis in mice. Next, we mapped the SBD of Rock to a stretch of 79 amino acids in

its coiled–coil region which is highly conserved across species. Using mutational analysis as well as *in vitro* and *in vivo* assays I have identified surface patches of highly conserved residues in Rock SBD that are important for Shroom binding, co-localization with Shroom, and apical constriction of MDCK cells. These results supplemented by the crystal structure of Rock SBD have facilitated a better understanding of the dynamics of Shroom-Rock interaction and ultimately cell morphogenesis. Overall, elucidating the Shroom-Rock interaction has helped establish an evolutionarily conserved signaling module as a paradigm for cellular and tissue morphogenesis.

TABLE OF CONTENTS

PREFACE ..... **XIV**

1.0 INTRODUCTION **1**

1.1 EPITHELIAL MORPHOGENESIS **2**

1.2 ROLE OF THE CYTOSKELETON IN CELLULAR AND TISSUE MORPHOGENESIS **5**

1.2.1 Actomyosin Contractility **5**

1.2.2 Role of actomyosin in cellular morphogenesis **9**

1.2.2.1 Stress fiber formation **9**

1.2.2.2 Cell migration **10**

1.2.2.3 Cell division **12**

1.2.2.4 Cell adhesion **13**

1.2.2.5 Cell polarity **14**

1.2.2.6 Cell morphology **15**

1.2.2.7 Wound closure **15**

1.2.2.8 Vesicular transport **16**

1.2.3 Role of actomyosin in development. **18**

1.2.4 Regulation of actin cytoskeleton by the Rho-family of GTPases **19**

1.3 APICAL CONSTRICTION AND NEURAL TUBE MORPHOGENESIS . **22**

1.3.1 Apical Constriction 22

1.3.2 Neural Tube Morphogenesis 23

1.4 SHROOM-FAMILY PROTEINS 26

1.4.1 Shroom3 28

1.4.2 Shroom2 31

1.4.3 Shroom4 33

1.4.4 Shroom1 34

1.4.5 Invertebrate Shroom proteins and its evolutionary implications..... 35

1.4.6 Conserved domains of Shroom implicated in Shroom localization and activity…. 36

1.5 RHO-ASSOCIATED KINASE/ROCK 37

1.5.1 Rock1, Rock2 and dRok 38

1.5.2 Rock domain structure and regulation 39

1.5.3 Rock activation 44

1.5.4 Rock effectors and function 46

1.6 SHROOM-ROCK SIGNALING PATHWAY IN CELLULAR AND TISSUE MORPHOGENESIS 49

1.7 DISSERTATION AIMS 52

2.0 CHARACTERIZING THE SHROOM SD2 DOMAIN TO IDENTIFY RESIDUES CRITICAL FOR MEDIATING SHROOM-ROCK INTERACTION, SHROOM DIMERIZATION AND APICAL CONSTRICTION 54

2.1 INTRODUCTION 54

2.2 RESULTS 56

2.2.1 Structure of Drosophila Shroom SD2 56

2.2.2 Making mShroom3 SD2 mutants 58

2.2.3 Residues in central coiled-coil body segment of Shroom SD2 are important for Shroom-Rock interaction 61

2.2.4 Interiorly buried residues in Shroom SD2 are required for Shroom dimerization 63

2.2.5 Shroom-Rock binding is essential for apical constriction and myosinII activation 65

2.2.6 The Shroom-Rock binding interface is evolutionarily conserved 68

2.3 DISCUSSION 69

2.3.1 The Shroom SD2 possess a unique fold with implications in Shroom structure and function 69

2.3.2 Molecular models of Shroom-Rock complex formation 71

3.0 INVESTIGATING THE ROLE OF SHROOM-ROCK INTERACTION IN NEURAL TUBE MORPHOGENESIS 73

3.1 INTRODUCTION 73

3.2 RESULTS 75

3.2.1 The Shroom3$^{m1/Nisw}$ allele harbors a substitution mutation in Shroom3 SD2……..... 75

3.2.2 Shroom3 SD2 R1838 is specifically required for Rock SBD binding..... 78

3.2.3 Shroom3 SD2 R1838 variants fail to colocalize with Rock 82

3.2.4 Shroom3 SD2 R1838 is required for apical constriction of polarized epithelial cells..... 85

3.2.5 Shroom3 SD2 R1838 variants causes decreased activation of the Rock-MyosinII pathway 87

3.2.6 dShroom SD2 R1838 variants behave similarly to mShroom3 SD2 mutants. 89

3.3 DISCUSSION 91

3.3.1 R1838 is essential for Rock binding and Shroom3-induced changes in cell morphology 92

3.3.2 The Shroom SD2-Rock interaction is evolutionarily conserved 94

3.3.3 Implications of understanding the Shroom-Rock interaction 95

4.0 CHARACTERIZING THE SHROOM BINDING DOMAIN OF ROCK TO IDENTIFY RESIDUES CRITICAL FOR SHROOM-ROCK INTERACTION AND ROCK LOCALIZATION 97

4.1 INTRODUCTION 97

4.2 RESULTS 99

4.2.1 Identifying the minimal SBD of Rock and making SBD mutants 99

4.2.2 Identifying conserved surface patch residues on hRock SBD critical for Shroom SD2 binding 102

4.2.3 Conserved surface patch residues are important for Shroom-Rock colocalization 107

4.2.4 The Rock SBD is required for Shroom3 induced apical constriction .. 110

4.3 DISCUSSION 113

4.3.1 Key conserved patches at N-terminus of hRock SBD are important for Shroom binding 114

4.3.2 Shroom-Rock binding is important for Rock localization and apical constriction 119
4.3.3 Implications of a distinct SBD in close proximity of RBD 120
5.0 DISCUSSION AND FUTURE DIRECTIONS 122
5.1 DIFFERENTIAL ACTIN BINDING ABILITY AND LOCALIZATION OF SHROOM 123
5.2 SHROOM REGULATION 125
5.3 ROLE OF SHROOM-ROCK INTERACTION IN ROCK ACTIVATION AND CELL MORPHOLOGY 127
5.4 CLINICAL IMPLICATIONS OF SHROOM-ROCK-MYOSIN II PATHWAY 131
6.0 MATERIALS AND METHODS 134
6.1 MUTAGENESIS OF SHROOM SD2 AND ROCK SBD PROTEINS 134
6.2 PROTEIN EXPRESSION AND PURIFICATION 135
6.3 IN VITRO PULL DOWN ASSAYS 136
6.4 COMPLEX FORMATION 137
6.5 CELL CULTURE AND IN VIVO ANALYSIS 137
6.6 LIMITED PROTEOLYSIS 139
6.7 SIZE-EXCLUSION CHROMATOGRAPHY 139
6.8 CHEMICAL CROSSLINKING 140
APPENDIX A 141
APPENDIX B 144
BIBLIOGRAPHY 150

LIST OF TABLES

Table 1: Sequence and position of mouse Shroom3 SD2 mutants created..... 61

Table 2: Position and sequence of hRock1 SBD mutants created..... 101

Table 3: hRock SBD mutants created to test for Shroom colocalization 108

LIST OF FIGURES

Figure 1 : Epithelial morphogenesis forms the basis for cellular and tissue remodeling 4

Figure 2: Actomyosin motors in cell contractility 8

Figure 3: Role of Actomyosin contractility in cellular morphogenesis 17

Figure 4: Neural Tube Morphogenesis 25

Figure 5: Shroom family of Proteins 27

Figure 6: Rho-associated kinase 43

Figure 7: Model of Rock activation 45

Figure 8: Rock effectors and their function 48

Figure 9: Shroom-Rock pathway in cellular morphogenesis 52

Figure 10: Ribbon diagram of dShroom SD2 protein 57

Figure 11: Alignment of Shroom SD2 protein sequence and SD2 mutants created 60

Figure 12: The Rock binding interface in Shroom SD2 is composed of surface exposed residues in the body segment of the SD2 protein 62

Figure 13: Shroom homodimerization mutants fail to dimerize and abrogate Rock binding 64

Figure 14: Rock binding is essential for Shroom mediated apical constriction 68

Figure 15: Model of Shroom-Rock complex formation 72

Figure 16: Arginine 1838 of Shroom3 SD2 is required for neural tube closure in mice but does not regulate protein expression or localization 78

Figure 17: Arginine R1838 is required for the interaction between Shrrom3 and Rock 81

Figure 18: Shroom3 SD2 R1838 mutants fail to colocalize with Rock SBD *in vivo.* 84

Figure 19: Shroom3 R1838 variants fail to induce apical constriction in MDCK cells 86

Figure 20: Shroom3 R1838 substitution mutations causes decreased activation of the Rock-MyosinII pathway 88

Figure 21: dShroom SD2 variants R1474A and R1474C behave similarly to mShroom3 SD2 mutants 90

Figure 22: Identification of a minimal binding region in the central coiled-coil domain of Rock 100

Figure 23: In vitro pull down assays with hRock SBD mutants and untagged mouse Shroom3 SD2 105

Figure 24: Shroom-Rock colocalization to actin stress fibers in cos 7 cells 109

Figure 25: Key residues in hRock SBD are important for Shroom3-induced apical constriction 112

Figure 26: Different models of Shroom-Rock complex formation and Rock regulation 119

Figure 27: hRock1 SBD mutant proteins expression and purification 142

Figure 28: hRock1 RBD mutant proteins expression and purification 143

PREFACE

I would first like to thank my advisor Dr. Jeffrey Hildebrand for entrusting me with such an exciting project. He infused in me that passion to explore the molecular nuts and bolts of a signaling pathway that is important in embryonic development. He had been a wonderful mentor and a true teacher to me and without his constant support and encouragement this thesis would not have been possible. His passion for research is contagious and it is this enthusiasm of his that made me realize that dedication and being passionate about science are the true colors of a scientist. Jeff, you have helped me grow in that direction and have proven integral in my pursuit of mysteries with relentless scientific fervor. I would be eternally thankful for all that I have learnt and imbibed from you.

I would secondly like to thank all my past and present lab members particularly Ryan, Matt and Erica. Ryan ensured that we always had all the necessary reagents that made doing experiments easy. Matt our past graduate student was always there to help me out during my initial phase in the lab and is a very amenable person too. Erica, a grad student in our lab has been a wonderful labmate. She is a very helpful and friendly person and has helped me out on countless occasions ungrudgingly. Erica, I want to thank you for all that.

I would specially like to thank my collaborator the VanDemark lab. Starting from sharing reagents, to using scientific equipments, to discussing and analyzing data, they have helped me

in every way imaginable. I could not have asked for a better collaboration and have benefitted tremendously from them. I would like to specifically thank Swarna, Jenna and of course Dr. VanDemark for all their help, support, encouragement and insights that have contributed to the completion of my thesis project. Thank you everyone for being such a great collaborator.

I would like to thank my committee Dr. Brodsky, Dr. Stronach, Dr.VanDemark and Dr. Schwacha for all their insightful comments and suggestions during my committee meetings that have shaped my thinking and have helped me sharpen my critical thinking skills. They always showed me ways to think out of the box and come up with appropriate hypothesis and reasoning that had helped me tremendously in growing as a scientist. I really appreciate all your help and would treasure all that I have learnt from you all.

I would like to thank all the labs in the Life Science Annex, who participate in our big lab meeting as well as cordially share their equipments with us. I would like to specifically thank the Boyle lab and Chapman lab for being so helpful over the past few years and have gladly allowed me to borrow reagents from them as well as use their computer for special software. Thank you everyone for being such helpful people and friends.

I would also like to thank everyone in the Main Office and the Fiscal office for helping me smoothly transition into the graduate program regardless of being an international student and making my stay in Pittsburgh a pleasant one. Cathy, I owe you more than words could ever say. Thank you so much for always being there. I would like to thank my friends who have been an important part of this journey. To name them would make the list endless and hence suffice me to say that I will be forever indebted for all the moral support and encouragement you have provided when things were rough.

I would lastly like to thank my family, my parents, grandparents, siblings and my husband for their continued support and undeterred faith in me. This journey certainly would not have been possible without the support system you provided me. They have always uplifted me during my moments of doubt and have reassuringly reinstated my confidence to move ahead and overcome all the hurdles. Ma, Bapi, Dada, Sohinidi and Bhaiu, I cannot thank you enough for all that you have done for me. Neel, you have made me a better person and have stood by me through all that I have undergone. Your faith and belief in me dispels all fear and encourages me to take the step forward. My life without you would not have been complete and I feel lucky and blessed to have you as my best friend for life. Thanks for everything that you all have done for me and I will be eternally grateful for all the blessings showered on me.

1.0 INTRODUCTION

During embryonic development epithelial cells undergo well synchronized and dynamic morphogenetic movements to pattern the complex 3D architecture of different organs and tissues like the central nervous system, vasculature, eye and kidney. When these morphogenetic movements occur synchronously in a group of cells, they can promote alterations in stiffness or architecture that facilitate tissue invagination, bending, folding, elongation and convergent extension [1, 2]. Although all these tissues are derived from polarized epithelial cells, they each undergo a unique morphogenetic program that defines their association and interaction with other cells to form different structures with distinct organization and function. Therefore any impairment in the cell's ability to execute the correct morphogenetic program results in myriad human birth defects and diseases involving formation of the neural tube, vasculature, eye and kidney.

At the cellular level this remodeling is brought about by spatially and temporally regulating the dynamics and organization of the cytoskeleleton. A wide array of cytoskeleton associated proteins have also been implicated in regulating cell behavior like adhesion, migration, shape and polarity that prove critical for normal embryonic development. In non-muscle cells, the key cytoskeletal proteins actin and myosin II play a major role in altering epithelial cell shape by exerting cortical tension and elliciting apical constriction. Together they form a contractile actomyosin network whose localization and activation is tightly regulated by

cytoskeleton-associated proteins and kinases. This contractility of the actomyosin cable is dependent on the localized activation of myosinII brought about by phosphorylation of its regulatory myosin light chain [3]. Rho-kinase/Rock serves as the major regulator of RMLC phosphorylation in non-muscle cells and activates the ATPase activity of myosinII [4]. Rock recruitment to specific subcellular locales to bring about this localized activation of myosinII is however dependent on binding to various effector molecules like RhoA, lipid or Shroom3 [5-7].

Shroom is a class of actin-binding proteins that is required for various developmental processes [8-14]. Shroom has the ability to regulate cell and tissue architecture by binding to Rock and activating the Rock-myosinII pathway [11, 15]. This Shroom-Rock interaction triggers a phosphorylation cascade that leads to the formation of a circumferential contractile actomyosin network that ultimately brings about change in cell shape and behavior. Though much is known about the downstream events of this Shroom-Rock signaling module, there is no sequence or structural homologs for the domain of Shroom that interacts with Rock and therefore the molecular mechanism and dynamics of this interaction still remain elusive. My dissertation aims to dissect the molecular nature of the Shroom-Rock interaction to unravel the basis for cellular and tissue morphogenesis and the spatio-temporal regulation of cytoskeletal dynamics.

1.1 EPITHELIAL MORPHOGENESIS

Epithelial cells are typically characterized by a monolayer of polarized cells with a distinct apical surface facing a lumen, a lateral surface adjoining neighboring cells and a basal surface that connects with the underlying extracellular matrix. Cellular adhesion encompasses stable but dynamic interactions which are important for maintaining tissue integrity, transducing

extracellular signals as well as integrating cytoskeletal dynamics across a tissue, especially during embryonic development when the tissue undergoes dramatic changes in morphology. During embryogenesis cells undergo highly coordinated morphogenetic movements like invagination, convergent extension, elongation, and tube formation that lead to the formation of complex structures of different tissues and organs (Figure 1C).

At the cellular level, these morphogenetic processes are driven by cytoskeletal proteins actin and motor protein myosinII. Localized activation of myosinII via phosphorylation of its regulatory light chain in conjunction with actin filaments forms a contractile actomyosin meshwork that exerts cortical tension and generates force required to transform a columnar shaped cell into wedge shaped form [2, 16] (Figure 1A). Regulation of the localized assembly and activation of this contractile actomyosin network proves crucial for different cell processes like adhesion, migration, division, polarity and cell morphology. As each cell connected to its neighbors, pulls the plasma membrane inward it cumulatively causes coordinated apical constriction across the epithelial sheet that leads to tissue bending (Figure 1B). Epithelial morphogenesis thus serves as the basis for tissue remodeling and its regulation is important for coordination of these complex and dynamic changes during embryonic development (Figure 1C).

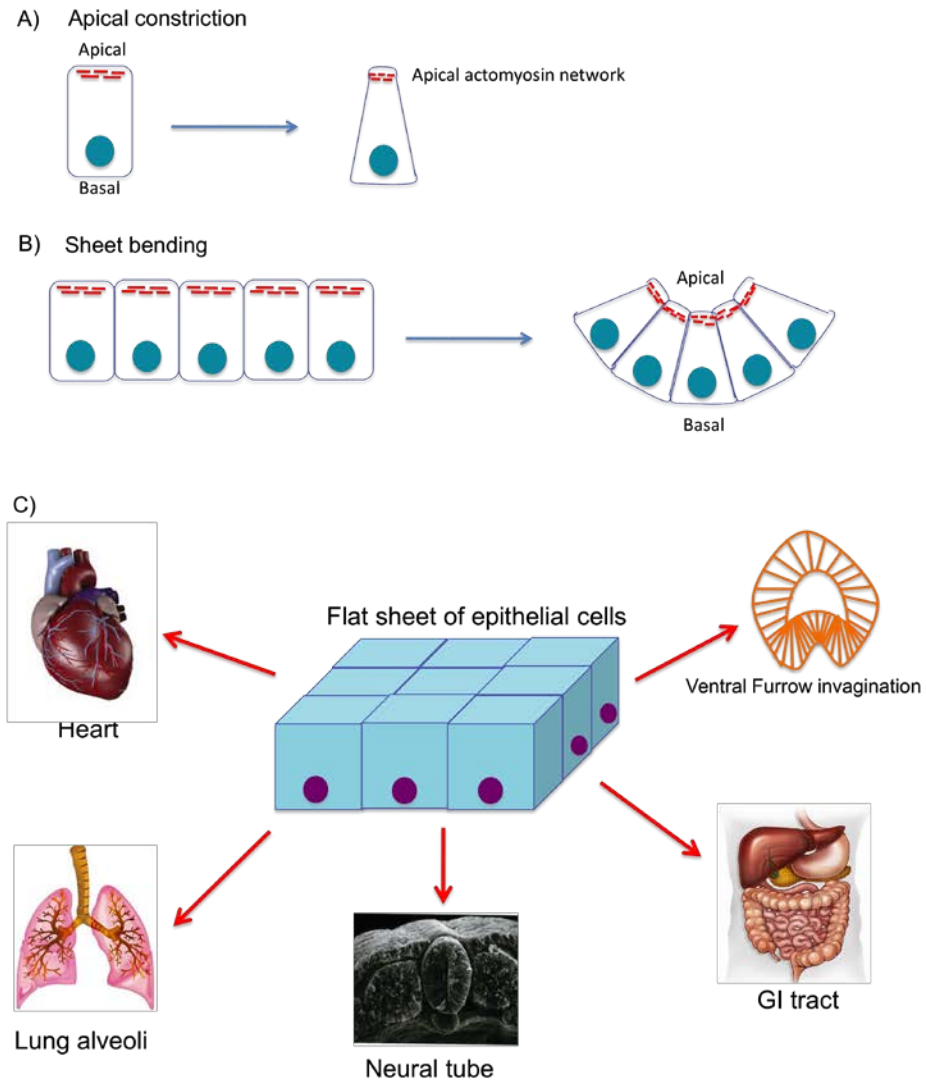

Figure 1 : Epithelial morphogenesis forms the basis for cellular and tissue remodeling

A). Epithelial cell shape change at the individual cell level.

B). Bending of flat epithelial cell sheet due to contraction of apical actomyosin network.

C). Morphogenetic movements in a group of cells causes remodeling of the cytoskeletal architecture leading to patterning of complex 3D structures of different organs. Images of different organs adapted from online google image.

1.2 ROLE OF THE CYTOSKELETON IN CELLULAR AND TISSUE MORPHOGENESIS

Spatiotemporal regulation of cytoskeletal dynamics is imperative for precise coordination of morphogenetic movements during embryonic development and organogenesis. Actomyosin networks, the key mediators of this process, can thus have ramificatons at both the cellular level and the organismic level. A combination of these two levels of cytoskeletal regulation can help understand the molecular mechanics of how cells change shape and regulate tissue architecture. The sections below will elaborate on the structure of this contractile apparatus of cells and how actomyosin dynamics can influence cell bahavior and development.

1.2.1 Actomyosin Contractility

The cytoskeleton forms the basic supporting framework of cells. This framework is composed of actin filaments, microtubules and intermediate filaments each with unique functions that can either impart mechanical strength, direct intracellular transport or determine cell shape and guide locomotion. The actin and microtubule filaments however cannot function without the motor proteins myosin, kinesin and dynein which regulate assembly of these cytoskeletal filaments spatially and temporally. Molecular motors like myosin utilize the energy of ATP hydrolysis to either pull actin filaments together or deliver cargo along these polymerized filaments.

Actin and myosinII are the major cytoskeletal proteins that bring about cell and tissue morphogenesis. Actin monomers are globular proteins (G-actin) which polymerizes in a head to tail fashion to form helical filamentous actin (F-actin) [17]. These filaments are structurally polar with a fast growing plus end and a depolymerizing minus end (Figure 2A). Actin filaments underlie the plasma membrane of cells and hence their dynamic nature can influence cell shape and behavior, migration, adhesion and contractility. MyosinII is a heteromer composed of two heavy chains (MHC), two essential light chains (MLC) and two regulatory light chains (RMLC). Each heavy chain consists a globular head domain followed by a short neck region and an extended coiled-coil region that mediates heavy chain dimerization (Figure 2B). The MLC and RMLC bind close to the MHC head and neck regions and the long coiled-coil region forms tail-tail interactions with other myosin molecules to generate a large thick bipolar filament [18]. Non-muscle myosinII is an actin-based motor that can bind to ATP, undergo a conformational change and utilize the energy from ATP hydrolysis to walk towards the plus end of an actin filament. By virtue of its opposing orientation of the heads in the thick filament the movement of the myosin motor effectively slides oppositely oriented actin filaments towards each other [19] (Figure 2C). This leads to contraction of the F-actin fibers generating tensile forces on the adhesion structures to which they are attached that can cause cell shape changes. On expending this energy from ATP hydrolysis actin filament dissociates from myosin. This cyclical actin binding and force generation motor activity of myosinII is greatly enhanced by phosphorylation of the Ser19 residue of the RMLC [20, 21] which alters the conformation of the myosin heavy chain and increases flexibility at the head-neck junction of myosin facilitating actin binding and stimulation of ATPase activity [22].

Several kinases have been implicated in the phosphorylation of RMLC including myosin light chain kinase (MLCK), Rho-associated kinase (Rock), p-21 activated kinase [23], citron kinase, integrin-linked kinase (ILK), myotonic dystrophy protein kinase-related cdc42-binding kinase (MRCK) and death-associated protein kinases (DAPK) and its dephosphorylation by myosin phosphatase targeting subunit (MYPT) [21, 24-28]. The major contributors being MLCK, Rock, and its dephosphorylation by MYPT [21, 24-31]. All these kinases phosphorylate either Thr18 or Ser19 or both and cause myosinII activation, however the mode of myosinII activation differs with each kinase [32]. Of the three different isoforms of myosinII namely A, B and C, myosinIIA shows increased stroke activity due to increased rate of ATP hydrolysis whereas myosinIIB binds to actin in a force generating state for a prolonged time to maintain tension [33, 34].

The localized activation of myosinII by kinases and subsequent actin binding leads to the formation of a contractile actomyosin network in cells. These tensile forces when communicated across a cell sheet, brings about tissue morphogenesis. Thus tissue sculpting requires a fine balance between contractility and stiffness of the extracellular matrix which is achieved by spatial and temporal regulation of the actomyosin activity.

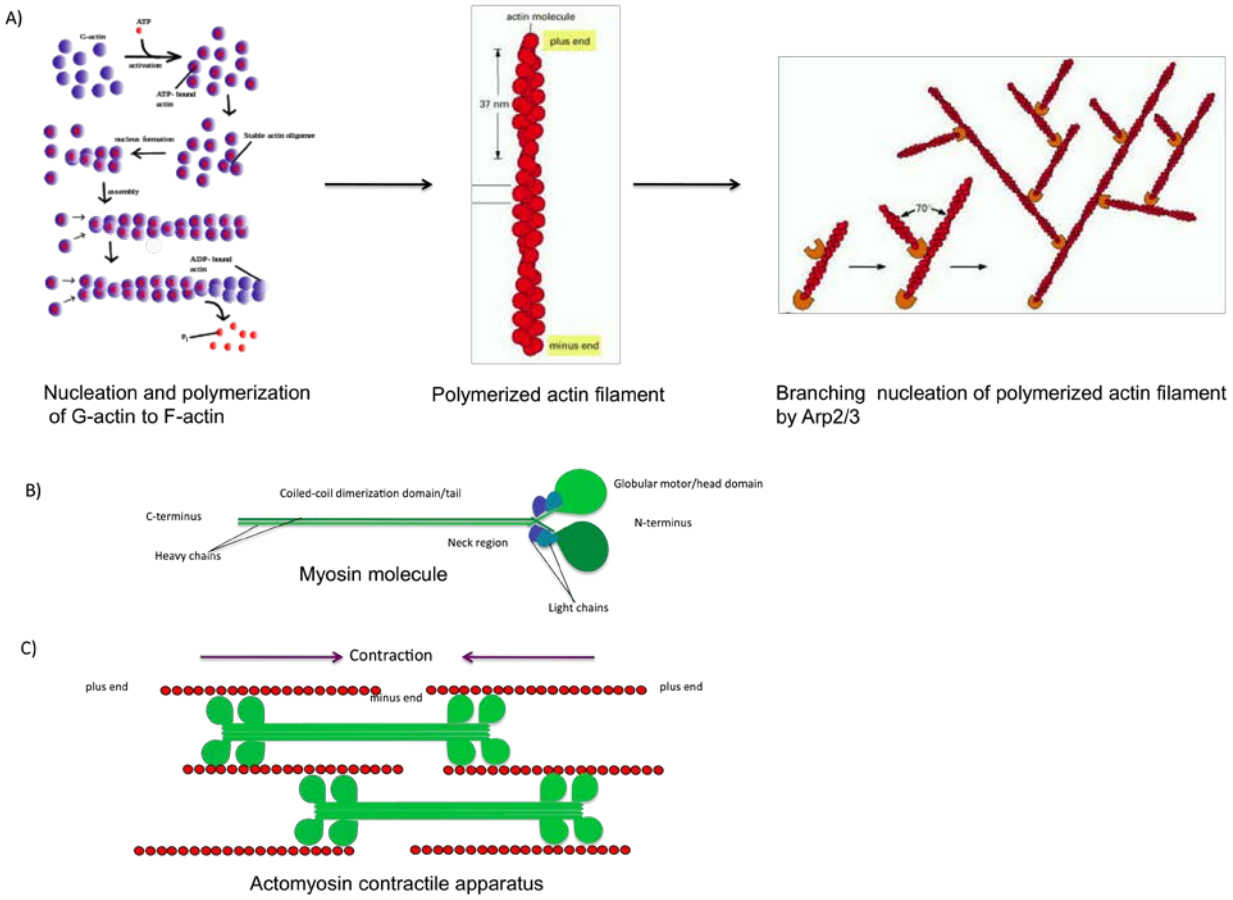

Figure 2: Actomyosin motors in cell contractility

A) Process of nucleation of monomeric globular actin and formation of polymerized polarized filamentous actin. Nucleation and branching web formation by the ARP complex (depicted in green). Adapted from Molecular Biology of the Cell, Fifth edition, Bruce Alberts et al.

B) Myosin motors: composed of two heavy chains and four light chains.

C) Oligomerized myosin bipolar filament and contractile stroke action due to ATPase activity causing sliding of actin filaments towards each other.

1.2.2 Role of actomyosin in cellular morphogenesis

1.2.2.1 Stress fiber formation

Stress fibers are bundles of antiparallel actin filaments with intermittent insertion of myosinII and forms an actomyosin based contractile network in cells (Figure 3). Various actin-myosin based contractile proteins like tropomyosin, α-actinin, filamin and others play a major role in bundling and maintenance of stress fibers as well as formation of cell-matrix adhesion sites called focal adhesions [35-37]. Rho proteins are known to be major modulators of organization of actin filaments including formation of stress fibers and focal adhesions [38, 39]. Of the known downstream effectors of RhoA, Rock and mDia have been shown to cooperatively activate myosinII to induce actin reorganization and formation of stress fibers [40]. Overexpression of Rock induces the formation of stress fibers and focal adhesions in several cell types [38, 41, 42] however they are not identical to Rho-induced stress fibers [43]. GTP-bound Rho activates mDia by disrupting its intramolecular interactions. mDia alone induces thin loosely bundled actin stress fibers in the absence of Rock. Additionally active mDia transforms Rock-induced condensed actin fibers into structures more reminiscent of Rho-induced stress fibers. Thus mDia and Rock work concurrently downstream of Rho during stress fiber formation [40]. It is the combinatorial effect of both Rock and mDia that leads to the formation of organized contractile actomyosin bundling in stress fibers [40]. While Rock induces formation of actomyosin stress fibers, mDia localizes to focal adhesion where it is involved in nucleating actin filaments [44]. Inhibiting either mDia or Rock activity leads to disruption of stress fiber and focal adhesion formation [45-48].

Stress fibers are important determinants of cell dynamics. They impart tissue rigidity that is important for cellular remodeling during morphogenetic movements. They are important for establishment of cell-matrix connections through termination in dense plaques called focal adhesions. Stress fibers also help endothelial cells sustain shear stress due to blood flow by maintaining a smooth luminal surface [49]. Rock mediated phosphorylation of myosin regulatory light chain enhances its actin-binding and actin-induced ATPase activity thereby triggering contractility. As myosin is highly efficient in crosslinking F-actin the enhanced binding of myosin to actin by virtue of its phosphorylated state promotes reorganization of actin filaments into higher order structures namely actin bundles or stress fibers and formation of focal adhesions. Therefore actomyosin contractility is the key step in the formation and assembly of stress fibers and focal adhesions [50].

1.2.2.2 Cell migration

Cell motility and locomotion is a complex process involving coordinated activity of cytoskeletal, membrane and adhesion systems. Directional cell motility is characterized by forward protrusions, substrate attachment and tail retractions [51, 52]. F-actin is required for each step of the cycle and its spatio-temporal regulation by specific binding proteins and myosin motors is required to perform such diverse mechanical functions. Cells form actin based finger like projections called filopodia or wave like protrusions called lamellopodia at the leading edge and makes contact with the substratum (Figure 3). Adhesion to the substrate triggers tail retraction allowing the cell to migrate in a specific direction. As one can imagine this forward protrusion, traction and retrograde retraction is mediated by dynamic polymerization and depolymerization of the underlying actin cytoskeleton in the cell.

Protrusive structures like filopodia or lamellopodia at the leading edge of the cell are highly dynamic being composed of dense arrays of actin filaments. They are organized with their barbed/plus/growing ends oriented towards the direction of protrusion. Protrusion of the membrane is tightly coupled to actin polymerization. Actin polymerization or nucleation is brought about by Arp2/3 and profilin in the lamellipodium and myosinII does not seem to be essential for its formation [53-55]. The lamellopodium, along with actin rich adjoining lamellum, undergo retrograde actin flow that counteracts actin polymerization at the leading edge of the lamellipodium. Inhibiting myosinII activity collapses the lamellum and delays frontal protrusion of the cell [54]. On the other hand, excessive myosinII activity also impedes cell migration [56]. Adhesion to the substratum via formation of focal adhesion contacts exerts traction that balances these two opposing forces, the frontal protrusion and retrograde actin flow resulting in net protrusive activity [57]. MyosinII plays a major role in the formation and maturation of these focal adhesions utilizing other cytoskeletal proteins like vinculin and talin [58-60]. These focal adhesion sites therefore serve as a 'molecular clutch' to generate forces required for forward directional protrusion and effective migration [61].

The two different isoforms of myosinII, A and B have exclusive roles in cell motility and migration. MyosinIIA is dynamic and localizes to frontal protrusions as well as at the cell rear to mediate retraction and adhesion disassembly. MyosinIIB on the other hand, is non-dynamic and mediates actin cross-linking to establish front-back polarity in the cell [62, 63]. This differential localization of the two isoforms of myosinII ensures different actin dynamics at the front and rear of the cell. MyosinII inhibition deforms cell shape and causes cell elongation as they fail to undergo tail retraction [64]. MyosinII mutant mice embryos exhibit embryonic lethality stemming from brain, cardiac, and endodermal maturation defects or simply cell adhesion

defects further confirming the importance of the cytoskeleton during normal development [65, 66]. Germ line ablation of the two different isoforms of myosinII in mice has revealed different phenotypes, thereby suggesting their unique functional roles. Also, knocking-in alternate myosinII isoform into a myosinIIA or IIB deficient mice partially rescues the developmental defects however they are still embryonic lethal [67, 68]. These results thus suggest a partially overlapping but non-redundant function of the different isoforms of myosinII. Several studies have noted differences in RNA expression patterns in tissues, intracellular localization biochemical properties and modes of regulation between the different myosin II isoforms [69-73]. However it is hypothesized that the actomyosin dependent contractile apparatus of cells requiring only the actin cross-linking ability of myosinII and is not isoform specific [74].

1.2.2.3 Cell division

Cell division is a precisely regulated process ensuring equal distribution of genetic material between two daughter cells. The dynamic nature of the cytoskeleton tightly controls the fidelity of this process both spatially and temporally. Cytokinesis begins after the segregation of the sister chromatids in anaphase and is marked by the assembly and appearance of a contractile ring called the cleavage furrow at the equator of the cell cortex. Contraction of this contractile ring results in the pinching off and formation of two daughter cells at the end of telophase (Figure 3). MyosinII is the primary motor protein responsible for cytokinesis [75, 76]. Myosin activation by phosphorylation of its regulatory light chain (RMLC) at residues Thr18/Ser19, allows it to interact with actin filaments to assemble a contractile actomyosin complex required for cell division [77]. RMLC phosphorylation also favors filament formation apart from filament assembly [22, 78, 79]. Genetic experiments using different model systems have shown the critical role of RMLC phosphorylation in cell division [3, 80]. Additionally, activated

phosphorylated myosin accumulates at the equator of a dividing cell after chromosomal segregation [81]. RMLC activation is tightly regulated by several kinases and phosphatases. Localized activation of myosin involves a tight balance between positive phosphorylation and negative dephospohrylation. Of the previously mentioned kinases, MLCK, Rock, citron kinase and MYPT are the key candidate regulators found to be localized to the cleavage furrow [82]. Therefore cells employ different kinases and phosphatases to regulate RMLC phosphorylation spatially and temporally to reorganize the cytoskeleton at the cleavage furrow for efficient cell division.

1.2.2.4 Cell adhesion

Cell adhesion is critical for integrating signals for cytoskeletal rearragements required for different morphogenetic processes as well as transition between mesenchymal and epithelial behavior. The adhesive properties of a cell, whether it needs to make cell-cell contacts via tight junctions or adherens junctions or anchoring to the underlying extracellular matrix via focal adhesions, requires F-actin [83, 84] (Figure 3). A tight balance between actomyosin networks and Ras superfamily of GTPases (Rho, Rac and Cdc42) is required to promote and maintain cell adhesion.

In epithelial cells localized activation of Rac induces formation of actin-based filopodial projections enriched with a transmembrane adhesion protein E-cadherin, which extend into neighboring cells and establish nascent cell-cell contacts along with other actin binding proteins like α-catenin, vinculin, Mena, VASP and formin-1 [85-88]. Rac indirectly activates Cdc42 and Arp2/3, known actin polymerizing agents, via phosphatidylinositol 3-kinase and creates cellular contacts through extensive E-cadherin interactions [88]. Rac and Cdc42 also activate Par6 and

aPKC, key components of cell polarity machinery to form epithelia specific cell-cell adherens junctions [89]. RhoA mediates E-cadherin based cell adhesion through Rock and Dia1 [90].

Actomyosin networks play a formative role in mediating cell adhesion and tissue organization. Knocking down myosinIIA leads to loss of E-cadherin and beta-catenin localization to cell adhesion sites in both cell culture and intact embryos [65]. Further, myosinII isoforms have been shown to mediate distinct functions required for cell adhesion and tissue integrity [91]. MyosinII is also required for adherens junction formation and maintenance and involves key actin binding proteins like vinculin and α-catenin that serve as mechanosensors for remodeling cell-cell junctions [92, 93].

1.2.2.5 Cell polarity

Cell polarity refers to spatial differences in shape, structure and function of cells. Epithelial cells grow as monolayers on a flat surface comprising tightly adherent cells via structures like tight junctions, adherens juctions and desmosomes and anchored to an underlying extracellular matrix by focal adhesions. When grown in three-dimension, like in collagen gels these cells form cysts with a central lumen. Epithelial cells exhibit either an apical-basal polarity or planar cell polarity or mostly both. Establishment of apical-basal polarity requires asymmetric distribution of membrane associated protein complexes like Par3-aPKC-Par6-Cdc42, Scribble or Crumbs to tight junctions to maintain polarization by interacting with cytoskeletal elements and separating apical and basal domains of the cell [94-98]. Planar cell polarity is mediated by yet another signaling pathway comprising Wnt, Frizzled, Dishevelled and its various tissue specific downstream targets [99-107]. These multiple cell polarity complexes execute their function by regulating and reorganizing the cytoskeleton (Figure 3). Rho-GTPases like Rac and Cdc42 have also been shown to play a formative role in establishment and maintenance of polarity [108-111].

1.2.2.6 Cell morphology

Cell shape changes like apical constriction, apical-basal lengthening or shortening and cell elongation are required universally by different species during development [112-114]. Actomyosin networks are required for these behaviors and when this shape change occurs synchronously in a group of neighboring cells it can alter the geometry of a tissue [16] (Figure 3). The actomyosin cytoskeleton is composed of networks of actin filaments cross-linked by myosinII. MyosinII oligomerizes in a tail-to-tail fashion to form bipolar filaments that allow anti-parallel actin filaments to be pulled towards each other thereby generating a contractile or tensile force. These tensile forces when transmitted across neighboring cells through cell-cell junctions or cell-matrix focal adhesions, brings about change in cell shape and tissue architecture [115].

Apico-basal cell elongation is sometimes concomitantly accompanied with apical constriction in different organisms [116-118]. Microscopy as well as pharmacologic inhibitor studies have shown microtubules to be the key cytoskeletal component in cell elongation [116, 119-121]. γ-tubulin, the key promoter of microtubule nucleation possibly plays an important role in cell elongation by organizing robust parallel array of microtubules that drive apicobasal cell lengthening [120].

1.2.2.7 Wound closure

Individual epithelial cells function in the context of the entire epithelium where tissue integrity poses to be a crucial requirement for cell function. Closure of wounds or tissue lesions involves coordinated cell migration into the wound as well as cell adhesion. This epithelial resilience is mediated by thick actomyosin cables at the leading edge of the wound that function as a purse-string in drawing cells together and closing the wound [122, 123] (Figure 3). Differential recruitment of myosinII as a contractile ring in tight junctions near the apical surface of the cell

or basally in lamellopodia immediately after wounding has been shown to be responsible for wound healing in polarized epithelial cells. Also Rock seems to be the primary effector molecule mediating this actomyosin dynamics in wound healing [124]. The tight junction protein ZO-1 performs multifaceted roles as it localizes to apical myosinII to initiate purse string contractions at the leading edge during the wound healing process and regulates localization and assembly of cell polarity proteins for directional cell migration [125].

1.2.2.8 Vesicular transport

Intracellular transport by random vesicle diffusion would be slow in a crowded cytoplasmic environment of a cell. Therefore a cell needs molecular motors to assist in the delivery of specific vesicles to assigned destinations. Cytoskeletal motor proteins associate with their filament tracks and move unidirectionally along these tracks by utilizing energy from ATP hydrolysis. There are three groups of cytoskeletal motor proteins: myosins which associate with actin filaments and kinesin and dyneins which are microtubule motor proteins. The structural similarity of myosin and kinesin motor domain core indicates a common evolutionary origin of these motor proteins. Although kinesin and dynein are the most well known mediators of intracellular transport of membrane enclosed vesicles, myosin motors have a significant role in organelle transport along actin filaments. MyosinV was the first to be shown to mediate intracellular transport of membrane bound pigment granules called melansomoes to the overlying keratinocytes of the skin [126]. Actin filaments provide the track for vesicle transport in the endocytic pathway [127, 128] whereas myosin motors utilizes this actin track as a scaffold for transporting the cargo inside a cell (Figure 3). The myosin superfamily of molecules is characterized by a globular motor domain and a α-helical rod domain in the heavy chain [129].

The motor domain binds to actin filaments in an ATP-dependent manner whereas the rod domain oligomerizes to form a coiled-coil that can bind to different cargo thus forming an intracellular transport system where the myosin can walk along the actin filament [130, 131]. The coil-coil domain also tethers multiple motor domains to facilitate processive transport along the actin filament. This intracellular transport machinery is fueled by the host of GTPases of the endocytic machinery and it is probable that regulation of actin dynamics or myosin via the Rho-Rock pathway can play a role in vesicular trafficking [132].

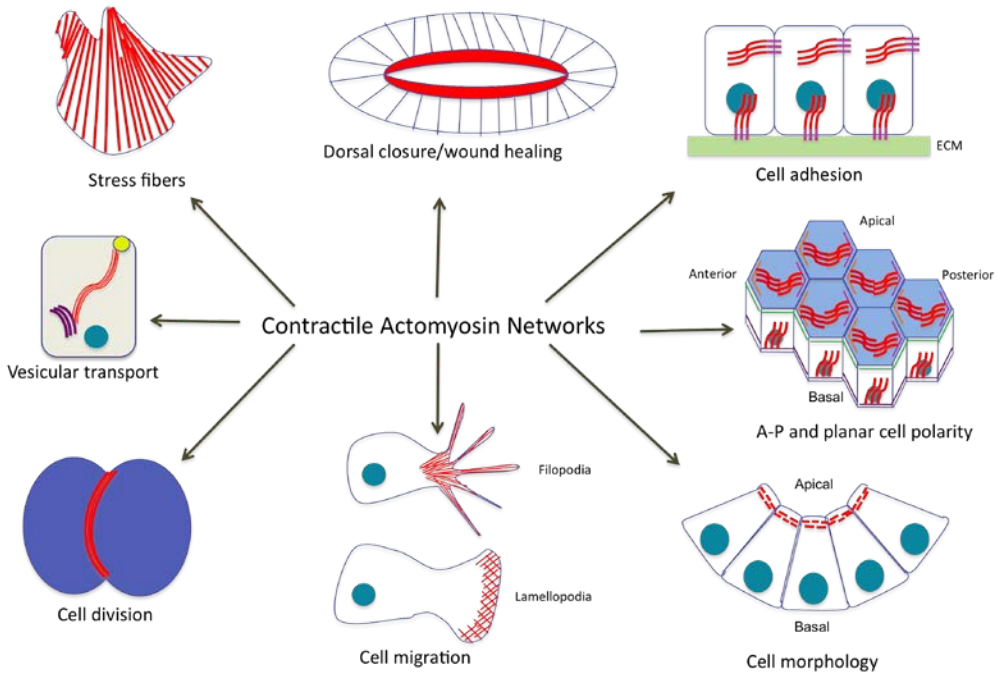

Figure 3: Role of Actomyosin contractility in cellular morphogenesis

Contractile actomyosin network forms the basis for various cell processes. Diagrammatic representation of some of them has been shown above. Actomyosin networks/filaments are labelled red and nucleus by turquoise circles.

1.2.3 Role of actomyosin in development.

The ability of the cytoskeleton to respond to external as well as internal cues to elicit changes within a single cell or a field of cells proves critical for the normal progression of development. This remodelling of the cytoskeletal architecture serves as the core of many morphogenetic programs. Fully activated and tightly regulated actomyosin networks thus emerge as a recurring theme in different developmental processes, some of which are discussed below.

Neural tube closure is a complex morphogenetic process involving well synchronized and coordinated cell movements that involve extensive reorganization of the cytoskeleton. The crucial role of the cytoskeleton in this process has been explicitly demonstrated by cytochalasin treatment (a potent disruptor of actin) experiments where mice embryos exhibit cranial exencephaly, a signature neural tube closure defect caused by loss of an intact actin cytoskeleton [133-135]. During vertebrate eye development formation of a contractile actomyosin network is essential for lens formation, eyelid closure, failure of which leads to eye open at birth phenotype (EOB), and various eye deformities [136, 137]. Gut morphogenesis is yet another example of orchestrated action of Rho/Rock/myosinII mediated cellular rearrangements for proper tube lengthening and luminization [138]. Axon guidance and neurite tail retraction are all mediated by tight regulation of actin polymerization and depolymerization where actomyosin networks prove indipensable for proper neuronal architecture and function [139-141] and also for immunologic function of the natural killer (NK) cell [142]. Tissue vascularization or sprouting of blood vessels from existing ones is an important event in development. Angiogenesis is brought about by the leading migrating tip cell forming filopodial extensions to provide guidance cues for directional

migration [143]. VEGF, a tip cell specifying morphogen, works via activation of Rho GTPases namely Rac, Cdc42 and RhoA to induce tip cell migration [144, 145]. Abrogating RhoA or Rock activity blocks VEGF mediated cytoskeletal rearrangements and prevents angiogenesis [146, 147]. Also Rock negatively regulates sprouting in a myosinII dependent pathway [148]. Glomerular epithelial cells of the kidney known as podocytes are critical determinants of normal kidney function. Podocytes form actin-rich projections known as foot processes required for effective glomerular filtration and kidney function. Specialized myosin motors, in conjunction with actin, form these foot processes, thereby illustrating the role of the cytoskeleton in normal kidney development and function [149-152]. Germ line ablation of myosinII isoforms in mice leads to embryonic lethality with severe brain, cardiac, and endodermal maturation defects or simply cell adhesion defects, further confirming its importance during normal development [65, 66]. Lastly, *Drosophila,* an excellent invertebrate model system, portrays the importance of actomyosin based contractile networks in myriad cellular functions and tissue morphogenetic events like ventral furrow invagination, dorsal closure, compartmentalization and germ band extension [16, 113, 153-155]. Thus precise spatio-temporal regulation of cytoskeletal dynamics proves crucial for proper embryonic development.

1.2.4 Regulation of actin cytoskeleton by the Rho-family of GTPases

There are different pools of actin in a cell. The variety of actin networks in a cell must undergo remodeling to bring about epithelial morphogenesis. This reorganization of the cytoskeleton is mediated by actin binding proteins and nucleation promoting factors. The Rho-family of small GTPases regulate a variety of these actin binding proteins, kinases and polarity proteins to regulate cell behavior like adhesion, migration, polarity and proliferation. Rho family GTPases

act as molecular switches cycling between an inactive GDP bound form and an active GTP bound form to interact with downstream effectors in transducing signaling pathways [156, 157]. GTP hydrolysis by GTPases is accelerated through interactions with GTPase activating proteins (GAPs) causing Rho inactivation whereas Rho activation is facilitated by guanine nucleotide exchange factors (GEFs) that exchanges GDP for GTP [158, 159]. The GTP or GDP bound to Rho GTPase dictates its affinity towards its downstream targets leading to very specific effector recognition in the 'on' state only [160]. Another means of GTPase regulation comes in the form of guanine-nucleotide dissociation inhibitors (GDIs), which block effector activation by binding to GDP-bound GTPases and prevent nucleotide exchange [161].

The Rho family of GTPases namely RhoA, Rac1 and Cdc42 have been shown to be key cytoskeletal regulators based on overexpression studies in Swiss3T3 fibroblasts. RhoA induced stress fibers and focal adhesions formation, Rac1 caused flat lamellipodial projections and Cdc42 induced filopodial extension [39, 162-164]. Therefore it is important that the cortical actin is tightly regulated. This regulation of actin polymerization is orchestrated by Rho GTPases. To date the Rho GTPases have been shown to play a role in numerous actin-dependent cellular processes such as platelet aggregation, lymphocyte and fibroblast adhesion, cell motility, contraction and cytokinesis [165]. Thus these observations indicate that Rho regulates cytoskeletal dynamics in a cell by linking extracellular stimuli to the reorganization of the actin cytoskeleton. The different external stimuli that can activate Rho GTPases are signaling through receptor tyrosine kinase (RTK), lysophosphatidic acid (LPA), integrins and cadherins [166-168]. As stated above Rho induces formation of focal adhesions in addition to stress fibers. However it is currently debatable whether the two are sperate or inter-dependent events.

Rac also transduces a similar type of signaling pathway and can mobilize the cytoskeleton to generate lamellipodia or membrane ruffles. Rac signals to a complex of proteins called the WAVE or SCAR complex (a member of the WASP family of proteins) consisting of Arp2/3 activating protein WAVE, two Rac binding proteins (Nap125 and PIR121), HSPC and Abi2 [169, 170]. Active Rac causes this complex to dissociate resulting in derepression of WAVE and enhancing Arp2/3 actin polymerization and induce branched actin networks as found in lamellipodia [171, 172]. Rac is also able to signal through other serine threonine kinases like PAK, which signals to downstream effectors to promote actin polymerization and stabilization of existing actin filaments [157].

Both Rac and Cdc42 have been shown to induce assembly of multimolecular focal complexes at the plasma membrane of fibroblasts [163]. These complexes are morphologically distinct from Rho-regulated focal adhesions though the protein components of both complexes appear similar. Moreover other labs have shown the involvement of Rac in cell motility in MDCK cells [173], actin and microtubule polymerization towards antigen-presenting cells [174], control of cytokinesis in fibroblasts, HeLa cells and *Xenopus* embryos [175-179]. WASP binds to Cdc42 in a GTP-dependent manner and links it to the actin cytoskeleton via another adaptor protein [180, 181]. Furthermore, over expression of WASP induces ectopic actin polymerization that could be blocked by dominant-negative Cdc42, suggesting that WASP-induced cytoskeletal rearrangements are controlled by Cdc42 [181]. Several potential targets of Rac and Cdc42 have been identified to date and several of them bind to both Rac and Cdc42. Though current evidence suggests that Rock is a downstream effector for RhoA only and not Rac and Cdc42, it is not surprising that the Rho-family signaling pathways often converge to either directly activate each other or utilize common downstream targets to elicit a response.

1.3 APICAL CONSTRICTION AND NEURAL TUBE MORPHOGENESIS

Apical constriction will be used to demonstrate how specific alterations in cytoskeletal organization and contractility can drive cell shape change during a developmental process.

1.3.1 Apical Constriction

A phenotypic readout of localized actomyosin contractility is apical constriction. Cells undergoing apical constriction exhibit dynamic apical enrichment of activated myosinII that colocalizes with actin filaments at the adherens junctions at the apical boundary of the cell. Together they form a contractile actomyosin cable, which undergoes pulsatile contractions to constrict the apical surface of cells, transforming a columnar shaped cell with roughly equal apical and basal surface into a wedge shaped form with narrow apical surface and wide basolateral surface. However these pulsatile contractions need to be stabilized for maintaining tension and retaining tissue integrity. Different models of epithelial morphogenesis have described these pulsatile contractions at the apical junctional complex to be a ratchet mechanism for maintaining tension across the cell sheet needed for tissue remodeling in fruit flies [182-184].

Apical constriction is widely utilized by polarized epithelial cells. In an epithelial layer, when this shape change occurs synchronously in a group of cells, it can cause cell sheet bending with a concave apical surface and convex basal surface. This leads to sheet invagination, tube formation and internalization of cells. Apical constriction forms the basis of many

morphogenetic events like gastrulation in invertebrates such as nematodes [185], sea urchins [186], *Xenopus* [187, 188] and *Drosophila* [189]. In *Drosophila*, apical constriction is also required for dorsal closure, eye development, formation of the salivary gland and tracheal tubes, ventral furrow formation and internalization of mesoderm [117, 190-193]. During vertebrate morphogenesis apical constriction is required for neural tube closure [194-196], lens placode formation and primitive streak formation [197]. Thus apical constriction is a conserved process used by different organisms for altering cell shape during embryonic development. In most of the above outlined cases Rho-GTPases and Rock activate myosinII and triggers formation of a contractile actomyosin network [198-205]. Thus, though these developmental processes differ greatly in their upstream regulators, actin and myosinII form the central effectors in bringing about apical constriction

One of the most widely studied examples of cells undergoing extensive morphogenetic movements is the process of neural tube closure which will be discussed next.

1.3.2 Neural Tube Morphogenesis

Neurulation is a critical event in the development of the vertebrate central nervous system. The neural tube serves as the embryonic precursor to the brain and spinal cord and failure of its closure leads to congenital malformations classified as Neural Tube closure Defects (NTDs). While less common in the developed world, NTDs including spina bifida and excencephaly are among the most common birth defects worldwide affecting approximately 1 in 1,000 child births [206-208]. While over 200 genes have been implicated in neural tube morphogenesis in mice, a clear understanding of the etiology of human NTDs has remained elusive [208-210].

The process of neurulation starts with a flat sheet of neural epithelial cells called the neural plate undergoing concerted morphogenetic movements to bend and form lateral folds. Further bending of the neural plate as a result of apical constriction of neural epithelial cells leads to formation of dorsolateral hinge points, elevations of the lateral folds and juxtaposition of the folds across the dorsal midline that fuse to form a closed neural tube [208-212] (Figure 4). Fusion of the neural folds is initiated at discrete locations along the neural axis and proceeds in a zipper-like fashion towards the anterior and posterior directions. The anterior part of this closed tube forms the brain and the posterior part becomes the spinal cord. Cranial NTDs cause anencephaly or exencephaly whereas caudal NTDs cause spina bifida [208-212].

The intrinsic forces driving neurulation are orchestrated by the contraction of the subapical actin microfilaments of the neural epithelial cells [213-217]. Inhibitor studies using cytochalasin, have shown the dependence of cranial neural tube closure on actin microfilaments [134, 135, 218]. Thus it has been suggested that this extensive morphogenetic event relies heavily on dynamic reorganization of the cytoskeletal components to provide necessary force and tension for proper closure of the neural tube. Indeed mutations in various cytoskeletal regulator proteins such as Nap1 [219], Abl1/2 [220], p190RhoGap [221], Mena/profilin [222], Vinculin [223], NF1 [224], paladin[225], Epb4.1l5 [226, 227] and Marcks [228], all cause neural tube defects.

Shroom3, is a member of one such class of cytoskeleton-associated or actin-binding proteins that is required for neural tube closure [11]. Shroom3 induces apical constriction in neural epithelial cells and is required specifically for hingepoint formation during neural tube closure [195]. A detailed description of individual members of the Shroom family of proteins can be found in the following section.

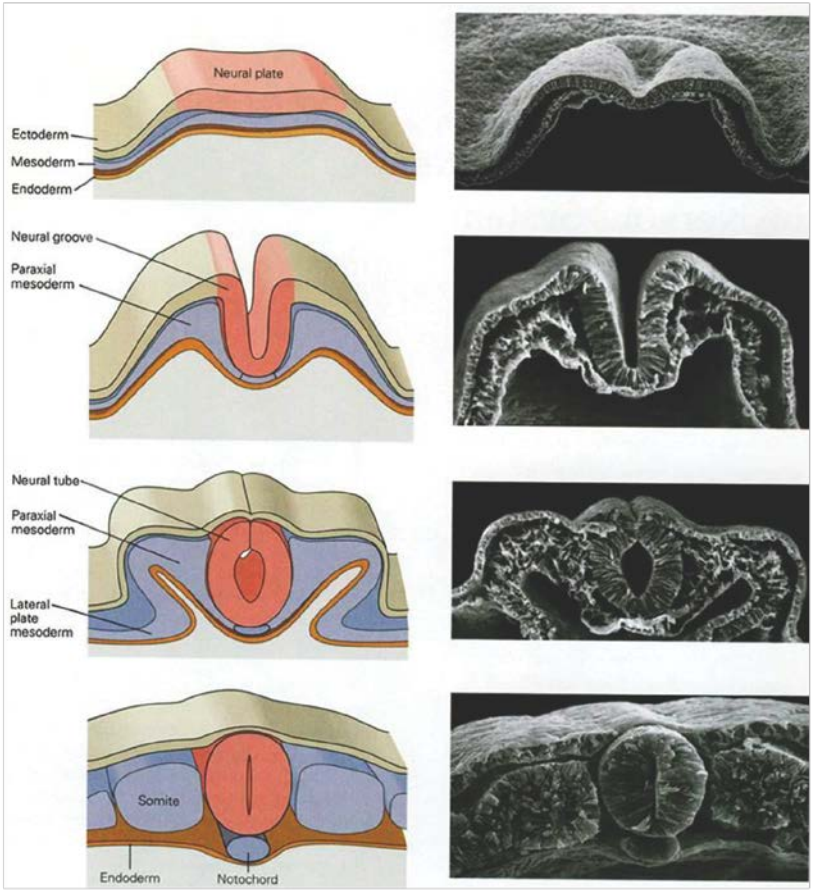

Figure 4: Neural Tube Morphogenesis

Process of neural tube closure a.k.a. neurulation whereby the neural plate undergoes complex morphogenetic movements to bend and form lateral folds which elevate and fuse along the dorsal midline to form a closed neural tube (Smith and Schoenwolf, 1997)

1.4 SHROOM-FAMILY PROTEINS

Shroom comprises a family of actin-binding proteins that are key regulators of the cytoskeleton and are implicated in different developmental processes. There are four family members in vertebrate Shroom which were originally named as Apx [229], Apxl [230], Shroom [11] and KIAA1202 [231] and later renamed as Shroom1, Shroom2, Shroom3 and Shroom4 respectively [232]. All the above mentioned Shroom family members are important mediators of epithelial morphogenesis during development [233].

Shroom proteins are characterized by some signature sequence motifs that are required for its localization and conserved *in vivo* activity. They possess an N-terminal Psd-95/DlgA/ZO1 (PDZ) domain, followed by a serine/proline rich region [10], a centrally located Shroom Domain1 (SD1) (except Shroom 4) and a highly conserved C-terminal Shroom Domain2 (SD2) [11] (Figure 5). The SD1 binds directly to F-actin and causes Shroom3 localization to the adherens junctions of cells whereas the SD2 is required for Shroom-mediated contractile activity [11, 231, 234]. All Shroom proteins identified to date bind both Rock (a serine-threonine kinase) and F-actin [9, 11, 15, 195, 234-236]. Shroom3, the best characterized member from this family has been shown to bind and bundle F-actin and recruit Ena/Vasp proteins to the zonula adherens of epithelial cells to induce apical constriction [11-13, 237]. Other Shroom family members differ in their actin-binding properties and subcellular localization [234]. Shroom2 and invertebrate *Drosophila* Shroom binds to cortical actin while Shroom4 localizes to a punctate cytoplasmic pool of F-actin [234, 235, 238]. Shroom3 can induce apical constriction in polarized epithelial cells whereas Shroom2 or Shroom4 lack this ability [234]. dShroom isoforms can induce varying degrees of apical constriction, depending on their subcellular distribution, and

their ability to bind Rock and assemble organizationally distinct actomyosin networks at specific locales [235]. This unique function of the different Shroom family members can be attributed to its differential subcellular localization conferred by association with distinct compartments of the actin cytoskeleton. However, all Shroom proteins reorganize the actomyosin network via a conserved interaction with another cytoskeleton regulator protein, Rock [5, 235].

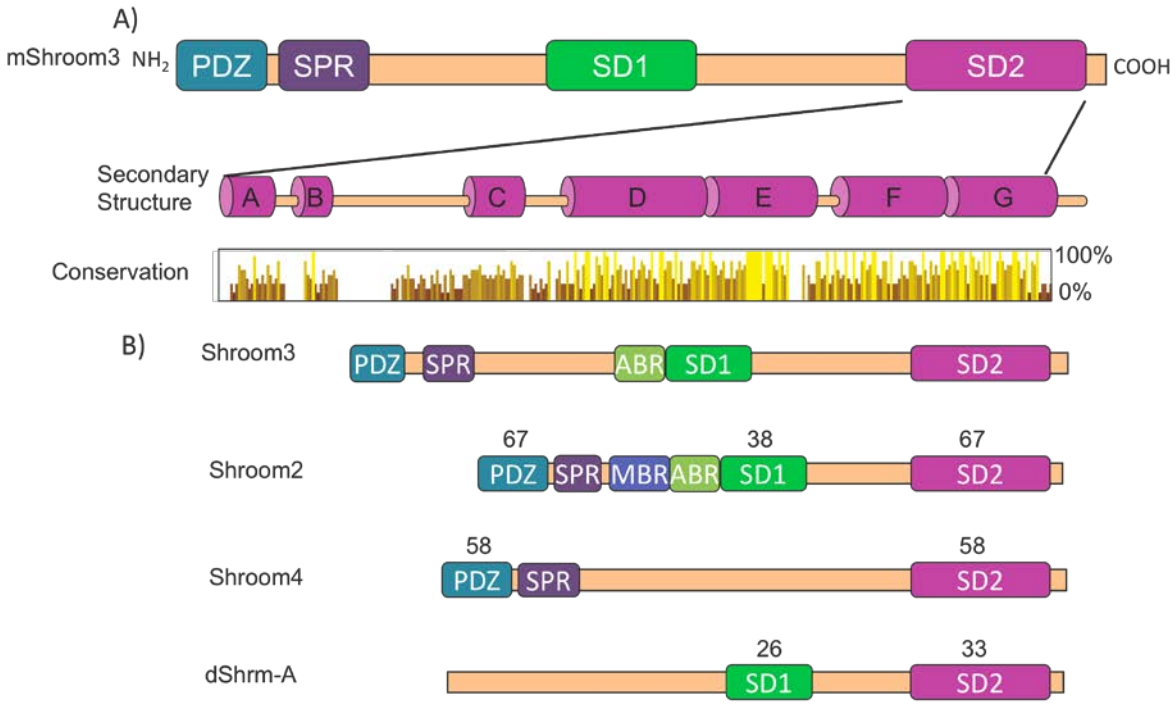

Figure 5: Shroom family of Proteins

A) Schematic representation of different domains of Shroom3, secondary structure prediction and conservation profile of SD2. PDZ: Psd-95/DlgA/ZO1, SPR: Serine Proline rich region, MBR: Myosin Binding Region, ABR: Actin Binding Region, SD1: Shroom Domain 1, SD2: Shroom Domain 2. Secodary structure predicts Shroom3 SD2 to be mostly α-helical represented by magenta bars A-G. Predominance of yellow bars in the sequence conservation

profile of SD2 across different Shroom SD2 constructs represents a highly conserved C-terminal region (helices D-G) and a slightly less conserved N-terminal region (helices A-C).

B) Comparison of domain structure of different Shroom family members. Numbers correspond to percentage identity of mouse proteins to mShroom3. dShroom = *Drosophila* Shroom.

1.4.1 Shroom3

Shroom3 was identified in a gene trap mutagenesis screen in mice where embryos homozygous for this mutant allele exhibited extensive NTDs including exencephaly, acrania, spina bifida, facial clefting and ventral closure defects resulting in organ herniation [11]. In these mutant embryos, the cranial neural folds, instead of converging and fusing along the dorsal midline, 'mushroom' out and have a poorly formed lumen [11]. The importance of Shroom3 in neural tube closure has also been demonstrated in other model systems like *Xenopus* and chick embryos [5] where morpholino mediated knockdown of xShroom3 or over expression of dominant-negative xShroom3 caused NTDs [195]. The neural epithelial cells that form the hingepoint undergo robust apical constriction and it is this cell shape change that ensures proper neural plate bending and elevation of neural folds critical for neurulation. Dominant-negative expression experiments in *Xenopus* have shown that inhibiting Shroom3 activity leads to failure of hingepoint formation, and subsequent errors in neural tube closure [195]. Shroom3 is sufficient to induce apical constriction in polarized epithelial cells in both cell culture and in the *Xenopus* blastula [195]. Apical constriction is thought to be brought about by contractile forces exerted by

a subapical actomyosin network in neural epithelial cells. Shroom3 mutant mice embryos do not show an apical enrichment of myosinII which can therefore explain the loss of apical constriction as well as failure of neural tube closure [15]. The defects caused by Shroom3 mutation however do not affect other apects of cell bahavior like proliferation, cell survival or tissue patterning, thereby demonstrating the critical role of Shroom3 in neural tube morphogenesis in vertebrates [11, 15, 195].

Shroom3 binds to F-actin, localizes to the apical junctional complex (AJC) of MDCK cells and forms a circumferential apical ring at the tip of adherens junctions of neural epithelial cells. In these cells, Shroom can induce apical constriction and apico-basal lengthening without perturbing apical-basal polarity [15, 195, 233]. However, in MDCK cells, not every cell expressing Shroom3 apically constricts, rather some constrict and the neighboring ones expand their apical surface and form taut tight junctions to balance the tension and maintain integrity of the monolayer [15]. However, in a mixed polulation of cells or in spheroidal cysts Shroom3 expressing cells show robust apical constriction and form clusters [15]. The apically constricting cells show an enrichment of actin filaments at the apical surface of cells thereby demonstrating that Shroom can redirect actomyosin distribution and modulate cytoskeletal organization for bringing about cellular morphogenesis [15]. Microtubules are the primary causative agents of apico-basal cell elongation and γ-tubulin serves as the key player in regulating its assembly into robust parallel arrays [120, 239]. In *Xenopus*, Shroom3 regulates γ-tubulin distribution and regulates assembly of robust parallel microtubules that drive apico-basal cell elongation [227].

The SD1 and SD2 motifs of Shroom have unique roles. SD1 is required for Shroom localization mediated by direct binding to F-actin and SD2 is required for apical constriction. The two domains however need to be present in a cis configuration to elicit cell shape change

[195, 234]. The SD2, when expressed by itself is diffusely localized in the cytoplasm and fails to cause apical constriction. However, targeting the SD2 to the apical plasma membrane causes robust apical constriction [15]. These results therefore suggest that Shroom localization is important for its activity.

However Shroom3 is not the only player in bringing about cell shape change. Shroom3 in addition to F-actin requires the molecular motor nonmuscle myosinII and another cytoskeletal regulator, a kinase, called Rock to bring about apical constriction [15]. The SD2 of Shroom3 mediates Rock binding and recruits it to specific subcellular locales. Rock on being activated triggers a phosphorylation event that causes localized activation of myosinII, binding of actin, formation of a contractile actomyosin network at the apical surface of cells and subsequent apical constriction [5, 15]. Ectopic expression of Shroom3 or apically targeted SD2 ellicit apical constriction by redistributing phosphorylated myosin and actin to the apical junctional complex of MDCK cells or apical tip of adherens junctions of neural epitheial cells [5, 15, 234].

Transcriptional regulators of Shroom3 identified to date are few. *Pax-6*, is a transcriptional factor expressed in the lens placode and has been shown to be essential for *Shroom3* expression [12]. *Pitx1* is another transcription factor shown to regulate *Shroom3* expression in Xenopus gut [240, 241]. In zebrafish, Shroom3 is as a transcriptional target downstream of FGF signaling during proneuromast assembly [236]. Some studies have also shown the importance of RhoA and RhoA-GEF Trio as upstream regulators in Shroom3 mediated apical constriction [242].

In addition to expression in the neural epithelium Shroom3 is also expressed in the eye, hindgut, foregut, lungs, kidney and somites [11] and presumably plays an important role in their morphogenesis as evidenced by Shroom3 mutant embryos which display defects in lens placode

invagination, foregut looping, neuronal architecture and function, pulmonary arterial hypertension [10, 12-14, 240, 243], chronic kidney disease (CKD) [23] and heterotaxy in humans [244]. Shroom3 can also act as a scaffold or adaptor protein by binding to Plenty of SH3 (POSH) protein and negatively regulating axon outgrowth [14] or to Mena/Vasp via its EVH1 domain and recruiting it to apical surface of cells [12]. Although Shroom3 has been shown to be required in numerous developmental processes the underlying theme of its function is universal where it redistributes and reorganizes the actomyosin cytoskeleton in conjunction with Rock and brings about cellular and tissue morphogenesis.

1.4.2 Shroom2

Shroom2 was first discovered in a large X-chromosomal deletion associated with the disorder Ocular Albinism TypeI (OA1) [230, 245]. OA1 is characterized by retinal hypopigmentation, visual impairment and defective melanosomes. Shroom2 is upstream of the *OA1* gene but its direct involvement in the disease still remains to be established. The retinal pigmented epithelium (RPE) is a layer of epithelial cells that prevents light scattering within the retina [246]. RPE mediates this function by melanosome pigmentation during retinal development. Many genes have been identified to play a role in melanosome biogenesis as well as its localization. Mutations in these genes lead to human disorders affecting retinal development [247]. xShroom2 has been shown to play a role in RPE development in *Xenopus* [8]. Ectopic expression of Shroom2 in naive epithelial blastomeres causes pigment accumulation at the apical surface. Morpholino mediated knockdown of Shroom2 in the developing eye leads to hypopigmentation and loss of RPE in *Xenopus,* all of which can be attributed to defective melanosome biogenesis and localization [8]. The exact role of Shroom2 in eye development is

still unclear, however it presumably plays an important role in melanosome transport and recruitment to the apical surface of RPE by apical accumulation of γ-tubulin and assembling parallel array of microtubules. This activity of Shroom2 specifically requires Rab27aGTPase [8]. Another human pigmentation disorder Ocular Albinism with Sensorineural Deafness (OASD) for which no causative mutation has been identified to date, also maps to the same X-chromosomal deletion region as *OA1*. The *Shroom2* locus lies within the critical region for these albinism-associated disorders, its loss of function leads to RPE pathologies similar to that found in patients with OA, and Shroom2 is expressed in the retina of mice [234, 248]. So it is possible that Shroom2 is a contributing factor in normal human visual system function [249, 250]. A *Shroom2* mutant mouse to look at the developmental defects associated with Shroom2 loss *in vivo* will greatly advance these studies.

Shroom2 has also been shown to bind to myosin VIIa, an unconventional myosin abundantly present at cell-cell junctions [248]. Mutation in myosin VIIa causes Usher syndrome characterized by congenital deafness and retinitis pigmentosa [251, 252]. Shroom2 binding to myosin VIIa proves dispensable for Shroom2 localization as myoinVIIa mutant *shaker-1* mice exhibit correct Shroom2 localization to tight junctions of hair cells [248, 253]. Since both Shroom2 and myosin VIIa are expressed in the inner hair cells of the ear they serve as interesting candidates in the development of auditory disorders associated with mutations in these genes [254, 255].

Shroom2 is also expressed in the vasculature, gut, neural tube and kidney and other epithelial tissues [8, 9, 233, 234, 248]. In the vascular endothelium Shroom2 binds to cortical actin for proper subcellular localization at the tight junctions. Rock and myosinII have been shown to be critical determinants of vascular architecture as inhibition of myosinII or Rock

promotes endothelial sprouting and angiogenesis [148, 256-258]. This negative regulatory effect of Rock and myosinII is thought to be due to cortical tension that prevents membrane protrusions and migration [148]. Shroom2 also plays a role in promoting contractility and regulating endothelial morphogenesis as depleting Shroom2 in vascular endothelia decreases Rock and myosinII activity and promotes endothelial sprouting and angiogenesis [9].

Previous work has shown that the PDZ domain along with the Serine/Proline rich region is required for efficient Shroom2 localization to tight junction of MDCK cells [234]. Results from a yeast two hybrid screen using the PDZ/SPR region of Shroom as bait against an inner ear cDNA library identified ZO-1 as an interacting partner of Shroom2 in the tight junctions [248]. The mechanism of Shroom2 localization at tight junctions is a little confounding as it is not dependent on the PDZ domain but on the SPR domain, although the PDZ domain is a common domain for scaffolding and tight junction proteins and shares substantial identity between different Shroom proteins [11, 248]. A closer investigation into the specific roles of the different domains of Shroom proteins in Shroom function is necessary for delineating the exclusive and overlapping roles of different Shroom family members.

1.4.3 Shroom4

Gross defects in morphogenesis can cause lethality however subtle defects in morphogenesis during development can still be tolerated though they can cause non-lethal debilitating diseases. Mental retardation is one such example of subtle impairment in neural development affecting1-3% of the world's population [259]. Over 10% of these cases have been attributed to gene mutations or chromosomal abnormalities in the X-chromosome and are collectively termed as X-linked Mental Retardation (XLMR). Of the different gene mutations that have been linked to the

development of XLMR, one of the most prominent categories involves gene products that regulate actin dynamics including several Rho effectors and actin binding proteins [260]. Additionally XLMR patients have shown X-chromosomal aberrations and several mutations within the Shroom4 locus [231]. Since Shroom4 is an actin-binding protein involved in myosinII dependent reorganization of the actin cytoskeleton required during vertebrate adult and foetal brain development, it is quite probable that it plays a crucial role in cognitive function and development [238]. Since Shroom4 is prominently expressed in different embryonic and adult structures like lung, neural epithelium, kidney and developing vasculature, it will be interesting to characterize Shroom4 and its interaction with upstream and downstream effector molecules to elucidate its role in normal vertebrate development.

1.4.4 Shroom1

One of the least characterized member of the Shroom family of proteins is Shroom1. It was identified in *Xenopus* oocytes where it is constitutively expressed and is required for amiloride sensitive sodium channel (ENaC) expression [261]. hShroom1 was recently identified in a yeast two hybrid screen as an interacting protein to the cytoplasmic domain of a membrane bound protein Melanoma Cell Adhesiom Molecule (MCAM) and is involved in linking MCAM to the cytoskeleton [262]. hShroom1 possesses both the signature SD1 and SD2 domains. However, hShroom1 SD2 shows relatively low similarity to the SD2 domain from hShroom 2, 3, 4 or the SD2 of xShroom1 which suggests that hShroom1 is not the human homlogue of xShroom1 [262]. hShroom1 is widely expressed in different tissues including brain, heart, skeletal muscle,

colon, small intestine, kidney, placenta, lung, melanoma cell lines and tumor tissues, however a clear role of Shroom1 in these tissues is yet to be established [262].

1.4.5 Invertebrate Shroom proteins and its evolutionary implications

Shroom proteins have been identified in several invertebrate animal phyla like cnidaria, ascidia, arthropoda and echinodermata, thereby hinting at its early appearance in the animal lineage [234]. The putative Shroom proteins from sea squirt and sea urchin do possess a PDZ domain unlike *Drosophila* Shroom (dShroom). Yeast and *Arabidopsis* do not contain Shroom-like proteins, suggesting that Shroom may be animal specific, however nematodes like *Caenorhabditis elegans* and flatworms *Schmidtea mediterranea* do not possess any Shroom homologs. Phylogenetic analysis of SD2 sequences in vertebrates suggest that a duplication of the ancestral *Shroom* gene gave rise to two homologs, one that became *Shroom4* and the other duplicated again to give rise to *Shroom2* and *Shroom3* [234]. Of all the invertebrate Shroom proteins characterized to date dShroom is the most thoroughly characterized.

dShroom lacks the N-terminal PDZ domain but possesses a loosely conserved central SD1 region and a conserved C-terminal SD2 domain [234, 235]. Two isoforms of dShroom, namely a longer dShroomA and a shorter dShroomB, are detected with dShroomA being the more abundant one. These isoforms exhibit different subcellular localization with dShroomA localizing to adherens junctions and dShroomB to the apical plasma membrane. This differential distribution can be attributed to differences in their N-termini where they employ different mechanisms for localization. dShroomA utilizes its SD1 to directly bind to F-actin and localize to the adherens junctions of cells. Since the shorter dShroomB isoform lacks this actin binding motif it localizes elsewhere [235]. Apart from differential localization, the isoforms exhibit

different functions, for example whereas dShroomA fails to elicit apical constriction in MDCK cells dShroomB induces apical constriction. Overexpression of dShroomA in the fly dorsal ectoderm induces apical constriction by aseembling a cicumferential actomyosin network whereas dShroomB assembles a disorganized actin network at the apical surface [235]. Over expression of either isoform in the *Drosophila* in the dorsal ectoderm leads to improper dorsal closure as a consequence of aberrant apical constriction of cells over expressing dShroom. Similar to vertebrate Shroom, dShroom induced apical constriction is mediated by apical enrichment of activated myosinII and F-actin at the adherens junctions. These Shroom mediated cytoskeletal reorganizations are Rock dependent and *in vitro* studies have indicated a direct interaction between dShroom SD2 and dRock [235]. These results suggest that the Shroom-Rock signaling module has been evolutionarily conserved and may serve as a paradigm for cellular and tissue morphogenesis.

1.4.6 Conserved domains of Shroom implicated in Shroom localization and activity

Shroom proteins are typified by the presence of signature sequence motifs, namely the N-terminal PDZ domain, the centrally located SD1 and the C-terminal SD2. Not all Shroom family members possess the PDZ or the SD1 motifs. However, strikingly all Shroom family members possess the C-terminal highly conserved SD2 and can regulate myosinII activity via this domain. Though only Shroom3 can cause apical constriction in polarized MDCK cells, other Shroom family members acquire the same capacity when their SD2 domain is apically targeted [234]. Shroom2, or Shroom4 by itself fail to elicit actomyosin based apical constriction however chimeric versions of Shroom protein encoding the N-terminal portion from Shroom3 and SD2 from any of the other Shroom proteins can induce apical constriction in MDCK cells. This

suggests that the SD2 from any Shroom members is capable of activating the constriction pathway provided they are localized at the apical surface of cells and the difference in function between the different Shroom members is due to their differential distribution in cells [234]. Shroom directly interacts with Rock via the SD2 and this interaction recruits Rock to specific subcellular locales [5], whereby Rock can phospohrylate RMLC and induce assembly of a contractile actomyosin network. Thus as evidenced above Shroom mediated changes in cell morphology are Rock and myosinII dependent. A detailed discussion of the cytoskeletal regulator Rock, follows next to better understand the interplay of Shroom-Rock and the cytoskeleton in bringing about cellular and tissue morphogenesis.

1.5 RHO-ASSOCIATED KINASE/ROCK

Rho-associated coiled-coil kinase or Rock, is a downstream target of the small GTPase Rho and is involved in reorganization of the actin cytoskeleton [41]. It was identified biochemically as a binding partner for RhoA-GTP [6, 263, 264]. Rock is a serine/thereonine kinase and is characterized by an N-terminal catalytic domain, a central coiled-coil region containing the Shroom Binding Domain (SBD) and the Rho binding Domain (RBD) and a C-terminal Pleckstrin Homology domain [265] split by a cysteine rich region. Structural insights into the above mentioned domains of Rock have shown it to be a parallel coiled-coil homodimer [266, 267].

1.5.1 Rock1, Rock2 and dRok

Vertebrate Rock is encoded by two different genes, Rock1/RockI/Rho-kinase β/p160-Rock and Rock2/RockII/Rho-kinase α. Rock1 and 2 share an overall 65% sequence identity with 92% identity in their kinase domains [41, 264, 268, 269]. Rock1 and 2 are both ubiquitously expressed in most mouse and rat tissues. However, Rock2 is more abundantly expressed in skeletal muscle and brain whereas Rock1 is found in the tissues of the lung, liver, heart, stomach, spleen, kidney, placenta and testis [268]. The C-terminus of Rock has been shown to negatively regulate Rock activity [270]. In that context Rock1 and Rock2 are differentially regulated by either caspase cleavage or granzyme B mediated cleavage of the C-terminus, respectively [271, 272]. Rock1 and 2 have been shown to play different roles during development. *Rock1-/-* mice exhibit defects in closure of eyelids and ventral body wall leading to Eye Open at Birth (EOB) phenotype and omphalocoele [136] whereas *Rock2-/-* mice display intrauterine growth retardation and fetal death due to placental dysfunction [273]. However, it was further shown that backcrossing *Rock2* knock out mice resulted in *Rock1* knock out phenotypes namely EOB along with umbilical herniation [137]. These data suggest that Rock1 and 2 have some specific roles but function redundantly in regulating the assembly of actin bundles essential for closure of the eyelid and ventral body wall in mouse embryos. In support of this, embryos heterozygous for either *Rock1* or *Rock2* showed no abnormal phenotype whereas *Rock1+/- Rock2+/-* compound heterozygotes showed EOB and omphalocoele phenotypes [137]. Also *Rock1-/- Rock2-/-* double mutant mice are embryonic lethal dying between embryonic day 3.5-9.5, but *Rock1-/- Rock2+/-* or *Rock1+/- Rock2-/-* embryos show impaired yolk sac vasculature [274]. Based on the above results and lack of information on Rock isoform specific substrates, it is presumed that Rock1

and Rock2 have largely redundant functions and will therefore be henceforth referred as simply Rock.

Drosophila possesses a single *dRok* gene which is homologous to vertebrate Rock [275, 276]. It contains a similar conserved N-terminal kinase domain which is 74% identical to hRock1, a central coiled-coil domain containing the Shroom binding domain (SBD), Rho binding domain (RBD) and a C-terminal split Pleckstrin homology (PH) domain which is 31% identical to human Rock PH domain. dRok has been shown to be a downstream effector of *Drosophila* Rho1 [275, 276]. dRok is ubiquitously expressed throughout embryogenesis, indicating a significant maternal contribution [275]. Embryos that are zygotic null for dRok do not survive beyond the 2^{nd} instar larval stage. Genetic analysis of loss-of-function mutation of dRok in the form of somatic clones of $dRok^2$ generated by recombination have revealed a role of dRok in Frizzled-Dishevelled, planar cell polarity pathway, to regulate ommatidial rotation during eye development and restrict actin bundle formation in fly wing [276]. dRok has also been shown to be essential for tissue morphogenesis during multiple aspects of oogenesis [277] during dorsal closure, ventral furrow formation and germ band extension [265]. dRok mediates these functions by phosphorylating the RMLC of myosin in *Drosophila* [278], thereby demonstrating the conserved mechanism which dRok employs to direct asymmetric cytoskeletal organization and cell polarity in fruit flies.

1.5.2 Rock domain structure and regulation

The N-terminal kinase domain is the most conserved region with 92% sequence identity between Rock1 and Rock2 [41] (Figure 6). Crystallographic studies have elucidated the structure of the kinase domain to be arranged into a head-to-head homodimer. Each monomer comprises an N-

terminal α-helical domain which aids in dimerization, a bilobed kinase domain, with a typical Ser/Thr kinase fold and a kinase tail. This dimerization domain links the two monomers together and spatially arranges the kinase active sites and regulatory sequences on a common face facilitating access to both kinases simultaneously for interaction with dimeric substrates or inhibitory domains [267]. Rock kinase domain shares close similarity to the PKA kinase domain and resembles the catalytically competent conformation of PKA in that its active sites are arranged similarly to PKA kinase domain active sites [267, 279]. However, unlike PKA, Rock does not exhibit phosphorylation of its serine or threonine residues in the activation loop suggesting a phosphorylation independent mode of activation [267].

Immediately following the kinase domain is an extended central coiled-coil region. Previous work by the Takeichi lab had identified amino acids 698-957 in the central coiled-coil region to physically interact with SD2 of Shroom3 and both Rock1 and 2 can bind equally well to the SD2 [5]. This region was named the Shroom binding domain (SBD) of Rock. Importantly, this region of the coiled-coil region is distinct from the Rho binding domain which spans amino acids 934-1015 [5]. This extended helical coiled-coil region exhibits high sequence conservation across different species thereby suggesting that it serves as a binding platform for Shroom, however it is important to map the boundaries of this domain and identify the critical residues mediating the Shroom-Rock interaction (Figure 6).

In close proximity to the SBD is a 79 amino acid long domain called the Rho-binding Domain (RBD) (amino acids 934-1015) that marks the end of the coiled-coil region of Rock [280]. This region contains a Rho-binding motif and binds specifically to the GTP-bound form of RhoA (Figure 6). The RBD contains two patches, amino acids 934-945 and 1005-1015, that seem to play a role in Rho recognition and binding [280]. The structure of Rock RBD indicates

that it forms a coiled-coil homodimer with differences in the N-terminal and flexible central portions of the coiled-coil but strong similarity in the C-terminal portions between the two Rock isoforms [281, 282]. Mutational studies have identified critical residues in the C-terminal part of the RBD that are important for mediating Rho-Rock interaction [41, 280-282]. The structure of the RhoA-Rock complex shows that the C-terminal portion of the RBD dimer binds to the switch regions of RhoA in a complementary manner and this interaction is primarily mediated by hydrophobic interactions [281].

Rock proteins remain in an auto-inhibited, folded inactive state. This autoinhibitory conformation is thought to be mediated by intramolecular interactions between the N-terminal kinase domain and the C-terminal domain containing the RBD and PH domains of Rock forming a head-to-tail closed, catalytically inactive state [267] (Figure 7). One of the most extensively studied examples of effector activation by small GTPases is the Cdc42-PAK interaction, where Cdc42 binding to PAK induces a conformational change in PAK resulting in its disassociation and phosphorylation to an activated state [283]. The hydrophobic interactions at the Cdc42-PAK interface resembles the hydrophobic interactions between RhoA-Rock [283, 284]. It can therefore be hypothesized that RhoA-GTP binding to Rock relieves the autoinihibitory conformation of Rock and renders it catalytically active. Indeed there is evidence that RhoA-GTP physically interacts with Rock RBD and activates Rock [6, 263]. Though the SBD and RBD of Rock are in close proximity to each other, Shroom and RhoA bind independently and simultaneously to the respective domains without competing with each other [237].

The C-terminal region of Rock contains a Pleckstrin Homology Domain (PH) domain (Figure 6). The structure of PH domain of Rock2 shows a canonical PH fold composed predominantly of β-sheets and is split into two halves by insertion of an internal cysteine-rich C1

domain [7]. Contrary to other known C1 domain proteins Rock lacks the phorbol ester/DAG binding motif and probably does not bind to these proteins [7]. Interestingly Rock2 lacks the signature phosphoinositide-binding motif and instead possesses a flat positively charged surface made up of seven basic amino acids that mediate lipid membrane binding [7]. Thus lipid binding to the PH domain of Rock not only activates it but also localizes Rock subcellularly [269, 285].

The C-terminus of Rock acts as a negative regulator of Rock activity and Rock activation can be brought about by enzymatic cleavage of the C-terminus [271, 272]. The C-terminal PH domain of Rock has been implicated in mediating this autoinhibitory function by establishing intramolecular interactions with the N-terminal kinase domain, rendering Rock catalytically inactive [270]. Rock activation can also be brought about by lipid binding to the PH domain such as Arachidonic acid [256] and phosphatidyl-inositol triphosphate (PIP_3) [269, 285].

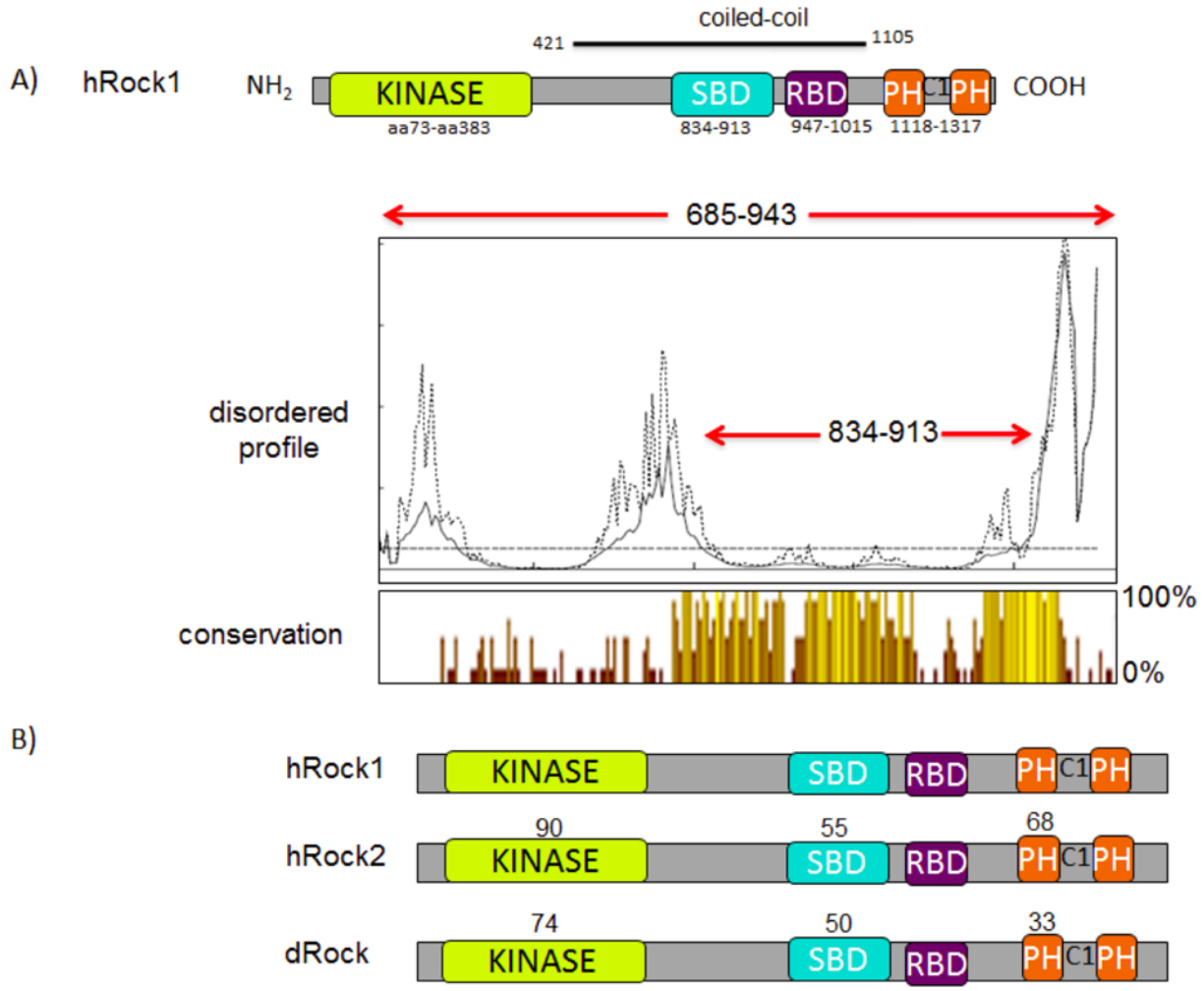

Figure 6: Rho-associated kinase

A) Schematic representation of different domains of Rock, its disordered profile and sequence conservation across SBD. The numbers denote the amino acid residues spanning that domain. SBD: Shroom Binding Domain, RBD: Rho Binding Domain, PH: Pleckstrin Homology Domain. Disordered profile of hRock1 SBD spanning amino acids 685-943. Peaks are representative of disordered regions and troughs are representative of ordered regions. hRock1 SBD fragment spanning amino acids 834-913 is the most ordered and shows

highest sequence conservation represented by yellow bars in the sequence conservation profile.

B) Comparison of domain structure between human Rock and *Drosophila* Rock. Numbers indicate percentage identity between different Rock proteins.

1.5.3 Rock activation

Rock shares 44% sequence identity to myotonic dystrophy kinase and remains in a similar folded autoinhibitory conformation mediated by intramolecular interactions between the N-terminal kinase domain and the C-terminal region rendering the kinase non-functional [270, 286]. This autoinhibiotry C-terminal region comprises of the SBD, the RBD and the PH domain of Rock [266, 270]. Several lines of evidence support the negative regulation of Rock activity by this autoinhibitory C-terminal region. First, deletion or proteolytic cleavage of the C-terminus of Rock constitutively activates Rock [41, 271, 272]. Second, binding of lipids especially Arachidonic acid, to its PH domain [287] relieve this intramolecular inhibition and activate Rock. Third, DynaminI, a membrane regulator protein involved in protein trafficking has also been shown to bind to the PH domain of Rock and induce its catalytic activity [288]. Finally, the C-terminal region of Rock acts as a dominant-negative and inhibits constitutively active form of Rock [270]. Lastly, binding of small effector molecules or proteins to the autoinhibted region [4, 6, 263, 264, 289] induces Rock activity [266].

However, there is also a well known repository of proteins that negatively regulate Rock function. Gem and Rad, GTP binding proteins of the Ras superfamily, bind Rock independently in the central coiled-coil region and function as spatially regulated inhibitors of Rock activity. Though they do not abrogate Rock kinase activity directly, they block the downstream effects of

Rock activation [46]. RhoE, a member of the Rnd subfamily of GTP-binding proteins is another well known inhibitor of Rock. RhoE specifically binds to Rock1, and not Rock2, near the kinase domain and inhibits phosphorylation of its downstream targets thereby abrogating Rock function [47, 290].

Apart from the above mentioned mechanisms of Rock activation there is growing evidence of a Rho-independent mode of Rock activation [15, 195]. Rho binding presumably cooperates with Shroom in bringing about apical constriction but is not required for Shroom-induced apical constriction [242]. Also, Shroom3 and RhoA have seperate binding sites on Rock and can bind to Rock simultaneously *in vitro*, indicating that they do not compete with each other [12]. Relief of intramolecular inhibition and opening up the folded autoinhibitory conformation seems to be the key theme for Rock activation. In addition to the known activators of Rock, it is possible that other protein-protein interactions in the SBD domain or other parts of the coiled-coil region can be potential contributors to Rock activation.

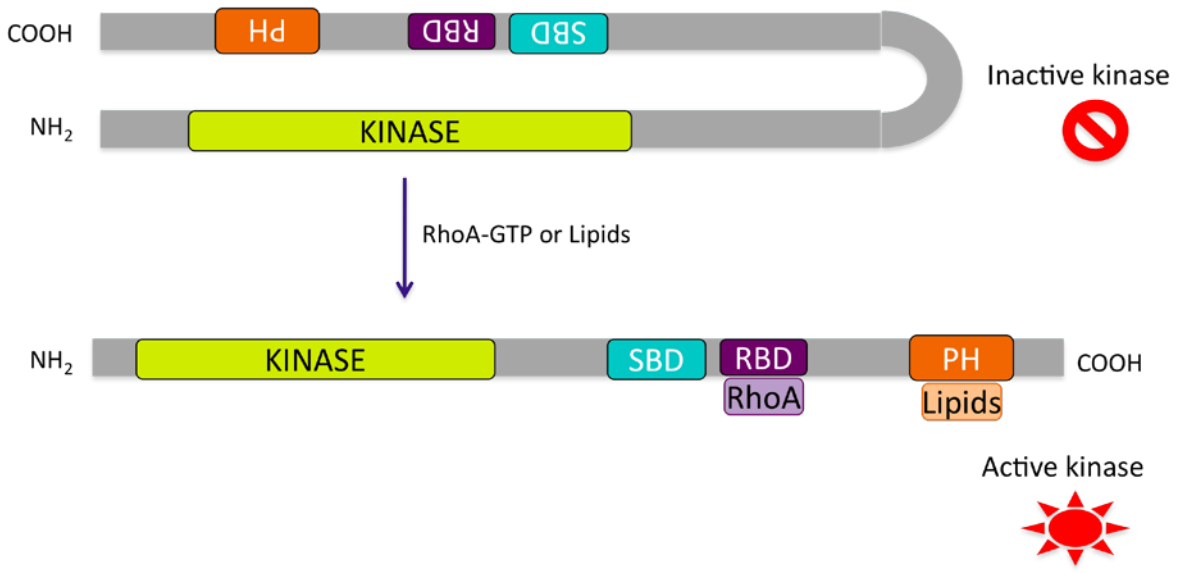

Figure 7: Model of Rock activation

Rock remains in a folded autoinhibitory conformation mediated by intramolecular interactions between the N-terminal kinase domain and C-terminal region. Binding of RhoA-GTP or lipids relieves this inhibition and renders Rock catalytically active

1.5.4 Rock effectors and function

Rock is a major cytoskeletal regulatory protein and it does so by bringing about localized activation of myosinII. The activated myosinII along with actin filaments can remodel the cytoskeletal architecture required for various important cell processes like smooth muscle contraction, formation of stress fibers and focal adhesion complexes, intermediate filament disassembly, neurite retraction, microvilli formation, cytokinesis, cell migration and centrosome positioning [38, 41, 42, 291-298]. Thus the actomyosin network needs to be tightly regulated both spatially and temporally. Phosphorylation at the Thr-18/Ser-19 of the RMLC allows myosinII to interact with actin, assembling an actomyosin network and initiating contraction. On the other hand removal of the phosphate moiety from this residue by myosin phosphatase targeting subunit (MYPT1) renders myosinII inactive [299-301]. One of the key regulatory mechanisms responsible for the induction of actomyosin networks is the fine balance between kinases that phosphorylate RMLC and MYPT1 that inactivates myosinII. Rock lies at the fulcrum of this balance as it can directly phosphorylate RMLC and activate its ATPase activity [4] and also phosphorylates and inactivates MYPT [289, 302-304], thereby increasing the population of activated myosinII in the cell. Rock can also phosphorylate ZIPK which can subsequently phosphorylate RMLC and MYPT, but its contribution in Rock-mediated actomyosin contractility still needs to be investigated [30].

In addition to RMLC and MYPT, Rock phosphorylates other downstream targets that can regulate cytoskeletal dynamics. One such example is LIM kinase (LIMK), a serine/threonine kinase also implicated in cytoskeletal dynamics. Rock phosphorylates and activates both LIMK1 and LIMK2 leading to phosphorylation of its downstream target ADF/cofilin [305]. Phosphorylation of cofilin by LIMK abolishes its actin depolymerizing activity [306]. Cofilin is essential for turnover of actin filaments [307, 308]. Hence there are more free ends of actin, which allows for more polymerization. Thus, Rock phosphorylation of LIMK, results in decreased cofilin activity and stabilizes F-actin. Rock also phosphorylates members of the Ezrin/Radixin/Moesin (ERM) family of proteins which link the actin cytoskeleton to transmembrane proteins in the plasma membrane [309]. The carboxyl termini of these proteins bind actin filaments while the amino termini bind the transemembrane proteins in the plasma membranes using other binding partners. ERM phosphorylation by Rock disrupts its head-to-tail inactive folded conformation and unmasks its protein and actin interaction domains. This facilitates actin filament and plasma membrane association and stabilizing the open conformation. This open active conformation of ERM can then act as an actin filament/plasma membrane linker [309-311]. The Sodium-Hydrogen-Exchanger (NHE-1), another target of Rock, gets activated and regulates Rho-induced stress fibers and focal adhesion formation [312-314]. Adducin, a filamentous protein, is phosphorylated by Rock and binds growing ends of F-actin, arrests polymerization and recruits spectrin. Adducin phosphorylation by Rock enhances its F-actin binding activity and is required for membrane ruffling and cell motility [293, 315]. Rock also phosphorylates several sites in intermediate filament proteins such as Vimentin, glial fibrillary acidic protein (GFAP) and neurofilament L protein (NF-L) to induce depolymerization and filament disassembly during cytokinesis [294, 296, 316]. Rock phosphorylation of other

actin-binding proteins like eukaryotic elongation factor 1α, myristylated alanine-rich C kinase substrate (MARCKS) and calponin inhibits their actin-binding function [317-320]. Rock mediated phosphorylation of neuronal proteins such as CRMP2 and other receptors facilitate axon outgrowth, growth cone collapse and cell migration [321-326].

Thus Rock has a plethora of downstream effector molecules mediating different functions but playing the central role of regulating the cytoskeletal dynamics in the cell to affect changes in cell shape, behavior and tissue architecture. Shroom has been shown to directly interact with Rock and this interaction regulate epithelial morphogenesis. A more detailed description of the Shroom-Rock signaling module is discussed next.

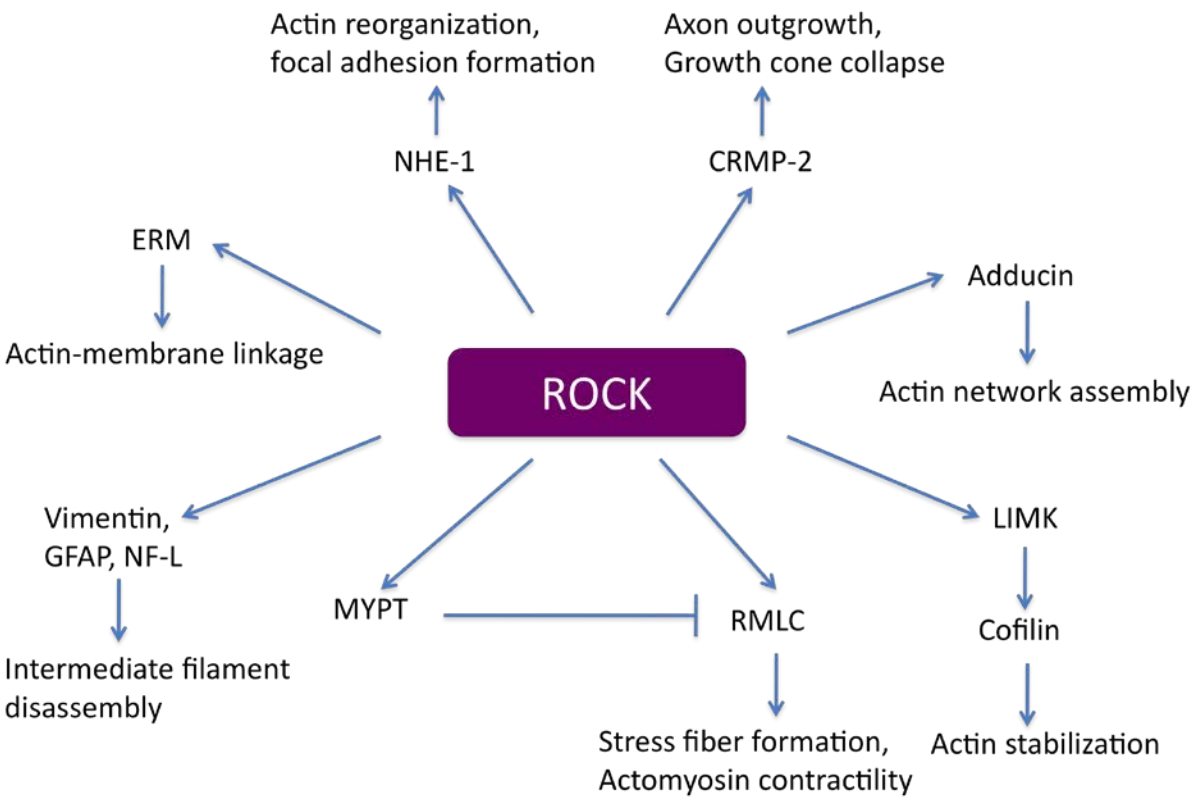

Figure 8: Rock effectors and their function

Schematic representation of different Rock effectors and their role in the regulation of cytoskeletal dynamics

1.6 SHROOM-ROCK SIGNALING PATHWAY IN CELLULAR AND TISSUE MORPHOGENESIS

Vertebrate Shroom family of proteins consists of Shroom1-4, whereas most invertebrates contain a single *Shrm* gene [232]. Each Shroom family member has been implicated in regulating various morphogenetic events during embryonic development, including neural tube closure [11], remodeling of the vasculature [9], eye development [8, 12], gut morphogenesis [10, 13], neuronal architecture and function [14, 231], ENaC channel regulation [261], renal function [23], arterial hypertension [243] and heterotaxy in humans [244]. Though not all Shroom proteins possess all the signature sequence motifs, the highly conserved C-terminal SD2 is shared among all members and it is this domain that physically interacts with Rock. It is presumed that all the above mentioned developmental processes are orchestrated by this Shroom-Rock pathway and it is highly conserved between vertebrates and invertebrates [234]. Thus we think that a Shroom-Rock signaling module operates in cells undergoing cytoskeletal remodeling and this forms the basis for epithelial morphogenesis during embryonic development.

The Shroom-Rock signaling pathway entails Shroom directly binding to F-actin. This interaction recruits Shroom to the correct subcellular locale. Shroom then binds to the central coiled-coil SBD of Rock via its SD2. This Shroom-Rock interaction causes subcellular localization of Rock. Rock, once localized and activated, phosphorylates RMLC and MYPT, thereby positively increasing the population of activated myosinII in cells locally. This localized

phosphorylated myosinII then binds to F-actin and forms a contractile actomyosin network. All Shroom proteins can regulate cell morphology and tissue architecture by regulating the subcellular distribution of actomyosin networks and use this to elicit apical constriction or cortical contractility [9, 15].

Shroom function is dependent on its correct subcellular localization as well as its ability to bind Rock. Shroom3 mediated apical constriction is dependent on its ability to bind both F-actin and Rock [5, 15]. Shroom3 binding to F-actin targets it to the zonula adherens of polarized epithelial cells. Shroom3 can then bind to Rock via its SD2 and recruit it to the apical surface of cells. This results in Rock- mediated localized activation of non-muscle myosinII as described above. As a result, the subcellular distribution of the actomyosin network within these cells is reorganized to form an apically positioned contractile ring. This contractile actomyosin ring then exerts tensile forces at the apical surface of the cell, causing the apical surface to shrink or constrict transforming a columnar shaped cell into a wedge shaped one. When this cell shape change occurs synchronously in a group of cells, it facilitates bending or invagination that ultimately leads to tissue remodeling.

Though much is known about the Shroom-Rock pathway, their role in developmental processes and its regulation of the cytoskeletal dynamics to bring about epithelial morphogenesis, a clear understanding of the molecular mechanism of Shroom-Rock interaction still evades us. Mapping the binding domains in both Shroom and Rock that mediates this interaction and determining the stoichiometry would thus prove extremely helpful in delineating the mechanistic details of Shroom-Rock interaction and Rock-myosinII regulation. Also, identification of the critical binding interface of Shroom and Rock will provide structural insights of the role of these residues in protein-protein interactions and Rock dimerization. An

interesting facet to this signaling pathway is whether the Shroom-Rock interaction is sufficient for Rock activation or whether Rho binding is required for the same. Rock has been shown to undergo both a Rho-dependent [242] and Rho-independent mode of activation [15, 195, 327] and since it is involved in a multitude of cell processes, a clear understanding of the different steps of Rock activation and localization will prove beneficial for designing Rock inhibitors for therapeutic purposes.

In order to elucidate the mechanistic details of the Shroom-Rock interaction, my project uses a variety of biochemical and cell based assays to dissect the molecular nature of this interaction. By adopting a multipronged approach to investigate the molecular dynamics of Shroom-Rock interaction, we hope to establish this evolutionarily conserved signaling module as a paradigm for cellular and tissue morphogenesis.

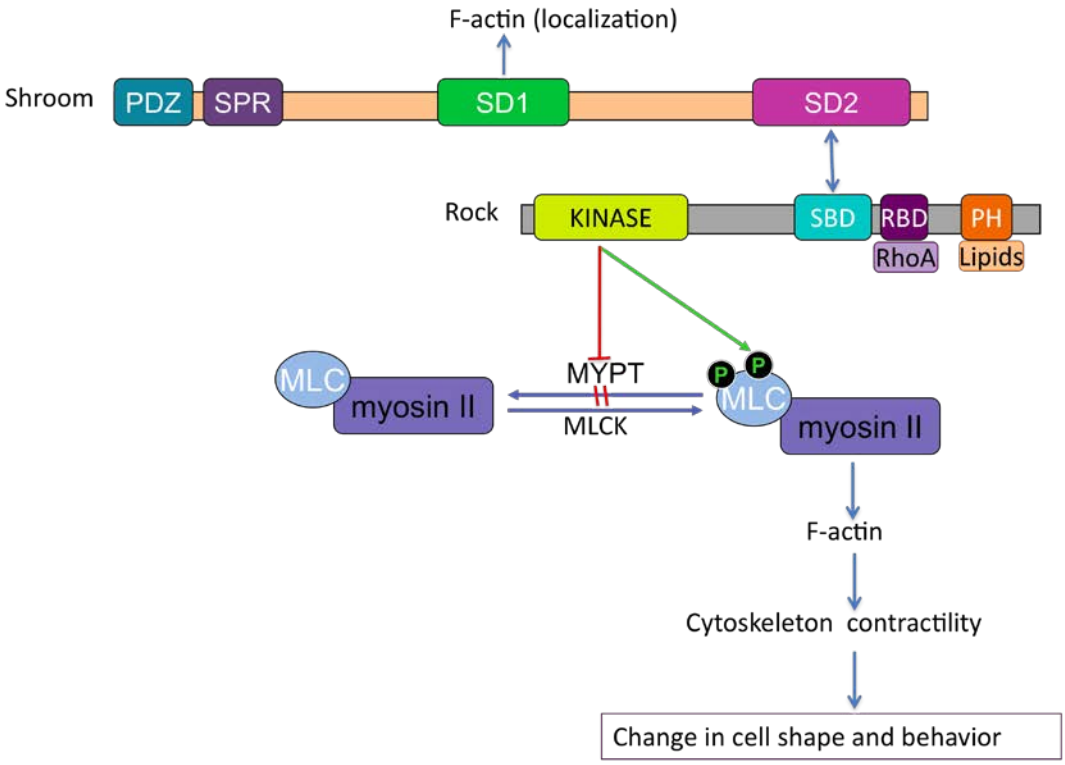

Figure 9: Shroom-Rock pathway in cellular morphogenesis

Schematic representation of the Shroom-Rock signaling pathway operating in cells to bring about cellular morphogenesis

1.7 DISSERTATION AIMS

The Shroom-Rock pathway is essential for numerous developmental process in both vertebrates and invertebrates. Though much is known about this pathway, a clear understanding of the molecular mechanism of this interaction still remains elusive. It has been clearly established that different Shroom members all mediate binding to Rock via its SD2. The SD2 physically interacts with the central coiled-coil SBD of Rock, however the mechanistic details of this interaction have not yet been characterized. My project aims to understand the molecular mechanism, stoichiometry and global consequences of this interaction.

Also, growing evidence suggests that Rock can undergo a Rho-independent mode of activation during Shroom induced apical constriction. We hypothesize two models of Rock activation. First, we suggest Shroom-Rock interaction proves sufficient for relieving the intramolecular inhibition and rendering Rock catalytically active. Second, Shroom-Rock interaction is required for Rock localization and Rock binding to other effector molecules, mainly RhoA, causes Rock activation. In order to dissect the intricacies of Shroom-Rock and Rho-Rock interaction it becomes imperative to map the binding domains mediating this interaction, namely Shroom SD2 and Rock SBD.

To this end, I identified amino acid residues in both Shroom SD2 and Rock SBD that are critical for mediating this interaction and analyzed the consequences of disrupting this interaction in embryonic development, especially neural tube morphogenesis. I then characterized the significance of the Shroom-Rock interaction in Shroom induced apical constriction and their contributions in Rock localization and activation. I used molecular biology techniques and adopted biochemical and cell based assays to analyze the molecular mechanism of Shroom-Rock interaction. These experiments were guided by structural studies performed by our collaborators, the VanDemark lab, and by the use of a novel Shroom SD2 mutant obtained from a genome wide ENU mutagenesis screen.

2.0 CHARACTERIZING THE SHROOM SD2 DOMAIN TO IDENTIFY RESIDUES CRITICAL FOR MEDIATING SHROOM-ROCK INTERACTION, SHROOM DIMERIZATION AND APICAL CONSTRICTION

2.1 INTRODUCTION

Shroom proteins are key regulators of cell morphology and tissue architecture. Shroom has been implicated in a variety of developmental processes including neural tube closure [11, 195], lens placode invagination, melanosome biogenesis [8, 12], gut morphogenesis [10, 13, 240], neuronal architecture and function in mice [14], lateral line morphogenesis in zebrafish [236] and has been linked to chronic kidney disease [23], pulmonary arterial hypertension [243] and heterotaxy in humans [244]. Shrooms proteins possess different domains that are required for its localization and activity. The central SD1 binds directly to F-actin and this interaction is necessary for Shroom3 localization to the apical surface of cells [234]. Though Shroom family members differ in the presence or absence of some sequence motifs, the C-terminal SD2 is highly conserved and is required for activity of all tested Shroom family members.

Shroom3 bind to Rock via its SD2. This Shroom-Rock interaction recruits Rock to the zonula adherens of cells [5] where it phosphorylates the RMLC and locally activates myosinII. The activated myosin then binds to actin to form a subapical contractile actomyosin meshwork in the cell. Tensile forces exerted by this contractile network at the cell circumference leads to shrinking of the apical region of the cell, transforming columnar shaped cells to wedge shaped

form. This Shroom3 induced apical constriction is both Rock and myosinII dependent [15]. In order to elucidate the molecular mechanism and dynamics of the Shroom-Rock interaction it is important to define the structure of these proteins and map the residues critical for mediating this interaction. In collaboration with the VanDemark lab we identified the critical amino acid residues in SD2 that are required for Shroom-Rock interaction and the role of this interaction in regulating cell morphology.

Analyzing the conservation profile of SD2 from Shroom proteins from different species revealed a core region of SD2 that is conserved. I selected for amino acid residues that were highly conserved in this region for site-directed mutagenesis to create Shroom SD2 mutants. To this end I was guided by structural data from the *Drosophila* Shroom SD2. The dShroom SD2 structure showed a novel fold and was a three segmented, antiparallel coiled-coil dimer. I generated multiple mouse Shroom3 SD2 mutants and tested their ability to bind Rock, cause apical constriction and activate the myosinII pathway. Using mutational analysis and other biochemical and cell based assays I successfully identified conserved surface exposed patches on the SD2 that are critical for Rock binding and apical constriction. Also we have shown Shroom dimerization to be important for Rock binding and Shroom function. Thus we have been successful in mapping the binding domain of Shroom and identifying the critical amino acid residues of the SD2 that mediate Shroom-Rock interaction [328].

2.2 RESULTS

2.2.1 Structure of Drosophila Shroom SD2

The VanDemark lab solved the structure of the core dShroom SD2 spanning amino acid residues 1393-1576 in dShroomA. Crystallization trials set up with this purified homogeneous protein produced cube like crystals that diffracted at 4Å. These crystals were subjected to multiple optimization trials to ultimately produce high quality crystals that diffracted at 2.7Å. Using these crystals an electron density map was generated using Coot software and the structure of dShroom SD2 was determined.

The dShroom SD2 structure revealed a three-segmented anti-parallel coiled-coil homodimeric conformation [328]. In each monomer there is a coiled-coil helical segment that is twice the length of the other two short helical segments (Figure 10). The long coiled-coil segments wrap around each other in a dimer to form the ‘body’ segment whereas the short helices wrap around each other to form the ‘arm’ segments. A predominance of hydrophobic residues observed at the junctions between the body segment and the arm segment are thought to play a role in stabilizing the arm segments in this conformation. Since no structural homologs were found for the dShroom SD2, this arrangement of three anti-parallel coiled-coil segments appears to be unique [328].

The dShroom SD2 crystal exhibits an extended surface with several conserved patches that might mediate protein-protein interactions by providing a binding interface to its partner. Extensive coiled-coil interactions in the protein form a dimerization interface with interiorly buried residues composed of conserved leucines and isoleucines characteristic of leucine zippers. These residues are predicted to function in either Shroom dimerization or intramolecular

interactions required for Shroom activity. A unique feature of this structure is the co-existence of symmetry as well as asymmetry in the protein. The protein displays internal symmetry with one half dimer possessing all the amino acid residues that comprise one whole monomer and thus, each half dimer is structurally identical to the other half. The protein is shaped asymmetrically such that the arm segments are rotated away from each other due to a twist in the body segment of the dimer. We term the region separating the left and right halves of the dimer as the symmetry point and it exhibits a predominance of glycine and proline residues making it highly disordered. This geometrical uniqueness of the protein poses important biological implications for Shroom function and activity as it now presents two potential binding sites for Rock on opposite faces of the dimer. Therefore, guided by the dShroom SD2 crystal structure, I designed mouse Shroom3 SD2 substitution mutants and tested their function and activity.

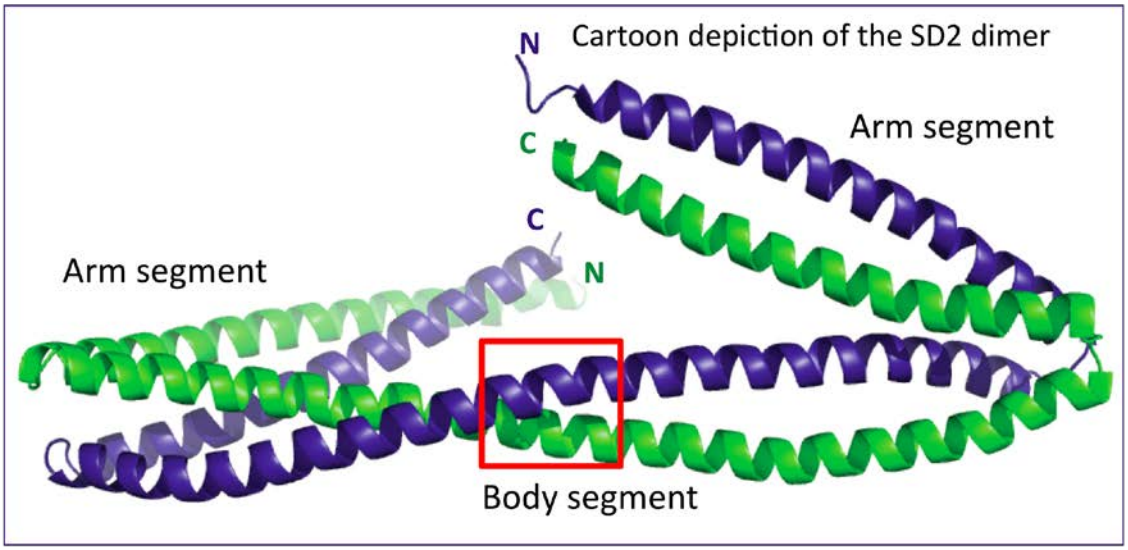

Figure 10: Ribbon diagram of dShroom SD2 protein

dShroom SD2 exhibits a unique three segmented anti-parallel coiled-coil structure. It consists of a long coiled-coil body segment flanked by two shorter arm segments that wrap around each other in the dimer. Each monomer is represented by a different color.The symmetry point location in the dimer is indicated by a box.

2.2.2 Making mShroom3 SD2 mutants

Since the dShroom SD2 exhibited an extended conformation with invariant residues and conserved patches broadly distributed on the protein, a major concern was the ability to develop assays that were sensitive enough to record any perturbations caused by single amino-acid substitutions in the SD2. These small changes in the SD2 might not destabilize the Rock binding interface or the dimerization interface enough to produce measurable or observable effects. In order to overcome this problem we used sequence conservation as well as structural data to identify regions which might have the greatest impact on Shroom structure and function (Figure 11A). We designed multi-residue variants that were either surface exposed, named Surface Cluster mutants (SC), or interiorly buried residues at the dimerization interface named Homodimerization mutants (HD) (Table 1) [328]. We hypothesized that the SC mutants target the Rock-binding interface and mutating them would disrupt Rock binding but not affect Shroom dimerization. Three patches of highly conserved residues were selected as potential candidates for SC mutations to be tested (Figure 11B). The HD mutants on the other hand targeted residues which were interiorly buried with the assumption that they are involved in Shroom dimerization and the structural integrity of the dimer but do not directly affect the Rock binding site. Based on sequence conservation and structural data, two highly conserved regions were selected as potential candidates mediating dimerization (Figure 11B). I created three SC mutants (one in the

arm segment and two in the body segment of the dimer) and two HD mutants (one in the body segment and the other in the arm segment) in mouse Shroom3 SD2 by site-directed mutagenesis (Table1). I selected for correct mutant clones based on the sequencing results and we tested them for their ability to bind Rock or dimerization [328].

Mouse Shroom3 SD2 spanning amino acids 1372-1986 in pCS2-endolyn-Shroom3 eukaryotic expression plasmid was used as a template to create the different SD2 mutants by site-directed mutagenesis. Since Shroom localization is dependent on F-actin binding via its SD1 domain, using only the Shroom SD2 domain might give us erroneous results stemming from its mislocalization in the cell. Therefore, a chimeric version of the protein consisting of Endolyn and Shroom3 SD2 was used to ensure constitutive targeting of Shroom to the apical surface of cells irrespective of its actin-binding capacity [15]. Endolyn is a transmembrane protein that trafficks to the apical plasma membrane in MDCK cells and can be over expressed without altering cell morphology [15]. These five different SD2 mutants were transiently transfected in polarized MDCK cells grown as a monolayer in transwell filters and then immunostained to detect Shroom3 and ZO-1 using specific antibodies. For *in vitro* biochemical studies the mutated sequence encoding amino acids 1562-1986 was cloned from the Endolyn-Shroom3 vector into the pGex-2TK expression vector, transformed into *E.coli* CodonPlus (RIPL) cells and expressed to produce recombinant proteins, which were subsequently purified using glutathione beads.

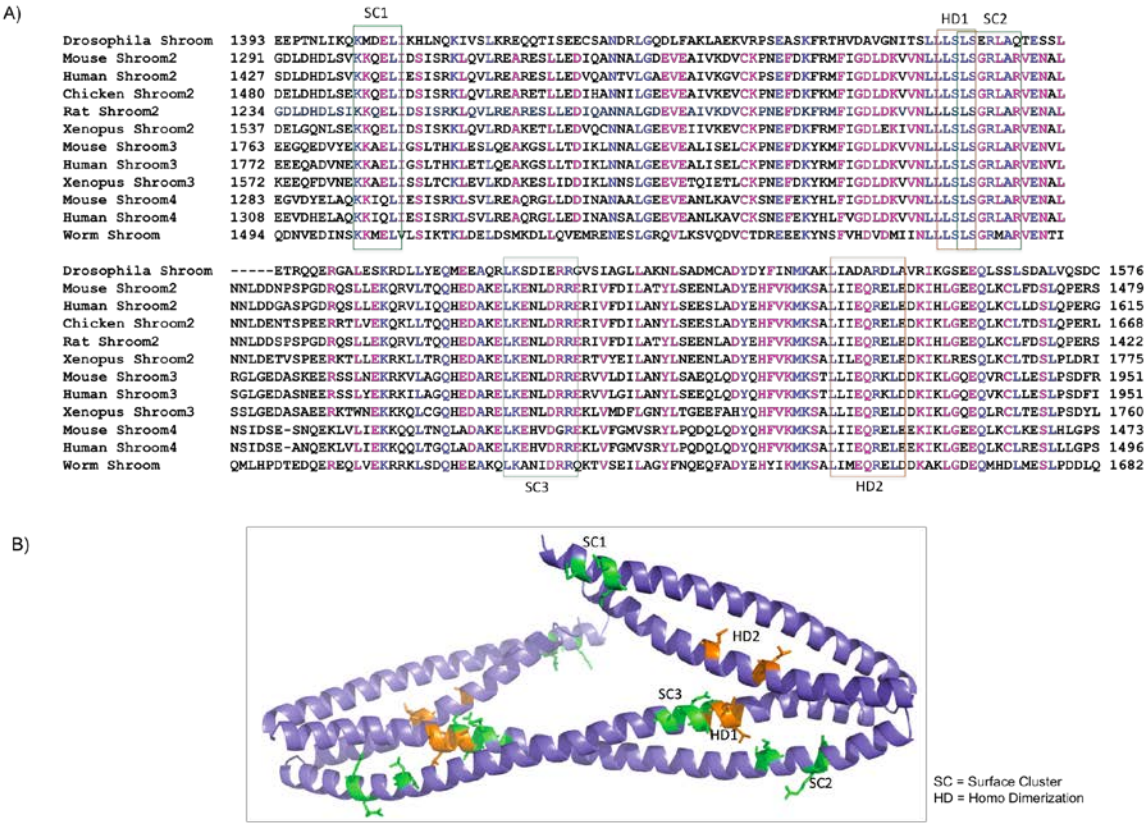

Figure 11: Alignment of Shroom SD2 protein sequence and SD2 mutants created

A) Sequence conservation of Shroom SD2 across different species using CLUSTAL W. Invariant residues are highlighted in blue, while highly conserved residues are highlighted in pink. Sequence of each SC and HD mutants are indicated by boxes.

B) Ribbon diagram of dShroom SD2 dimer showing the SC and HD mutants created.

Table 1: Sequence and position of mouse Shroom3 SD2 mutants created

Name	mShroom3 SD2 mutant sequence	Position in the dShroom SD2 structure
SC1	^{1766}KKAEL^{1770} ➔ ^{1766}AKARA^{1770}	Surface exposed
SC2	^{1840}SLSGRLA^{1846} ➔ ^{1840}ALEADLE^{1846}	Surface exposed
SC3	^{1878}LKENLDRR^{1885} ➔ ^{1878}AAENLDDA^{1885}	Surface exposed
HD1	^{1832}LLSL^{1835} ➔ ^{1832}AASA^{1835}	Interiorly buried
HD2	^{1915}LLIEQRKL^{1922} ➔ ^{1915}ALIEQAKA^{1922}	Interiorly buried

2.2.3 Residues in central coiled-coil body segment of Shroom SD2 are important for Shroom-Rock interaction

In order to test the ability of the Shroom SC and HD mutants to bind Rock, we performed an *in vitro* pull down assay using glutathione beads. The Shroom SD2 mutant proteins were expressed as GST-fusion proteins and added to glutathione beads. Purified human Rock SBD protein was added in solution and incubated at room temperature for 1 hour and the complex resolved on a 12% SDS- PAGE gel and then stained with Coomassie Blue. The wild type Shroom3 SD2 protein can bind Rock and both protein species are detected in the bead fraction. The SC1 mutant behaves similarly to WT SD2 in being able to bind Rock, however all other SC and HD mutants fail to bind Rock and Rock can be seen only in the supernatant fraction with Shroom3 in the bead fraction (Figure 12). Thus the data clearly suggests that the surface exposed residues in the Shroom3 SD2 body segment SC2 and SC3 play a role in Rock binding whereas the surface

exposed residues in the SD2 arm segment, SC1, seem to be dispensable for Rock binding [328]. The HD mutants also fail to bind Rock, indicating that disrupting the Shroom-Shroom dimerization interface affects Shroom's ability to bind Rock and implies that the Rock-binding interface on Shroom SD2 is composed of residues from both chains of the dimer. Alternatively the HD mutant protein might be non-functional due to its structural deformity and proteolytic sensitivity and hence fail to bind Rock.

Our data suggest that the Rock-binding interface is molecularly conserved with surface exposed residues within the SD2 body segment playing a critical role in Rock binding whereas the conserved residues in the arm segment are dispensable for Rock binding.

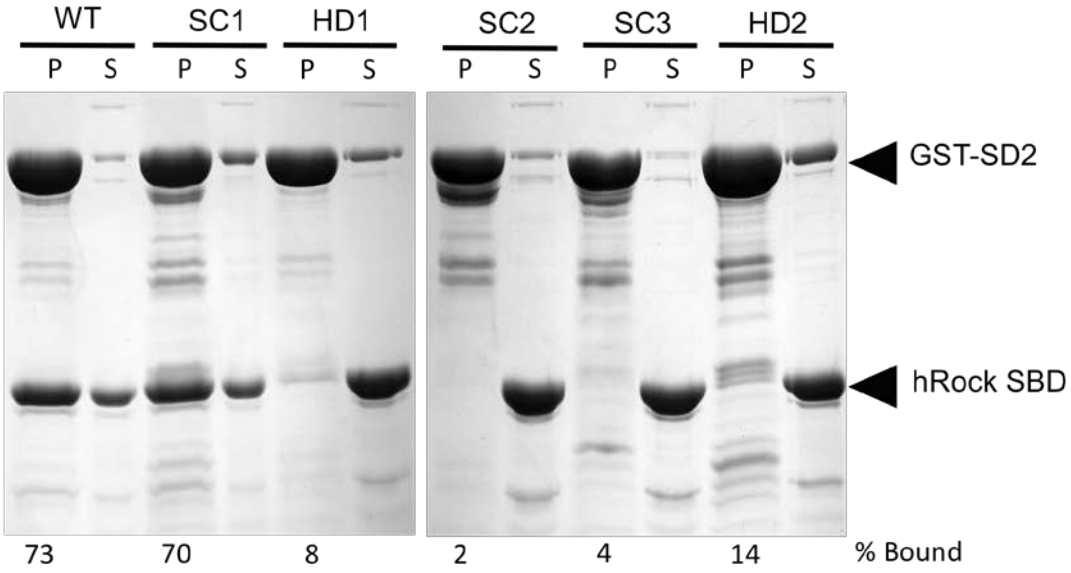

Figure 12: The Rock binding interface in Shroom SD2 is composed of surface exposed residues in the body segment of the SD2 protein

GST-tagged versions of WT or mShroom SD2 mutants were tested for their ability to bind Rock via an *in vitro* pull-down assay. WT or mutant SD2 proteins were bound to Glutathione beads and Rock added in solution. The ability of the WT or mutant Shroom SD2 proteins to bind Rock was assayed by resolving the pellet and supernatant fraction to detect

bound complexes by SDS-PAGE. Quantification of the amount of Rock bound to Shroom was assessesed using ImageJ software and represented as percentage. This experiment was performed by Ryan Rizaldy.

2.2.4 Interiorly buried residues in Shroom SD2 are required for Shroom dimerization

These mShroom3 SD2 mutants were next tested for their dimerization ability with the prevailing hypothesis that the surface exposed residues are probably required for mediating Shroom-Rock interactions whereas the interiorly buried residues are required for dimerization and do not affect the Rock binding interface. All five different GST-tagged mShroom3 SC and HD mutants were bound to glutathione beads and untagged mShroom3 SD2 added in solution and incubated for 1 hour at room temperature. The bound complexes were then resolved on a 12% denaturing SDS–PAGE gel and stained with Coomassie blue. As expected, the WT mShroom3 SD2 protein bound to Shroom3 SD2 to form dimers whereas the HD mutants failed to dimerize. The SC mutations on the other hand did not impair Shroom3 dimerization (Figure13). Similar results were obtained with dShroom SD2 mutants using *in vitro* pull down assays, crosslinking assays and native gel mobility shift assays [328]. Since HD mutants failed to bind Rock as well as dimerize, our data suggests that Shroom dimerization is critical for Rock binding but not the other way around.

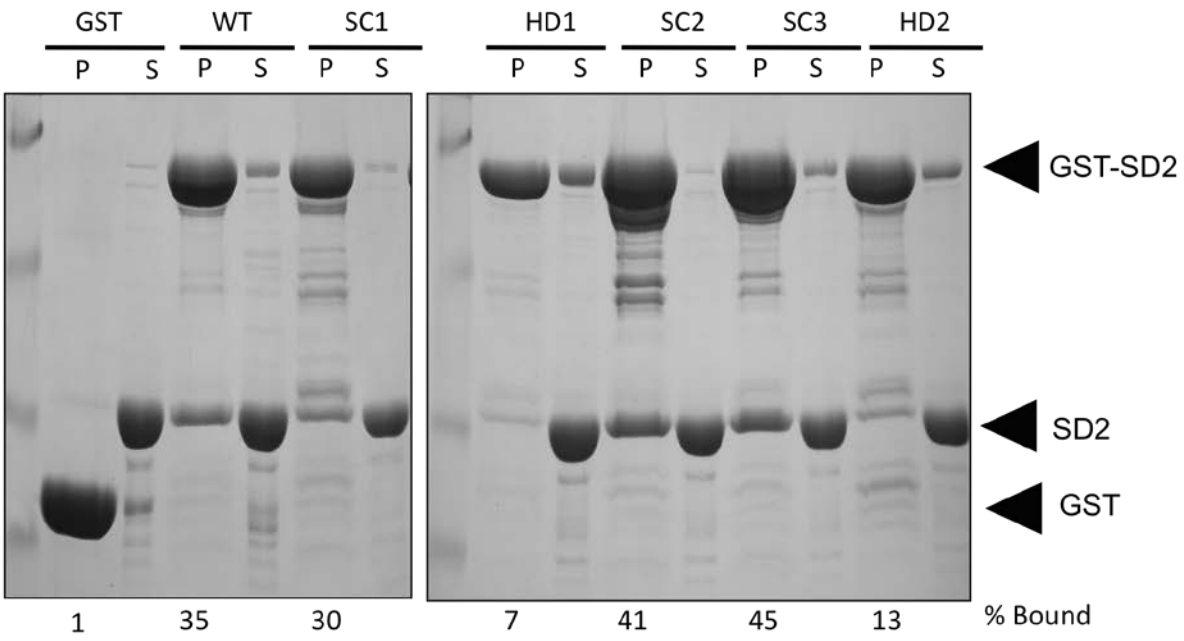

Figure 13: Shroom homodimerization mutants fail to dimerize and abrogate Rock binding

GST-tagged versions of Surface Cluster or Homodimerization mutants were tested for their ability to bind untagged mShroom SD2 using a GST-pull down assay. As evident, the HD mutants fail to dimerize whereas the dimerization ability of SC mutants remain unaffected. Quantification of the amount of untagged Shroom bound to GST-Shroom was assessesed using ImageJ software and represented as percentage. This experiment was performed by Ryan Rizaldy.

2.2.5 Shroom-Rock binding is essential for apical constriction and myosinII activation

In order to assess the importance of these amino acid residues in the Rock-binding interface or dimerization interface in mediating Shroom induced changes in cell morphology, we transiently transfected WT or mouse Shroom3 SD2 mutants in a pCS2-endolyn-Shroom3 eukaryotic plasmid into polarized MDCK cells. MDCK cells were grown as a monolayer on transwell filters and 24 hours post transfection, cells were stained with tight junction marker ZO-1 and anti-Shroom3 antibody to assess Shroom3 expression and apical constriction (Figure 14A). The WT as well as Shroom3 mutant proteins were apically localized in the cell as evidenced by Shroom3 staining and distribution of ZO-1 indicative of apical boundaries of the cell. In accordance with the *in vitro* results, the SC1 mutant that retained the ability to bind Rock showed apical constriction, whereas the remaining SC and HD mutants that failed to bind Rock, also failed to elicit apical constriction in MDCK cells (Figure 14A). Western blot analysis using anti-Shroom antibodies confirmed comparable expression of WT and mutant mShroom3 SD2 proteins, thereby suggesting that the phenotypic effect of loss of apical constriction is due to disruption in the Rock-binding interface of Shroom and not due to insufficient protein expression or protein degradation (Figure 14B).

Apical constriction is brought about by localized activation of myosinII by Rock. Phosphorylation of the regulatory myosin light chain at Thr-18/Ser-19 is the key step of myosinII activation and is considered as a readout of activated myosinII. This phosphorylated RMLC along with F-actin forms a contractile actomyosin network at the apical surface of the cells that exerts tension to apically constrict the cell surface. In order to assess whether these mShroom3 surface cluster or homodimerization mutants are capable of activating the Rock-myosinII

pathway mShroom3 WT or SD2 mutants were transiently transfected into MDCK cells and stained with anti-Shroom antibody and pMLC to assess for an enrichment of activated myosinII in cells expressing Shroom proteins. Confirming our *in vitro* binding results and apical constriction assay, the SC1 mutant behaved similarly to WT in exhibiting apical recruitment of activated myosinII at the apically constricted cell surface whereas all other surface cluster or homodimerization mutants that failed to induce apical constriction failed to show apical enrichment of pMLC (Figure 14C) [328]. Collectively, the data suggest that Rock binding is critical for Shroom induced apical constriction and this apical constriction activity is dependent on both Rock and myosinII. Thus alterations that disrupt the Rock-binding interface or the dimerization interface in Shroom negatively affect its apical constriction activity.

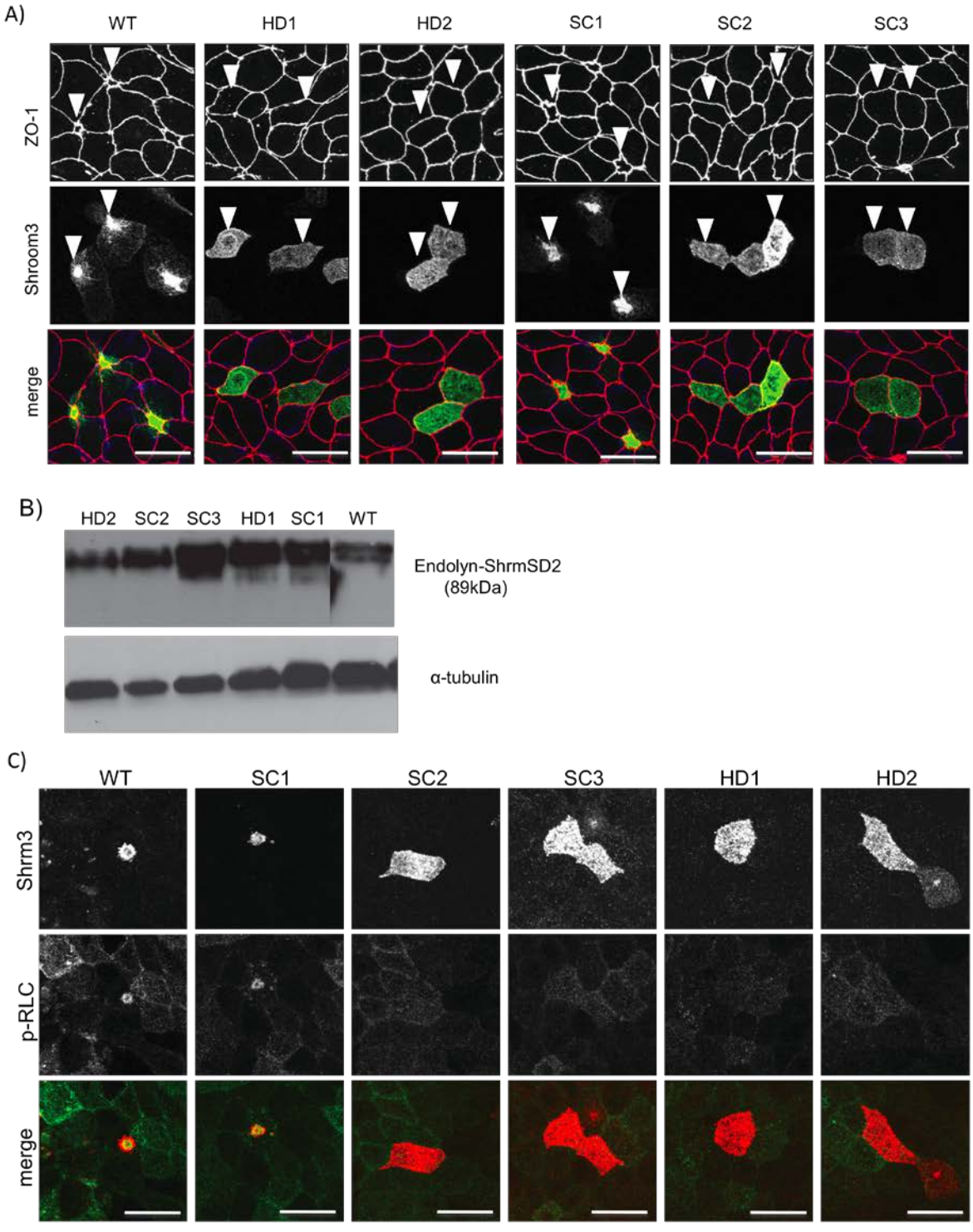
A)
WT
HD1
HD2
SC1
SC2
SC3
ZO-1
Shroom3
merge
B)
HD2
SC2
SC3
HD1
SC1
WT
Endolyn-ShrmSD2
(89kDa)
α-tubulin
C)
WT
SC1
SC2
SC3
HD1
HD2
Shrm3
p-RLC
merge

Figure 14: Rock binding is essential for Shroom mediated apical constriction

A). Endolyn tagged WT or mutant Shroom3 SD2 were transiently transfected in MDCK cells and stained for ZO-1(red) and Shroom3(green). The cells expressing either WT or mutant Shroom3 proteins are indicated by arrow heads. Scale bar 20 μm.

B). Western blot from cell lysates transfected with either WT or mutant mShroom3 SD2 was performed using anti-Shroom3 antibody. Blot was reprobed using anti-tubulin antibody to verify equal protein loading.

C). Endolyn tagged WT or mutant Shroom3 SD2 were transiently transfected in MDCK cells and stained for pMLC (red) and Shroom3 (green). Apart from SC1 mutant, no other mutant can elicit apical constriction and recruitment of active myosinII when targeted to the apical membrane in MDCK cells. Scale bar 20 μm. This experiment was performed by Dr.Jeff Hildebrand.

2.2.6 The Shroom-Rock binding interface is evolutionarily conserved

The C-terminal SD2 domain of Shroom is highly conserved across species [11, 234]. Drawing inference from the sequence conservation of Shroom SD2 across different species, equivalent mutations were made in *Drosophila* Shroom SD2 by the VanDemark Lab. Similar biochemical assays performed with the dShroom SD2 SC and HD mutants recapitulated the above results obtained with mShroom3 SD2 [328]. The dShroom SC1 mutant retained the ability to bind dRock whereas all other dShroom SC and HD mutants failed to bind dRock. The dShroom HD mutants failed to dimerize whereas dimerization capacity was not affected in the SC mutants when assessed by crosslinking assays using glutaraldehyde or native gel mobility shift assays

[328]. Chimeric version of Endolyn-dShroom SD2 when transfected in MDCK cells also triggered apical constriction. Thus the Rock-binding interface is evolutionarily and molecularly conserved and the Shroom-Rock pathway seems to be the universal signaling module employed by cells undergoing apical constriction.

2.3 DISCUSSION

2.3.1 The Shroom SD2 possess a unique fold with implications in Shroom structure and function

Solving the structure of the SD2 provided a wealth of testable hypotheses regarding the function of the SD2 motif. The *Drosophila* Shroom SD2 protein exhibited a unique fold consisting of an antiparallel dimer composed of three helical segments; a long coiled-coil body segment flanked by two short arm segments. Guided by the sequence conservation profile and the structural data, several conserved patches of residues were selected for mutation. In order to achieve the greatest impact of these mutations on Shroom structure and function multiple residues were targeted simultaneously. Given the large extended dimerization interface and the broad distribution of conserved patches, two classes of mutants were created; residues which were either surface exposed, and presumably implicated in Rock binding, and residues which were interiorly buried, and proposed to mediate Shroom dimerization.

Results from the mouse Shroom3 SD2 mutants suggest that among the conserved surface exposed patches, amino acid residues in the body segment of the protein mediate Rock binding, whereas conserved residues in the arm segment are not involved. The anitparallel nature of the

Shroom SD2 structure suggests that these surface patches lie on opposite sides of the molecule. Importantly, abrogation of Rock binding also affects Shroom's ability to induce apical constriction and results in a loss of activated myosinII enrichment at the apical surface of cells. As for the HD mutants, the dimerization interface is extended such that different mutations targeting the coiled-coil in either the body segment or the arm segment disrupt Shroom dimerization. However, it is difficult to predict whether these interiorly buried patches affect dimerization of the whole Shroom protein or just the structure of the SD2 domain. Structural data on other domains of Shroom or the protein as a whole still awaits discovery. Importantly these HD mutants are also defective for Rock binding and eliciting apical constriction, thereby suggesting that perturbing the Shroom-Shroom dimerization interface has dramatic consequences on its ability to bind Rock. Thus, the Rock-binding site on SD2 is probably made up of amino acid residues from both chains of the dimer, and the SD2 motif should retain the ability to both dimerize and bind Rock in order to trigger apical constriction. Interestingly the internal symmetry in the dShroom SD2 dimer suggests that there are two independent but identical Rock-binding sites. One half of the SD2 dimer is structurally identical to the other half and contains both the Rock-binding sites and should be competent for Rock binding. Alternatively, it can be proposed that each Shroom monomer can fold back on itself at the symmetry point to form a half dimer. In that case, the internal patches are still necessary for the monomer to fold properly and position conserved residues on the SD2 surface into an orientation competent for Rock binding. Similar biochemical results obtained with *Drosophila* Shroom SD2 mutants suggest that the Rock-binding interface has been both evolutionarily and molecularly conserved with important functional and biological implications [328].

2.3.2 Molecular models of Shroom-Rock complex formation

Other biochemical assays have elucidated the stoichiometry of Shroom-Rock binding to be in a 1:1 molar ratio and the binding affinity of Shroom-Rock interaction to be 0.58μM [328]. This quantification has prompted us to suggests two different models of the Shroom-Rock interaction. Previous studies have elucidated the structure of other regions of Rock including the kinase domain, PH domain, portions of the central coiled-coil domain, RBD domain and a RhoA-RBD complex to be a parallel coiled-coil homodimer [7, 267, 281, 282, 329-332]. It is therefore reasonable to predict that the SBD of Rock also forms a parallel coiled-coil homodimer. In view of its parallel coiled-coil structure it would suggest that there exists two independent Shroom binding sites in Rock SBD. With the identification of distinct surfaces required by Shroom for Rock binding or dimerization and its presence as a dimer, a probable mode of Shroom-Rock binding might be opening up of individual dimers and annealing to form a Shroom-Rock heterodimer (Figure 15A), however it is energetically unfavorable and conformationally impossible to position the two Rock-binding sites, each on a half-dimer of Shroom, to align with the two independent Shroom binding sites on the parallel coiled-coil of Rock SBD.

It is difficult to envision how the two independent Rock-binding sites on Shroom would contact the two independent Shroom binding sites of Rock without evoking large conformational remodelling. Thus it is reasonable to predict that these two independent and identical Rock binding sites probably form contacts with the two independent Shroom binding sites on Rock by positioning two half dimers on opposite side of Rock coiled-coil (Figure 15B, C). These half dimers can either be from a single Shroom SD2 dimer or from a Shroom SD2 monomer that has folded back on itself at the symmetry point to generate a half dimer. A probable model of Shroom-Rock complex formation would be Rock SBD dimer binding to Shroom SD2 and

inducing a huge conformational change that can position the two independent Rock binding sites to interact with the Shroom binding sites on the coiled-coil of Rock SBD simultaneously (Figure 15B, C). The latter tetrameric model is favored, however evidence of Shroom SD2 in other conformations or in a complex with Rock need to be analyzed to establish this model.

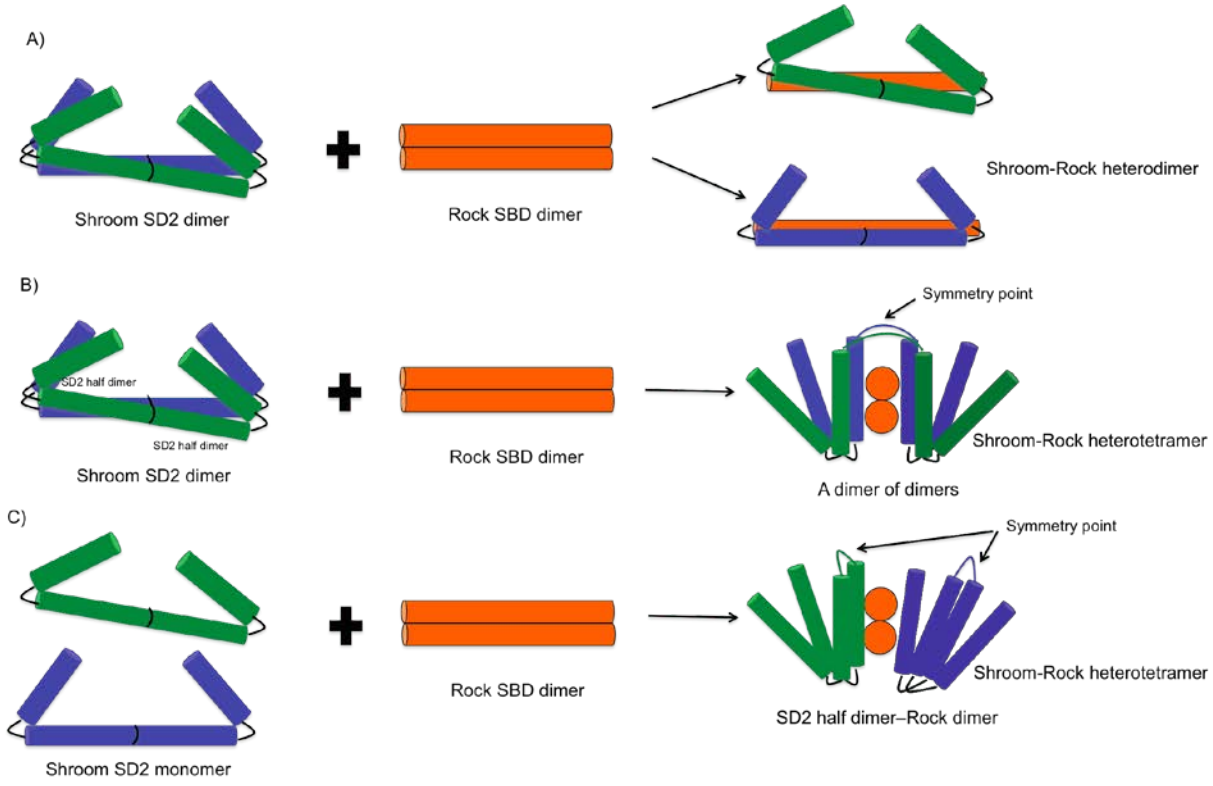

Figure 15: Model of Shroom-Rock complex formation

A) Opening of individual Shroom and Rock homodimers and annealing to form a heterodimer.

B) Each Shroom dimer hinging at the symmetry point to form half dimers and binding to opposite surface of Rock homodimer.

C) Each Shroom monomer hinging at the symmetry point to form half dimers and binding to opposite surface of Rock homodimer.

3.0 INVESTIGATING THE ROLE OF SHROOM-ROCK INTERACTION IN NEURAL TUBE MORPHOGENESIS

3.1 INTRODUCTION

Cellular remodeling, driven by the dynamic nature of the cytoskeleton, is critical for regulating cell processes like adhesion, division, polarity, migration, secretion and morphology [1, 2, 16, 139-142, 155, 333-340]. Through the use of genetic models systems and the mapping of mutations that cause human diseases, it is well-established that errors in these processes lead to a wide range of maladies, including birth defects, cancer, kidney disease, and neuronal degeneration. One example of a congenital birth defect associated with improper cell morphogenesis arising due to errors in cytoskeletal dynamics are those that affect closure of the neural tube, the precursor to the brain and spinal chord [206-208]. While less common in the developed world, neural tube closure defects (NTDs), including spina bifida and excencephaly, are among the most common birth defects worldwide affecting approximately 1 in 1,000 births [206, 207]. While over 200 genes have been implicated in neural tube morphogenesis in mice, a clear understanding of the etiology of human NTDs has remained elusive [208-210].

Shroom3, a class of F-actin associated proteins is one of over 200 genes that have been shown to be a key regulator of cell morphology in neural tube closure [11, 232, 234, 235, 238]. In vertebrates, the Shroom family is comprised of four members, Shroom 1-4 [232] each of

which has been implicated in the regulation of various developmental processes including neural tube closure [11], remodeling of the vasculature [9], eye development [8, 12], gut morphogenesis [10, 13], neuronal architecture and function [14, 231], ENaC channel regulation [341], renal function [23], arterial hypertension [243], and heterotaxy in humans [235, 238, 244, 262]. Importantly, Shroom-mediated cellular morphogenesis is dependent on its proper localization and protein-protein interactions. Most Shroom proteins (Shroom 2,3,4 and dShroom) bind to both F-actin and Rho-associated kinase (Rock) via signature sequence motifs known as Shroom domain 1 (SD1) and 2 (SD2), respectively. Shroom3 binding directly to F-actin localizes actin to the zonula adherens of polarized epithelial cells [15, 234]. Shroom3 binding to Rock ensures Rock localization to the zonula adherens of cells [5]. Rock, a Ser/Thr kinase, then phosphorylates the myosin regulatory light chain (RMLC), resulting in localized activation of non-muscle myosinII [5, 12, 15]. As a result, a contractile circumferential actomyosin ring gets sub-apically positioned in the cell. This ring exerts tension and elicits apical constriction, facilitating the transition of columnar shaped cells into a wedge-shaped form [15]. When this cell shape change occurs synchronously in a group of cells it alters tissue stiffness and causes invagination or bending, leading to tissue morphogenesis.

A new Shroom3 allele, *Shroom3*^{m1nisw} has been identified in mice using a genome-wide ENU mutagenesis screen to identify mutants that exhibit neural tube closure defects [342, 343]. *Shroom3*^{m1nisw} homozygous mutant mice embryos exhibit exencephaly and spina bifida similar to the gene trap allele of Shroom3, Shroom3$^{gt(ROSA)53sor}$. In order to investigate the molecular basis of this loss-of-function phenotype, I characterized the ENU-induced mutation, a substitution in a highly conserved arginine residue (R1838) in Shroom SD2 in the ENU-mutant embryos. In this study, I look at the role of R1838 directly, demonstrating the pronounced effect of alterations at

this position on the development of neural tube defects, Rock binding and Shroom-mediated apical constriction via activation of the Rock-myosinII pathway. This mutation in Shroom3 SD2 abrogates Rock binding and renders it incapable of triggering apical constriction. Thus my data suggest the essentiality of Shroom-Rock interaction in neural tube morphogenesis and apical constriction in polarized epithelial cells. I also demonstrate that the equivalent mutation in *Drosophila* Shroom results in a loss of Rock-binding activity, thereby showing that the Shroom-Rock signaling module is molecularly and functionally conserved across animal evolutionary history.

3.2 RESULTS

3.2.1 The Shroom3$^{m1/Nisw}$ allele harbors a substitution mutation in Shroom3 SD2

Previous studies have identified a novel, ENU-induced allele of Shroom3 called *Shroom3*^{m1Nisw} [342, 343]. Embryos homozygous for this allele phenocopy embryos homozygous for a gene trap null allele at the Shroom3 locus, *Shroom3*$^{gt(ROSA)53sor}$, suggesting that this allele is a functional null (Figure 16A). However, analysis of the *Shroom3*^{m1Nisw} allele indicates a C-to-T missense mutation at nucleotide position 5744 in the Shroom3 cDNA (accession number NM_015756), resulting in an Arginine to Cysteine amino acid substitution at position 1838 of Shroom3 (accession number NP_056571) (Figure 16C). This would suggest that the mutant allele should still express full-length protein that is localized to the apical adhesion sites of cells. Alternatively the substitution mutation could destabilize the protein, causing it to be degraded. Consistent with the first hypothesis, the staining of neural epithelium from wildtype or homozygous

Shroom3^{m1Nisw} embryos indicates that Shroom3 protein is expressed at approximately equal levels and exhibits similar subcellular distribution (Figure 16B). Additionally, this substitution mutation does not appear to affect the stability or folding of the protein (see below). Sequence analysis indicates that R1838 is within the SD2 of Shroom3 and maps to a highly conserved patch of amino acids that is surface exposed (Figure 16C, D). Our previous work on the SD2 has identified the cluster of residues ^{1834}SLSG**R**LA^{1840}, as being essential for Shroom-Rock interaction [344]. In fact, in all SD2 motifs identified to date, an arginine is conserved in this position (Figure 16C). Taken together, these data indicate that the Shroom3 R1838C protein is defective for a specific activity that is required for neural tube closure in mice.

A)

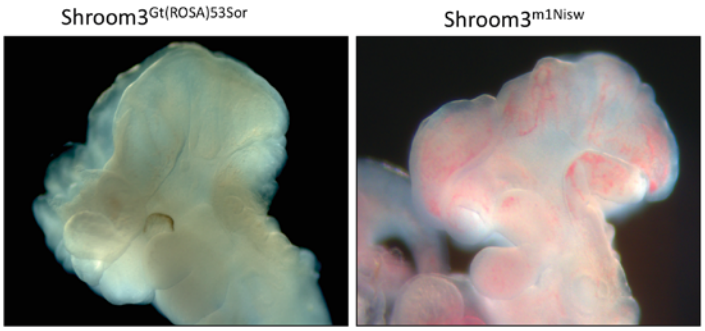

B)

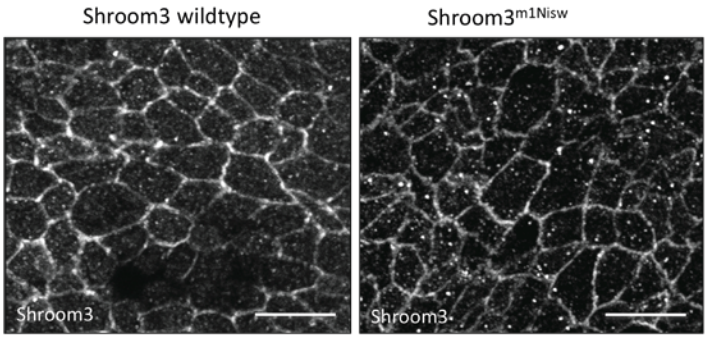

C)

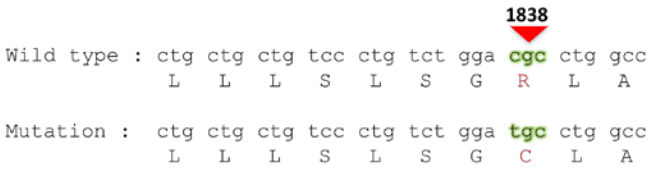

Mouse Shroom3	LLLSLSGRLA
Human Shroom3	LLLSLSGRLA
Chick Shroom3	LLLSLSGRLA
Frog Shroom3	LLLSLSGRLA
Mouse Shroom2	LLLSLSGRLA
Human Shroom2	LLLSLSGRLA
Chick Shroom2	LLLSLSGRLA
Frog Shroom2	LLLSLSGRLA
Mouse Shroom4	LLLSLSGRLA
Human Shroom4	LLLSLSGRLA
Chick Shroom4	LLLSLSGRLA
Frog Shroom4	LLLSLSGRLA
Fish Shroom4	LLLSLSGRLI
Fly Shroom	LLLSLSERLA
Beetle Shroom	LLLGLSGRLA
Urchin Shroom	LLLSLSRRLN
Ciona Shroom	LLLSLSGRMA
Anemone Shroom	LLLSLTQRMH
Hydra Shroom	LLLSLTQRLH

D)

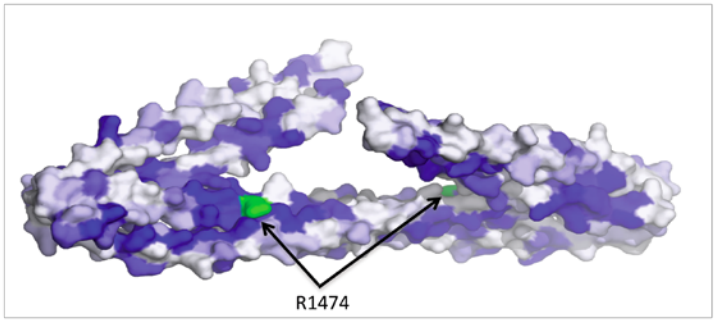

Figure 16: Arginine 1838 of Shroom3 SD2 is required for neural tube closure in mice but does not regulate protein expression or localization

A). Embryos homozygous for Shroom3 null allele Shroom3$^{Gt(ROSA)53Sor}$ exhibit the same phenotype as the ENU Shroom3 allele Shroom3^{m1Nisw}

B) Expression of the Shroom3 R1838C protein. Sections of either wild type or Shroom3^{m1Nisw} neural epithelium was analyzed by indirect immunofluorescence to detect Shroom3 and visualized by confocal microscopy. Scale bar, 10μm.

C) The Shroom3^{m1Nisw} mutation results in the substitution of a cysteine for a highly conserved arginine. Top panel shows the point mutation while the bottom panel shows the sequence conservation of the SD2 in the vicinity of arginine 1838.

D) Surface view of the Drosophila Shroom SD2 with the conserved arginine (R1474) residue highlighted in green. Blue patches are representative of highly conserved residues.

3.2.2 Shroom3 SD2 R1838 is specifically required for Rock SBD binding

Based on the above results and previous studies, we predicted that the Shroom3 R1838C protein is unable to interact with Rock. To test this hypothesis, I generated two substitution variants R1838A and R1838C of mouse Shroom3 SD2 and tested their ability to bind to the Shroom-Binding domain (SBD) of human Rock1 using *in vitro* binding assays. I created an alanine subsitution in addition to the cysteine substitution to replace the hydrophobic nature of arginine with alanine and also see the effect of replacing the long side chain of arginine with only a small hydrophobic methyl moiety in alanine. First, I performed pull-down assays by mixing GST-Shrm3 SD2 variants bound to beads with soluble, His-tagged Rock-SBD spanning amino acids 707-946. In this assay, the R1838A and R1838C variants exhibit an approximate 45% and 95%

reduction, respectively, in the ability to bind Rock protein relative to the wildtype SD2 (Figure 17A). To verify the results from the pull-down assay and assess the stability of the interaction, I tested this interaction by mixing GST-Shrm3 SD2 with His-tagged SBD in solution and resolved the proteins by native gel electrophoresis. In this assay, wildtype GST-Shrm3 SD2 and the SBD form a stable complex that has reduced mobility in the native gel (Figure 17B). In agreement with the pulldown assay, I found that the R1838C variant is incapable of forming a stable complex and essentially all of the SD2 and SBD proteins remain in the unbound state. In contrast, the R1838A exhibits an intermediate level of binding, with 51% of the GST-SD2 protein remaining unbound. These data suggest that the R1838 position is important for binding. However, since the alanine substitution results in an intermediate level of binding, it suggests that the cysteine mutation is more severe and that there may be some tolerance for different amino acids at this position. To further investigate this interaction and to verify that the GST moiety, because it is a dimer, didn't influence the binding, we assessed the ability of untagged SD2 and SBD proteins to form stable complexes using native gel mobility shift assays (Figure17C). In these experiments, we can readily detect a complex with wild type SD2 and Rock SBD whereas neither the R1838A nor the R1838C variant were able to form a stable complex, suggesting a significant decrease in the binding affinity for Rock SBD.

Although the *Drosophila* Shroom SD2 structure suggests that the R1838C mutation should be surface exposed, it is possible that the substitution mutation perturbs the intramolecular interactions and thus influences protein folding and stability. However, the R1838C and R1838A variants exhibit the same mobility on a native gel (Figure 17B and 17C), suggesting this is not the case. To further test this we analyzed the stability of these proteins in the presence of protease and their behavior in size-exclusion chromatography, which would

indicate if the proteins had a dramatically different conformation or were forming aggregates. Shroom3 WT, R1838A and R1838C proteins all exhibit the same stability when subjected to digestion by Subtilisin A for 15, 30, and 60 minutes, suggesting that they are all in a stably folded conformation (Figure 17D). Similarly, all of the proteins exhibit the same elution profile using size exclusion chromatography, suggesting there are no dramatic changes in overall protein tertiary structure or protein aggregation (Figure 17E). Taken together, these data indicate that the R1838A and R1838C proteins are virtually indistinguishable from the wildtype SD2, suggesting these substitutions do not effect the overall folding or stability of the protein. Thus, these results suggest that R1838 is playing a prominent role in mediating the Shroom-Rock interaction and not other aspects of the SD2 structure.

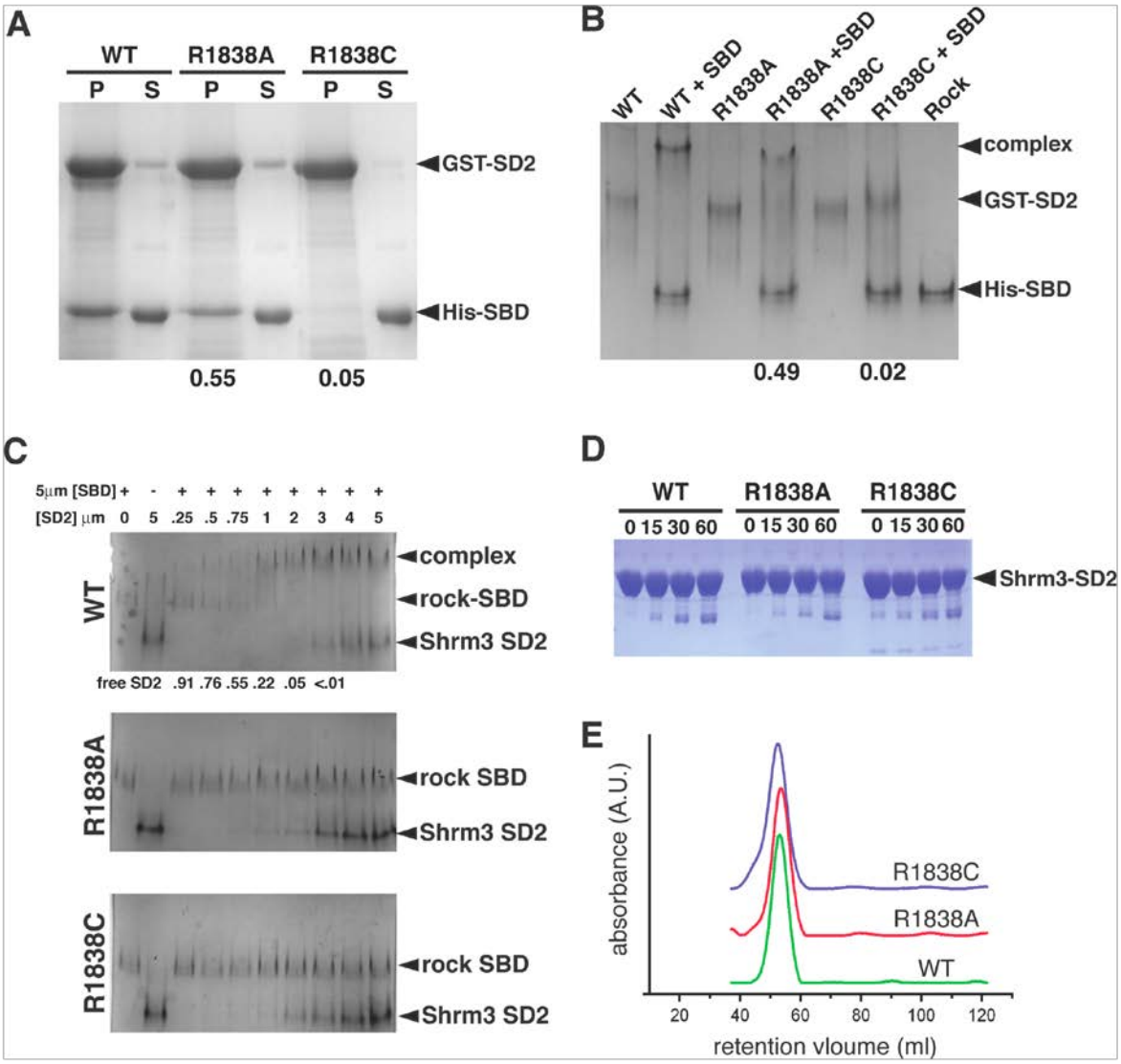

Figure 17: Arginine R1838 is required for the interaction between Shrrom3 and Rock

A). *In vitro* pull down assay using wild type and R1838 substitution variants of GST-Shroom3 SD2 (GST-SD2) bound to glutathione beads and His-tagged hRock SBD (His-SBD) in solution. The amount of Rock SBD in the pellet relative to wild type, is indicated under the gel.

B). Gel mobility shift assay to detect the binding of GST-Shroom3 SD2 variants to the SBD of hRock1. Purified GST-Shroom3 SD2 and SBD proteins were mixed in solution, resolved

on native PAGE gels, and detected by Coomassie Blue staining. The amount of complex formed relative to wild type is indicated beneath the gel.

C). Gel mobility shift assay to detect the interaction of untagged Shroom3 SD2 variants (Shrm3-SD2, amino acids 1642-1951) and untagged hRock1 SBD (Rock-SBD, amino acids 707-946). Increasing concentrations of SD2 proteins (indicated at top) were mixed with 5 μM SBD, resolved by native PAGE, and detected by Coomassie Blue staining. Values beneath the wild-type panel indicate the relative amount of free SBD.

D). Purified, untagged SD2 proteins were exposed to Subtilisin A for 0, 15, 30, or 60 minutes, resolved on SDS-PAGE gels, and stained with Coomassie Blue.

E). Elution profiles of size exclusion chromatography of purified Shroom3 SD2 substitution variants. Experiments shown in panel D and E were done by Jenna Zalewski from the VanDemark Lab.

3.2.3 Shroom3 SD2 R1838 variants fail to colocalize with Rock

Shroom proteins bind directly to the coiled-coil Shroom Binding Domain (SBD) of Rock via its C-terminal SD2 domain and recruits it to specific subcellular locales to regulate cell morphology and behavior [5, 9, 234, 327]. Based on the above data showing that Shroom3 variants R1838A and R1838C fail to bind Rock, we predict that these mutants would also fail to recruit Rock to proper subcellular locales *in vivo* and therefore fail to colocalize with Rock. To test this hypothesis, we co-expressed the Rock SBD with either wild type or substitution variants of Shroom3 in MDCK and Cos7 cells and assayed their co-localization (Figure 18). Shroom3 usually localizes to the cell-cell junctions in MDCK cells and to cortical actin and stress fibers in Cos7 cells, while the Rock SBD is typically cytoplasmic in these cells [5]. If Shroom3 is capable

of binding Rock and recruiting it, Rock will then colocalize with Shroom3. As expected, the wild type Shroom3 and Rock colocalize to cell-cell junctions in MDCK cells and to actin stress fibers in Cos7 cells (Figure 18A). A Shroom3 version lacking the SD2 domain fails to recruit Rock SBD and serves as the negative control (Figure 18B). Similar to the SD2 deletion variant, Shroom R1838A and R1838C mutants fail to colocalize with Rock when coexpressed in either MDCK or Cos7 cells (Figure18C). Colocalization analysis performed to quantify the degree of co-distribution between Shroom3 and Rock SBD in Cos7 cells demonstrate a linear relationship in cells expressing WT Shroom and Rock whereas it is greatly reduced in cells expressing R1838A and R1838C indicating a lack of co-distribution. Thus, our data suggest that Shroom-Rock binding is required for directing Rock to specific subcellular locales.

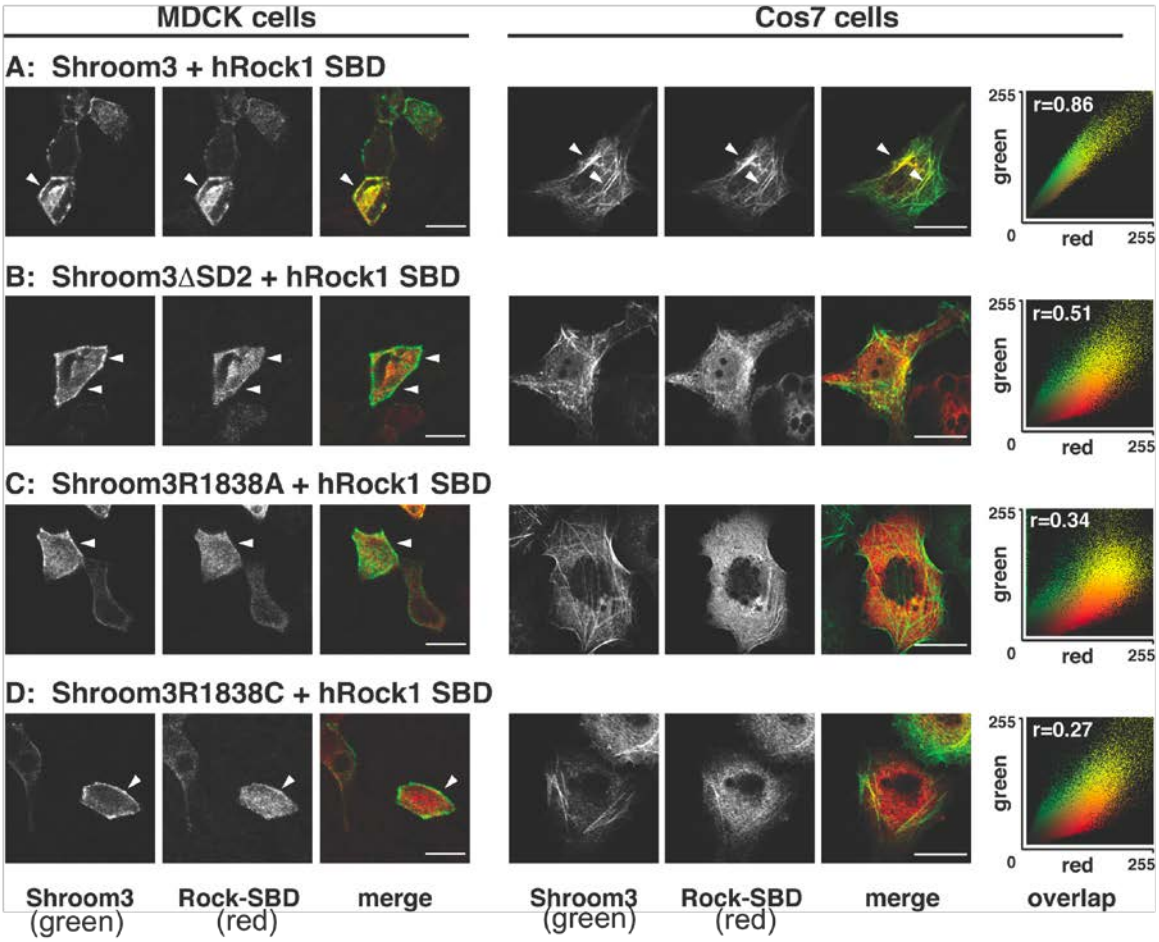

Figure 18: Shroom3 SD2 R1838 mutants fail to colocalize with Rock SBD *in vivo*.

MDCK and Cos7 cells co-expressing the hRock1 SBD and either wild type Shroom3 (A), Shroom3 ΔSD2 (B), Shroom3 R1838A (C) or Shroom3 R1838C (D) were grown on either transwell filters (MDCK cells) or fibronectin-coated coverslips (Cos7) and stained to detect Shroom3 (green) and the myc-tagged Rock SBD (red). The furthest right-hand panels are color scatter plots and indicate the degree of overlap between Shroom3 and the Rock-SBD with Pearson's *r* value indicated in each scatter plot. Scale bar, 10μm.

3.2.4 Shroom3 SD2 R1838 is required for apical constriction of polarized epithelial cells

Shroom3 directly interacts with F-actin through its SD1 domain and this interaction is required for Shroom3 localization to the apically positioned sites of cell-cell adhesion, the zonula adherens [15, 234]. Previous work has shown that the Shroom3 SD2 is both necessary and sufficient to cause apical constriction in polarized Madin-Darby canine kidney (MDCK) cells and this activity is dependent on the catalytic activity of both Rock and myosinII [15, 234]. To address whether alterations at R1838 prevent apical constriction, we expressed either wild type or R1838 variants of Shroom3 in MDCK cells and tested their ability to elicit apical constriction. MDCK cells expressing wild type Shroom3 show dramatic apical constriction, demonstrating a 89% decrease in apical area relative to non-transfected cells (Figure 19A, B). In contrast, cells expressing the Shroom3 R1838A or R1838C variants largely fail to induce apical constriction to the same extent as wildtype. Consistent with the *in vitro* binding data, the R1838A variant induces a small degree of apical constriction, a 22% decrease in apical area relative to non-transfected cells. The R1838C variant exhibits no apical constriction and is more severe, inducing a minimal decrease of 8% in average apical area (Figure 19A, B). We predict that these results are due to the inability of these proteins to bind Rock and not the degree of protein expression or stability as all of the Shroom3 proteins are expressed at comparable levels (Figure 19C). The above results are consistent with the hypothesis that the ability of Shroom3 to bind Rock directly correlates with the ability of Shroom3 to induce apical constriction and thus Shroom3-induced changes in cell morphology are the result of its interaction with Rock and not the actin cytoskeleton or other possible effectors.

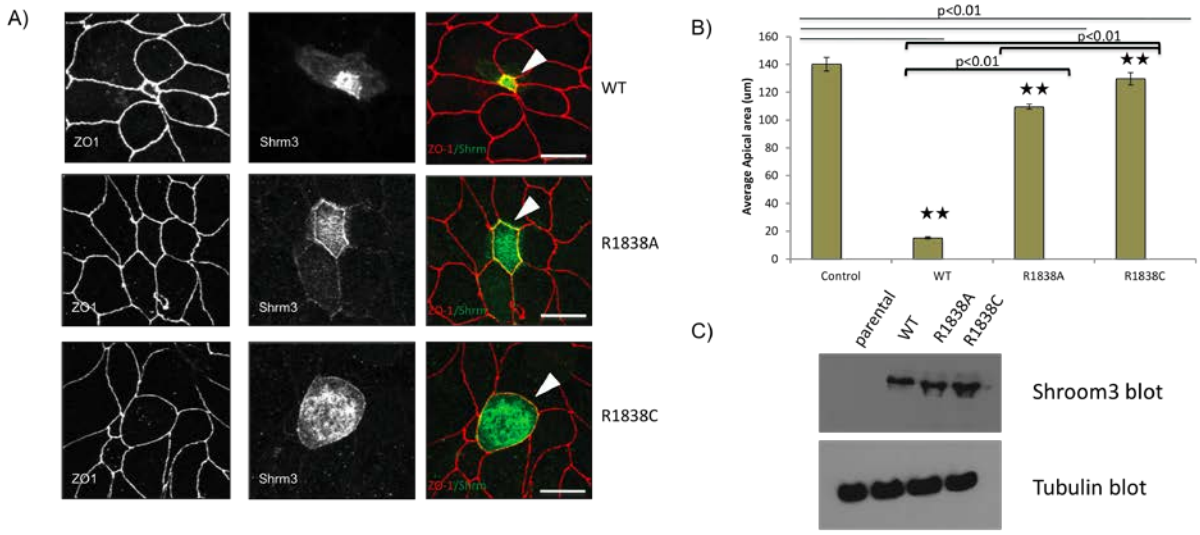

Figure 19: Shroom3 R1838 variants fail to induce apical constriction in MDCK cells

A). MDCK cells were transiently transfected with expression vectors for Shroom3, Shroom3 R1838A, or Shroom3 R1838C, grown overnight on transwell filters, and then stained to detect Shroom3 (green) and the tight junction marker ZO-1 (red). Scale bar, 10 μm.

B). Quantification of apical constriction induced by wild type, R1838A and R1838C Shroom3 proteins when expressed in MDCK cells. Apical area was determined by measuring the area encircled by ZO1 staining of cells expressing the indicated Shroom3 proteins using ImageJ software. Error bars represent standard error variation in the positive and negative range for 30 cells. The statistics are shown for 30 cells picked at random from a single experiment and the *p* value is <<0.01 for R1838A and R1838C relative to control cells, cell expressing wild type Shroom3 cells and in between R1838A and R1838C.

C). Equal amounts of total lysate from MDCK cells expressing the indicated Shroom3 proteins were assayed by western blot analysis using anti-Shroom3 sera. Membranes were reprobed to detect α-tubulin to demonstrate equal protein loading in each lane.

3.2.5 Shroom3 SD2 R1838 variants causes decreased activation of the Rock-MyosinII pathway

Shroom SD2 domain is both necessary and sufficient to induce changes in cytoskeletal organization and subsequent alterations in cell morphology [11, 15]. SD2 elicits changes in cell morphology by altering the cellular distribution of contractile actomyosin networks [15]. This function of SD2 is accomplished by the direct association of Shroom SD2 to Rock [5]. We hypothesize that this binding recruits Rock to specific subcellular compartments and activates it, resulting in the phosphorylation of its downstream targets, specifically Regulatory Myosin Light Chain (RMLC) and Myosin phosphatase targeting subunit (MYPT). This results in the localized activation of myosinII which then binds to F-actin to form a contractile actomyosin network at the zonula adherens of cells, which induces apical constriction. Since the Shroom3 R1838A and R1838C mutants fail to bind Rock or cause apical constriction I wanted to test if they are also incapable of activating the Myosin II pathway by assaying the phosphorylation status of RMLC in polarized MDCK cells expressing either wild type or Shroom3 SD2 variants. Consistent with our previous findings cells expressing either the R1838A or the R1838C mutant do not show enrichment of phosphorylated RLC at cell junctions contrary to the the cells expressing wild type Shroom protein (Figure 20A, B, C). Taken together, these results substantiate the role of this conserved arginine residue in the SD2 in mediating Shroom-Rock interaction and demonstrate that Rock binding and subsequent localized activation of actomyosin is required for proper neural tube morphogenesis.

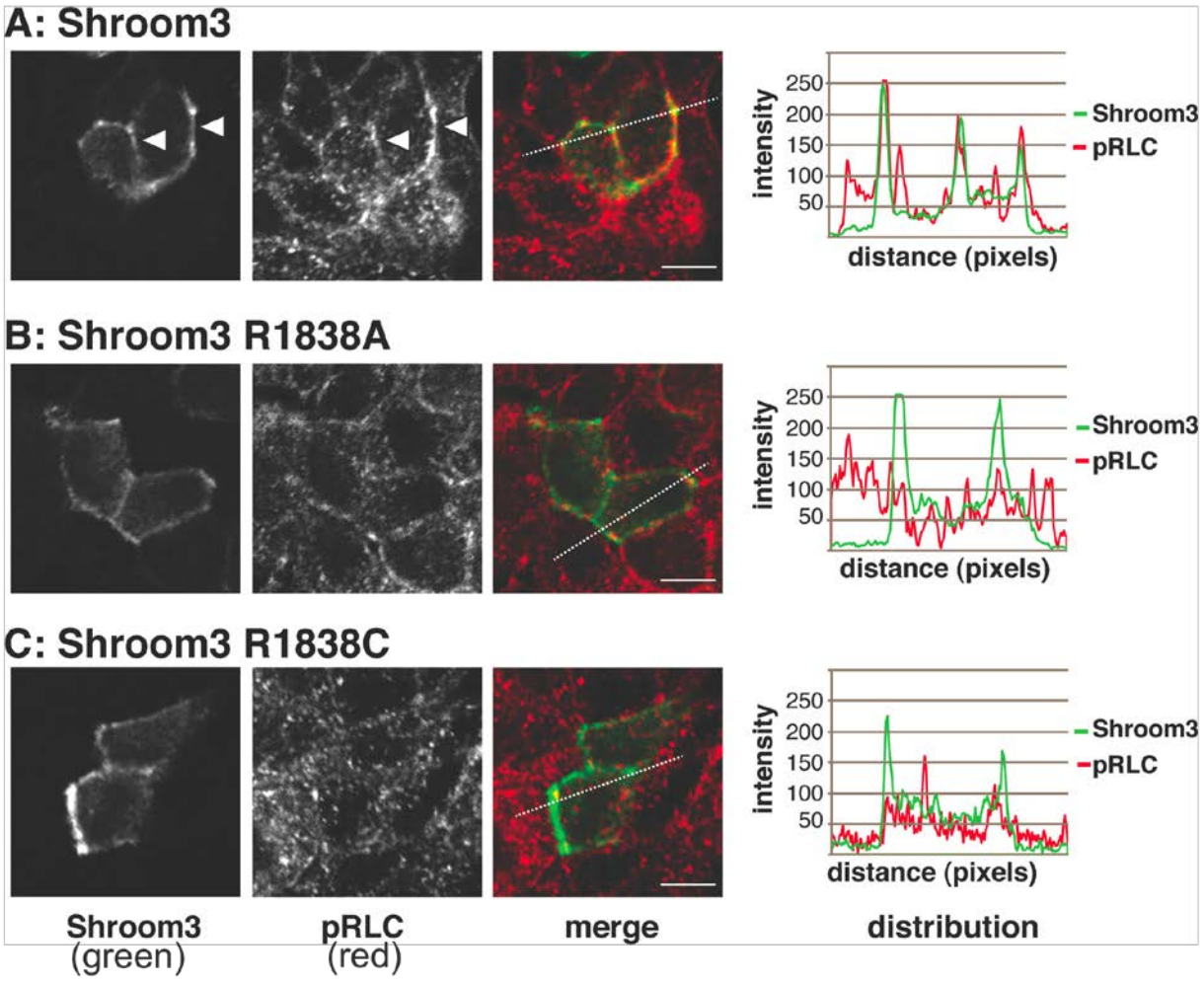

Figure 20: Shroom3 R1838 substitution mutations causes decreased activation of the Rock-MyosinII pathway

MDCK cells were transiently transfected with expression vectors for hRock1 and either Shroom3, Shroom3 R1838A, or Shroom3 R1838C and stained to detect Shroom3 (green) and phosphorylated RLC (pRLC, red). Right-hand panels show the fluorescent intensity of Shroom3 (green) and pRLC (red) at the position of the dotted line in the corresponding merge panels. Scale bar, 10 μm.

3.2.6 dShroom SD2 R1838 variants behave similarly to mShroom3 SD2 mutants

Our previous work had identified a Rock-binding interface on mouse Shroom SD2 that was conserved in invertebrate *Drosophila* Shroom [327, 328]. The mShroom SC2 mutant (^{1834}SLSG**R**LA^{1840}) behaved similarly to dShroom SC2 mutant in that it failed to bind Rock or cause apical constriction in MDCK cells. Since the R1838 is highly conserved across species I wanted to test whether this residue had an evolutionarily conserved role in Shroom-Rock interaction. To test this I created equivalent mutations in dShroom SD2, R1474A and R1474C and tested their ability to bind dRock. Purified untagged dShroom SD2 proteins wild type (2mg/ml), R1474A (2mg/ml) or R1474C (10mg/ml) were subjected to solution binding with dRock and complex formation assessed via native gel mobility shift assay. As expected, the wild type dShroom SD2 protein formed a stable complex with dRock, as represented by the higher molecular weight species on the native gel. In contrast, no complex formation was detected when the R1474A or R1474C variants were used (Figure 21A). These substitution mutations did not affect the overall structure or stability of the protein as evidenced by crosslinking and protease sensitivity assays (Figure 21B, C). Thus, this arginine residue plays an evolutionarily and molecularly conserved role in mediating the Shroom-Rock interaction.

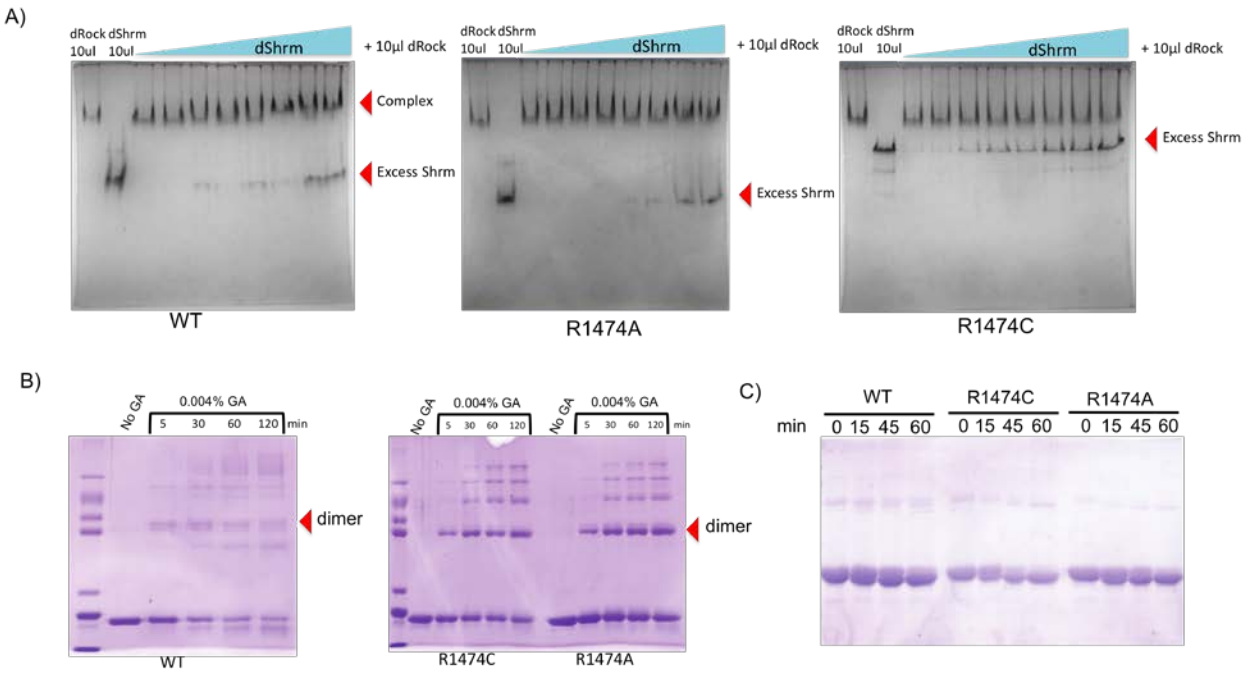

Figure 21: dShroom SD2 variants R1474A and R1474C behave similarly to mShroom3 SD2 mutants

A). Gel mobility shift assays to detect interaction and complex formation between untagged wild type or dShroom SD2 variants (dShroom-SD2, amino acids 1393-1576) and untagged dRock (amino acids 724-938). Increasing concentration of dShroom SD2 proteins were mixed with a constant concentration of dRock, resolved by native PAGE, and detected by Coomassie Blue staining.

B) Chemical crosslinking of dShroomSD2 wild type or R1474 variants to detect dimer formation in solution. Wild type or mutant dShroom SD2 proteins were incubated with 0.004% glutaraldehyde (GA) and samples taken at various time points were resolved by SDS-PAGE and detected by Coomassie Blue staining.

C) Limited proteolysis to detect protein stability of dShroom wild type or R1474 SD2 mutants. dShroom wild type or mutant proteins were treated with 40µg of the protease Subtilisin A for the indicated times and samples taken at each time point were resolved by SDS-PAGE and

detected by Coomassie Blue staining. Experiments shown in panel B and C were done by Swarna Mohan from the VanDemark Lab.

3.3 DISCUSSION

Neurulation is a complex morphogenetic event and an intensely studied field because of the high prevalence of congenital birth defects associated with failure of neural tube closure [207]. Shroom3 plays an important role in neurulation in *Xenopus*, chick and mouse embryos [5, 11, 195]. Shroom3 is a key regulator of tissue morphogenesis and cell morphology and it does so by modulating the cytoskeletal dynamics in the cell. Shroom3 directly binds to F-actin and Rock via signature sequence motifs and these interactions are required for its *in vivo* activity. We predict that other Shroom family members function analogously to Shroom3 [8, 9, 11, 15, 195, 229, 232, 234, 238], thereby suggesting that a conserved Shroom-Rock signaling module operates in a variety of cell types to regulate cell morphology and behavior. However the molecular basis of the Shroom-Rock interaction is still unknown.

Mutant mice embryos, obtained from a genome-wide ENU mutagenesis screen exhibiting neural tube closure defects similar to the null allele of Shroom3, lead to the discovery of a novel allele of Shroom3; *Shroom3*^{m1Nisw}. Molecular analysis of these *Shroom3*^{m1Nisw} mutants lead to the identification of a substitution mutation in a specific region of Shroom SD2 that fortuitously coincides with the highly conserved surface cluster patch of residues on Shroom SD2 that we previously identified to be important for Rock binding and apical constriction [328]. In this study I investigated the role of this Shroom SD2 substitution variant in Rock binding and apical constriction and showed that this specific region of SD2 is required for Rock binding and its

recruitment to the apical surface of cells to bring about Shroom induced apical constriction and neural tube morphogenesis.

3.3.1 R1838 is essential for Rock binding and Shroom3-induced changes in cell morphology

Shroom3^{m1Nisw} mutant mice exhibit severe exencephaly that is attributed to a point mutation in Shroom3 SD2 that changes a highly conserved arginine 1838 to a cysteine. One of our previously generated surface cluster mutants, SC2 of Shroom SD2 (^{1834}SLSG**R**LA^{1840}) removes this arginine residue and abrogates Rock binding as well as apical constriction [328]. In this study I showed that changing the positively charged arginine to either an uncharged polar amino acid cysteine, or to a nonpolar amino acid alanine, disrupts Rock binding. Out of the two Shroom SD2 variants, R1838C seems to be more severe in disrupting Rock binding thereby suggesting some tolerance at this position. It is probable that the R1838C mutant has a reduced binding affinity for Rock relative to the alanine substitution mutant. A more stringent quantitation of the binding affinity of these two SD2 variants using fluorescence anisotropy would address this issue. Our previously characterized SC2 mutant substitutes the R1838 with an aspartic acid and this dramatic change from a positively charged amino acid to a negatively charged one might account for its failure to bind Rock. Alternatively, it might be a cumulative effect of mutating multiple resiudes in the surface cluster patch. In our single R1838 variants it is a little surprising that the alanine substitution, which is hydrophobic, shows a milder effect compared to the cysteine substitution mutant which is hydrophilic, similar to arginine. The presence of a sulfhydryl group in cysteine might account for the severity of this mutation, as being a weak acid it cannot mediate hydrophilic interactions comparable to arginine. Also, cysteine can form

disulphide bonds to form a strongly hydrophobic and nonpolar cystine that mediate protein protein interactions. However the SBD of human Rock does not contain a cysteine residue and therefore forming disulphide bridges to strengthen Shroom-Rock interaction seems improbable. Rather the absence of a cysteine residue in Rock SBD might contribute to its inability to bind Rock. The R1838A mutant, because of its hydrophobic character, might cluster inside the SD2 however since it retains the helical propensity, it probably does not disrupt the secondary structure of the extended SD2 body segment and therefore has milder effects on Rock binding. Our native gel shift assays however predict a smilar behavior of both R1838 variants in their inability to bind Rock and form a stable Shroom-Rock complex. Solving the structure of these proteins will help us better understand the side chain interactions mediated by this residue in the Shroom-Rock complex. Nonetheless, both the mutants are severely affected in their ability to cause apical constriction in MDCK cells, suggesting that this arginine residue is essential for altering cell shape *in vivo*.

Neural tube closure is a complex embryological process requiring precisely orchestrated cell movements that are brought about by spatio-temporal regulation of cytoskeletal architecture and dynamics. Using mice as a genetic model system, other labs have demonstrated the importance of actin architecture and regulation in neural tube morphogenesis as mutations in cytoskeletal regulators like Nap1 [219], Abl1/2 [220], p190RhoGap [221], Mena/profiling [222], Vinculin [223], NF1 [224], paladin [225], Epb4.1l5 [226, 227], and Marcks [228], all cause neural tube closure defects. Shroom3 has been shown to directly bind and bundle F-actin and apart from Rock, it can also bind Ena/Vasp proteins and recruit them to the apical surface of cells to induce apical constriction [11, 12, 345]. Shroom can thus employ different mechanisms to regulate actin dynamics required during neural tube closure and mutating it could have global

consequences on embryonic development. That being said, the *Shroom3*^{m1Nisw} mutant embryos have neural tube closure defects that match the *Shroom3* null embryos. If they had a more severe phenotype it would be indicative of something else that is going on. Based on our previous results, I predict that the above-mentioned activities, though required for *in vivo* function of Shroom3, are not perturbed in the R1838 substitution variant and are thus dispensable for neural tube morphogenesis.

3.3.2 The Shroom SD2-Rock interaction is evolutionarily conserved

In *Drosophila*, apically localized contractile networks of actomyosin exert forces that are critical for germ band extension, ventral and dorsal closure, and various invaginations [153, 190, 202, 205, 265, 276, 346-352]. These processes exhibit extensive and robust apical constriction. Vertebrate Shroom protein has limited overall sequence homology to *Drosophila* Shroom, however the SD2 motif is highly conserved. Previous work from our lab has shown that *Drosophila* Shroom functions similarly to Shroom3 in binding to dRock, F-actin, inducing robust apical constriction, and localizing to specific subcellular compartments [235]. The VanDemark lab has solved the structure of the SD2 from dShroom and based on the structure we predict that R1838 of Shroom3 is surface exposed [344]. To verify that the Shroom-Rock interface is conserved, mutation of the analogous arginine in the dShroom SD2 (R1474 in dShroomA) renders the protein incapable of binding Rock. Additionally these dShroom SD2 proteins are proteolytically stable, confirming that these substitutions do not affect the overall structure or stability of Shroom protein. It would be interesting to knock-in the mutant allele in fly and assess the effect of this mutation *in vivo*. Thus, we conclude that the Shroom-Rock pathway is evolutionarily conserved.

3.3.3 Implications of understanding the Shroom-Rock interaction

An interesting facet of the Shroom-Rock pathway is whether Shroom binding can directly activate Rock or if it is merely required for Rock localization where Rock is activated by some other effector molecule. It is predicted that Rock adopts a folded, autoinhibited conformation via intramolecular interactions between the C-terminal tail and the N-terminal kinase domain that renders it inactive. It is thought that binding of proteins such as RhoA (in the GTP bound state), lipids, or caspase cleavage of the C-terminus, relieves this intramolecular inhibition and activates Rock [6, 41, 42, 263, 266, 269-272, 285, 287, 353, 354]. However, there is evidence for both Rho-dependent [237] and Rho-independent modes of Rock activation during Shroom3-induced apical constriction [15, 195, 344]. We predict that if Shroom binding is both necessary and sufficient for activation of Rock, then the Shroom3 R1838C substitution variant would be unable to localize as well as activate Rock.

It has already been shown that the Rock-MyosinII pathway controls vital morphogenetic processes in animals and is central to diverse signaling networks [136, 137, 273, 355, 356]. Therefore global disruption of Rock function affects multiple cellular processes with detrimental side effects. Targeted Rock inhibition hence serves as a potential therapeutic approach for many debilitating diseases including cancer [357-360], obesity [361-363], diabetes [364], hypertension [365], atherosclerosis [366] and cardiovascular diseases [367]. It would thus prove helpful to understand the different mechanism of Rock activation and its interaction with different downstream substrates for targeted modulation of Rock activity. Finally establishing our

proposed model of Shroom-Rock interaction to be necessary and sufficient for Rock activation, independent of RhoA, will provide a new paradigm of Rock activation and facilitate an improved understanding of disease pathogenesis associated with dysregulation of Rock activity. This will aid in designing strategies to alter Rock regulation for therapeutic purposes.

4.0 CHARACTERIZING THE SHROOM BINDING DOMAIN OF ROCK TO IDENTIFY RESIDUES CRITICAL FOR SHROOM-ROCK INTERACTION AND ROCK LOCALIZATION

4.1 INTRODUCTION

Rock proteins are required for various cellular processes such as cell motility, migration, adhesion, shape change, cytokinesis, centrosome positioning and cell polarity [292, 368-370]. It is a Serine/Threonine kinase that can regulate the cytoskeletal dynamics by phosphorylating various downstream targets, including RMLC, MYPT, LIMK, Adducin, ERM proteins and many others. Rock phosphorylates the MLC causing localized activation of myosinII [4] which contributes to the assembly of a contractile actomyosin network. Of the different Rock binding proteins that have been identified to date, Shroom is one such candidate that binds to Rock via its SD2 [5]. Previous work has shown the essentiality of Rock activity in Shroom mediated processes, especially Shroom3 induced apical constriction [5, 15, 235]. Rock is a multidomain protein characterized by several signature sequence motifs. Rock binds to the C-terminal SD2 of Shroom via its centrally located Shroom Binding Domain (SBD). The SBD is part of a larger central coiled-coil fragment that comprises the SBD, the Rho-binding domain (RBD) and spans amino acids 421-1105 in hRock1. The Shroom-Rock interaction recruits Rock to specific subcellular locales where it can locally activate myosinII and form a contractile actomyosin

network [5, 235]. Shroom3 SD2 mutations that abolish Rock binding also results in a loss of phosphorylated RMLC at the apical junctions of cells [328]. Thus it demonstrates that Rock is required for Shroom3 mediated apical constriction.

Rock remains in an inactive autoinhibitory folded conformation in the native state. This folded conformation is mediated by intramolecular interactions between the N-terminal kinase domain and C-terminus of Rock. Previous studies have shown the negative regulatory effect of the C-terminus of Rock [270]. Binding of RhoA, lipids, arachidonic acid or caspase cleavage is thought to relieve this autoinhibition [6, 41, 42, 263, 266, 269-272, 285, 287, 353, 354]. However there is evidence of Rho-dependent [242] as well as Rho-independent modes of Rock activation [15, 195] during Shroom3 mediated apical constriction. Though much is known about the expression pattern of Rock, its subcellular localization, downstream targets and function, regulation of its catalytic activity still remains confounding. It is unclear as to how Rock gets activated once it is recruited to the zonula adherens following Shroom binding. This questions the contribution of Shroom-Rock interaction in Rock activation, forming an alternate pathway contrary to the canonical Rock activation pathways known to date.

In order to dissect the role of Shroom binding in Rock localization and Rock activation, it becomes imperative to characterize the domains in both Shroom and Rock that are mediating this interaction. I have first characterized the SD2 domain of Shroom and identified surface patches important for Rock binding. Here, I characterize the highly conserved Shroom Binding Domain (SBD) of Rock to map the residues critical for Shroom binding. I, along with our collaborator, the VanDemark lab designed various human Rock1 SBD mutants, based on secondary structure prediction and sequence conservation, and identified residues that are critical for Shroom binding.

4.2 RESULTS

4.2.1 Identifying the minimal SBD of Rock and making SBD mutants

Rock is a 160kDa multidomain protein with signature sequence motifs required for its localization and catalytic activity (Figure 22A). A large central region in the coiled-coil domain of Rock was shown to mediate binding to Shroom SD2, however residues that specify this interaction have not yet been identified [5]. Since both Rock1 and Rock2 bind to Shroom SD2 we predicted that there is a conserved sequence motif in Rock that mediates this interaction. Previous work from our lab had identified the minimal core hRock SBD (amino acid 834-913) that is capable of Shroom binding and is proteolytically stable (Figure 22B, C). I analyzed the sequence conservation of this core region across different species using CLUSTALW sequence alignment (Figure 22D). I selected those amino acid residues that were highly conserved across species and targeted them by site-directed mutagenesis. Due to the extended helical coiled-coil region of the Rock SBD, I created multi-residue alanine substitution mutants and tested them for their ability to bind Shroom SD2. I used pET151D/TOPO expression plasmid containing the hRock1 template amino acids 707-946 or 834-913. The correct mutants were selected based on sequencing results and then transformed into *E.coli* CodonPlus RIPL cells. Protein expression was induced using 0.5 mM IPTG. Proteins were purified with Ni-NTA beads and then mixed with untagged mouse Shroom3 SD2 protein in solution. I then resolved the bead and supernatant fraction of the bound or unbound complex on a 12% SDS-PAGE and stained with Coomassie blue. A table summarizing the hRock SBD mutants created and their position on the hRock SBD protein structure is presented below (Table 2).

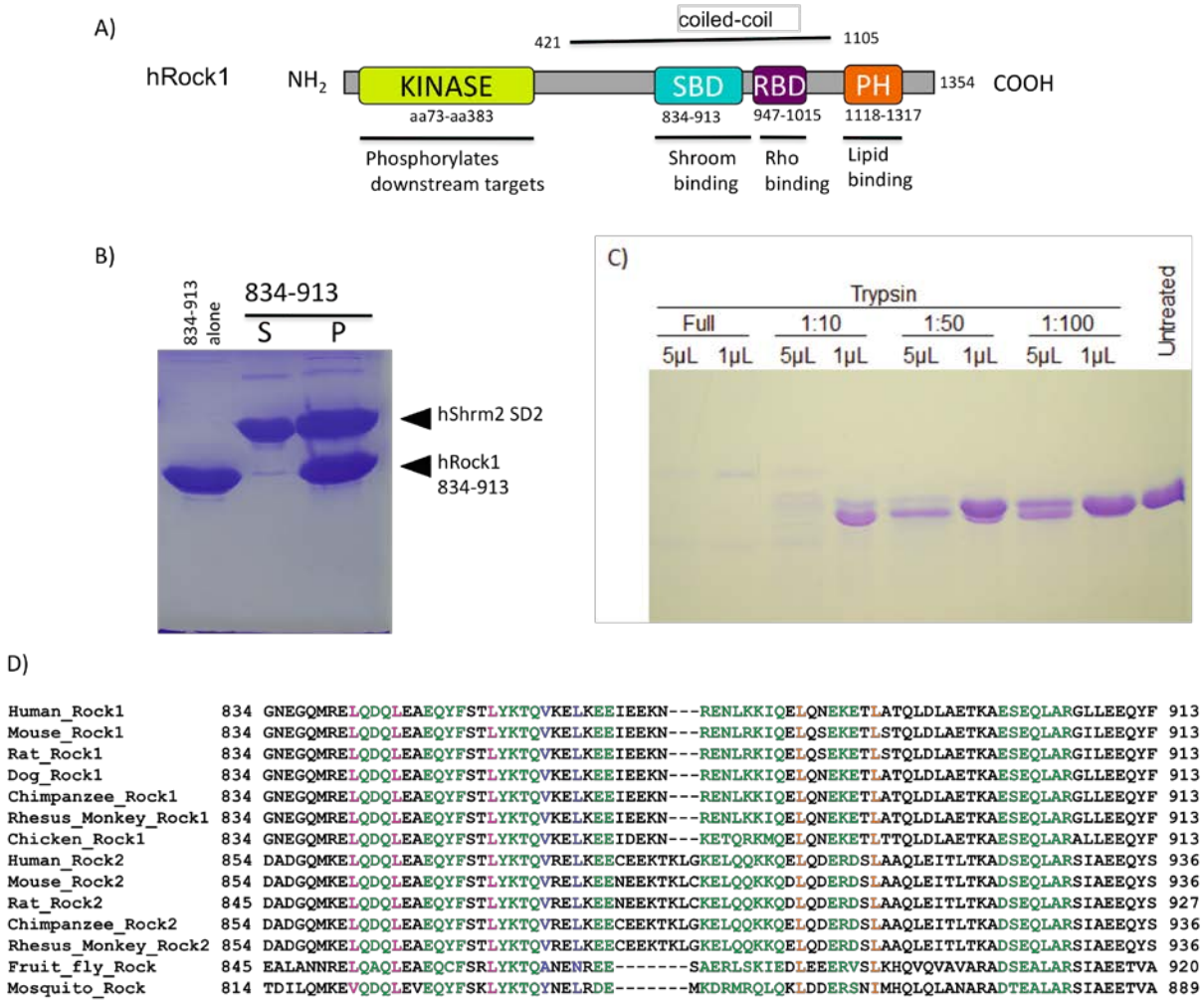

Figure 22: Identification of a minimal binding region in the central coiled-coil domain of Rock

A) Schematic of domain structure of human Rock1

B) hRock SBD spanning amino acids 834-913 is the minimal Shroom SD2 binding region in the central coiled-coil of Rock. *In vitro* pull down assay using His-tagged hRock SBD spanning amino acids 834-913 and untagged human Shroom2 SD2. Ni-NTA beads were bound to His-tagged hRock fragment and untagged Shroom SD2 was added in solution. Complexes were precipitated by spinning down beads and resulting samples were resolved by SDS-PAGE. This experiment was performed by Jenna Zalewski from the VanDemark lab.

C) Purified hRock SBD protein spanning amino acids 834-913 is proteolytically stable and is resistant to Trypsin at room temperature. This experiment was performed by Ryan Rizaldy from our lab.

D) Sequence conservation of Rock SBD (amino acids 834-913) across different species. Colored residues indicate highly conserved residues that were targeted for Site-directed mutagenesis. Green residues indicate different multiresidue SBD mutants created. Pink and orange residues are indicative of Leucines present in the N-terminal and C-terminal part of SBD and were mutated to alanine. Blue residues are indicative of buried residues that were targeted for mutational analysis.

Table 2: Position and sequence of hRock1 SBD mutants created

Residue number	Sequence	Position in SBD structure	hRock1 template
834-845	QDQ	Surface exposed	707-946
865-866	EE	Surface exposed	707-946
900-902	ESE	Surface exposed	707-946
850-852	QYF	Surface exposed	707-946
857-859	KTQ	Surface exposed	707-946
872,873,876,879	RE..K..Q	Surface exposed	707-946
842,846	Leu	Buried interiorly	707-946
860,863	V..L	Buried interiorly	707-946
849-852	EQYF	Both (E buried)	707-946

900-906	ESEQLAR	Both	707-946
842,846,855	3 LEU	Both (842,846Leu buried)	707-946
856-859	YKTQ	Both (Y buried)	834-913
855-859	LYKTQ	Both (L & Y buried)	834-913
881,888	2 LEU	Buried interiorly	834-913

4.2.2 Identifying conserved surface patch residues on hRock SBD critical for Shroom SD2 binding

Mapping the selected amino acid mutations onto the hRock SBD structure solved by the VanDemark lab showed some of them to be surface exposed, some to be interiorly buried and some a mixture of both. I tested each of the fifteen different hRock1 SBD mutants individually for their ability to bind Shroom via an *in vitro* pull down assay. hRock proteins were purified using Ni-resin and beads were mixed with untagged mShroom3 SD2 in solution and incubated for 2 hrs at room temperature. Both the bead and supernatant fraction were resolved on a 12% SDS-PAGE and subsequently stained with Coomassie blue. The wild type hRock1 SBD protein spanning amino acids 707-946 (Kd = 1.7 ± 0.2 μM) or 834-913 (Kd = 5.3 ± 1.5 μM) can bind to SD2 albeit with differing affinity and both the Rock and Shroom protein are detected in the bead fraction. The binding affinities for the two Rock1 proteins are comparable to that observed between Drosophila Rock and Shroom [327, 328]. A truncated hRock protein spanning amino acids 707-841, serves as a negative control and fails to bind Shroom and is detected in the supernatant fraction (Figure 23A). This indicates that this fragment does not contain the Shroom binding site. Blank beads, serving as a negative control fail to bind Shroom as evidenced by

Shroom in the supernatant fraction (Figure 23A). Of the different mutants tested, six alanine substitution mutants fail to bind Shroom as evidenced by absence of Shroom from the pellet fraction. Mapping these residues onto the hRock SBD structure reveals a surface patch of conserved residues at the N-terminus of the minimal SBD (Figure 23F). Some mutants with interiorly buried residues also affected Shroom binding whereas mutants containing residues in the central portion or C-terminal portion of SBD did not affect Shroom binding. The surface exposed residues ^{850}QYF^{852} and ^{857}KTQ^{859} were found to be critical for Shroom binding as mutating them abolished Shroom binding (Figure 23B) [327]. Two other mutants, ^{856}YKTQ^{859} and ^{855}LYKTQ^{859}, variants of the above KTQ mutant, as well as the ^{849}EQYF^{852} mutant a variant of the surface exposed QYF, were also defective for Shroom binding (Figure 23D). Also the leucine residues 842, 846, 855 seem to be critical, as alanine substitutions at these positions abrogated Shroom binding (Figure 23D). Since this triple leucine mutation targets residues which are both surface exposed and buried, I might have disrupted both the coiled-coil dimerization interface (mediated by residues ^{842,846}Leu) as well as the Shroom-Rock binding interface (mediated by the surface exposed residue ^{855}Leu) rendering Rock incapable of binding Shroom. Interestingly mutating interiorly buried residues like V860 and L863 or L842 and L846 did not affect Shroom binding (Figure 23C). Similarly, alanine substitutions made in the N-terminal part of the SBD (^{843}QDQ^{845}, ^{865}EE^{866}), or the central part (^{872}RENLKKIQ^{879}), or C-terminal part (^{884}EKE^{886}, ^{900}ESEQLAR^{906}, ^{881,888}Leu) did not affect Shroom binding (Figure 23B, D) [327]. This helped in the identification of a Shroom binding site on Rock SBD located between 839-860, with surface exposed residues between 850-859 serving as the critical binding determinants (Figure 23F) [327]. A summarization of the *in vitro* pull down results is presented below (Figure 23E).

A) Wild type, negative control and binding control for hRock1 SBD pull down assay

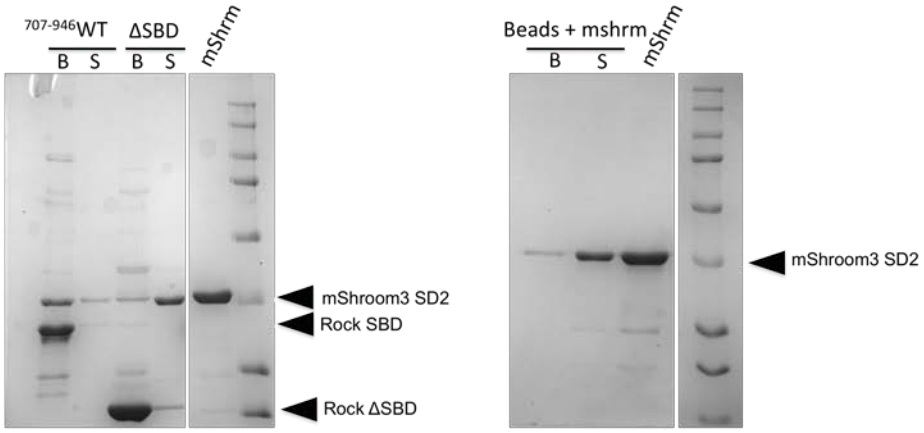

B) Surface exposed hRock1 SBD mutants

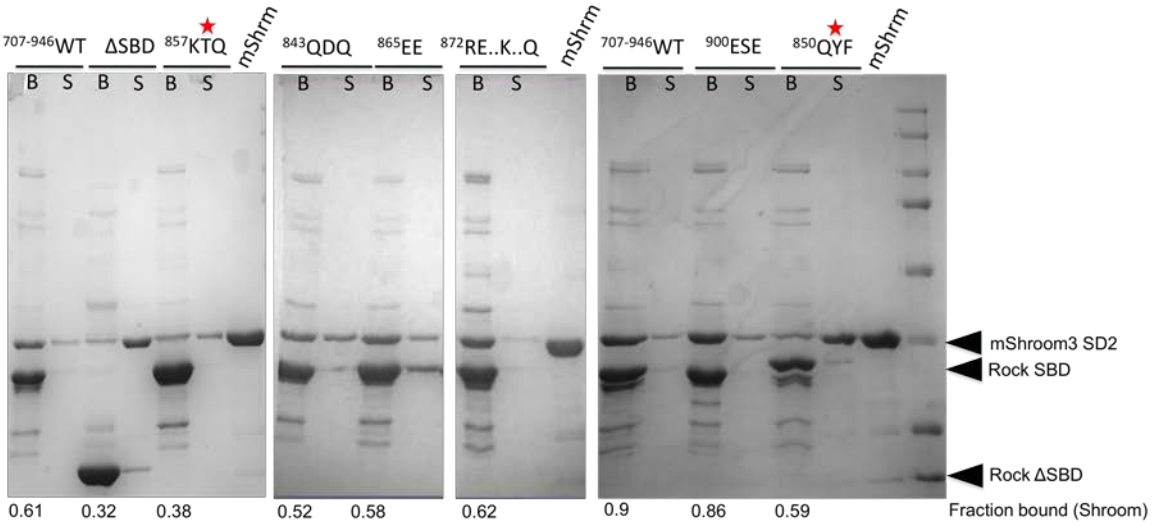

C) Interiorly buried hRock1 SBD mutants

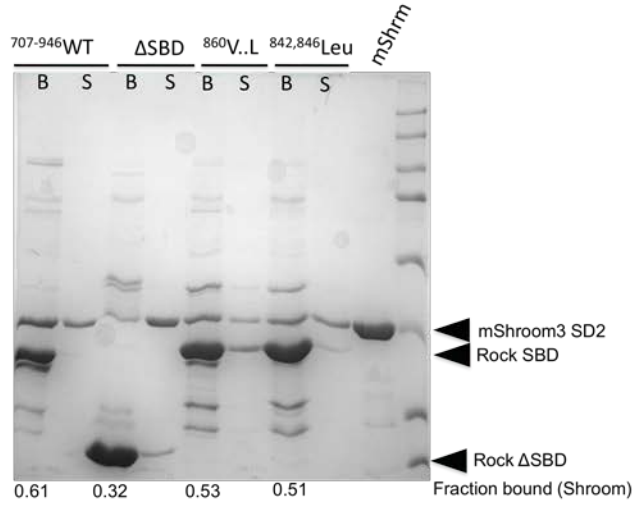

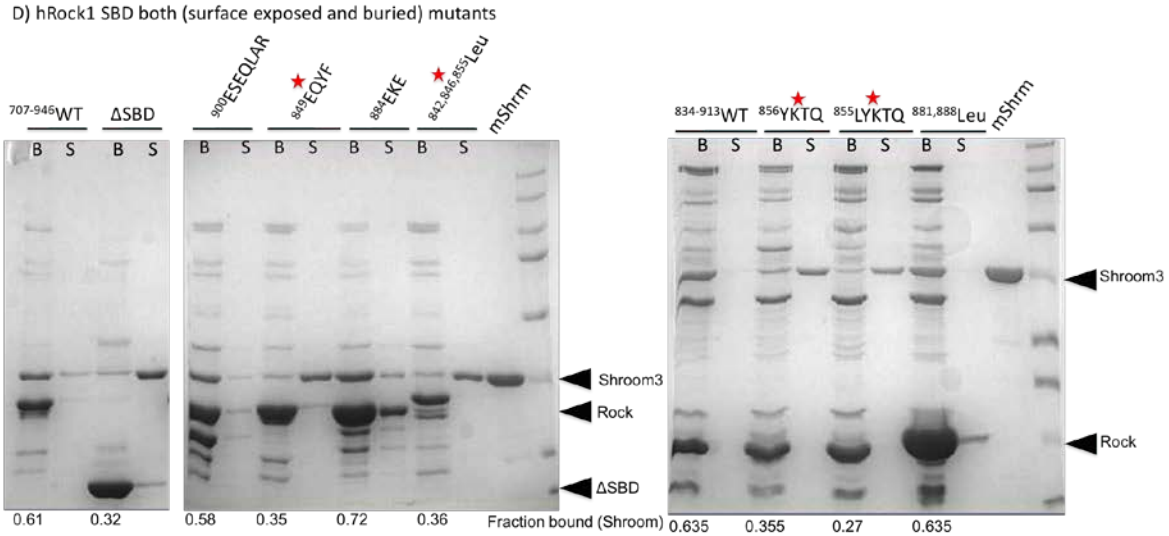

E)

Residue#	Sequence	Surface/ Buried	mShrm3 SD2 binding	hRock template
843-845	QDQ	Surface	+	707-946
865-866	EE	Surface	+	707-946
900-902	ESE	Surface	+	707-946
850-852	QYF	Surface	-	707-946
857-859	KTQ	Surface	-	707-946
872,873,876,879	RE..K..Q	Surface	+	707-946
842,846	Leu	Buried	+	707-946
860,863	V..L	Buried	+	707-946
849-852	EQYF	Both	+	707-946
900-906	ESEQLAR	Both	+	707-946
842,846,855	3 Leu	Both	-	707-946
856-859	YKTQ	Both	-	834-913
855-859	LYKTQ	Both	-	834-913
881,888	2 Leu	Buried	+	834-913

Figure 23: In vitro pull down assays with hRock SBD mutants and untagged mouse Shroom3 SD2

A) *In vitro* pull down assay using 20 µl of 10µM His-tagged hRock1 SBD (707-946) bound to Ni-NTA beads and 10 µl of 10 µM purified untagged mouse Shroom3 SD2 (B:beads, S:supernatant). ΔSBD hRock1 (707-841), a truncated version fails to bind Shroom and serves as the negative control. Blank Ni-

NTA beads fail to bind Shroom3 SD2 and Shroom is recovered in the supernatant fraction.

B) *In vitro* pull down assay using 20 µl of 10µM His-tagged hRock1 SBD wild type or surface exposed mutants and 10 µl of 10 µM purified untagged mouse Shroom3 SD2 (B:beads, S:supernatant). The fraction of Shroom bound to Rock is indicated below each gel (Fraction bound = Shroom Bound/Total Shroom input)

C) *In vitro* pull down assay using 20 µl of 10µM His-tagged hRock1 SBD (707-946) wild type or interiorly buried mutants and 10 µl of 10 µM purified untagged mouse Shroom3 SD2 (B:beads, S:supernatant). The fraction of Shroom bound to Rock is indicated below the gel (Fraction bound = Shroom Bound/Total Shroom input)

D) *In vitro* pull down assay using 20 µl of 10µM His-tagged hRock1 SBD (707-946)/(834-913) wild type or mixed mutants and 10 µl of 10 µM purified untagged mouse Shroom3 SD2 (B:beads, S:supernatant). The second gel in this panel is a 15% SDS-PAGE to better resolve the small wild type hRock fragment. The fraction of Shroom bound to Rock is indicated below each gel (Fraction bound = Shroom Bound/Total Shroom input)

E) Summarization of *in vitro* pull down results of hRock1 SBD mutants with untagged mouse Shroom3 SD2 highlighting the mutants that abrogate Shroom binding.

F) Cartoon ribbon diagram of hRock1 SBD (amino acids 834-913) highlighting the N-terminal residues critical for Shroom SD2 binding.

4.2.3 Conserved surface patch residues are important for Shroom-Rock colocalization

Previous work has shown that Shroom-Rock interaction is essential for directing Rock to specific subcellular locales. They identified that this recruitment of Rock to the apical junctions of polarized MDCK cells or neural epithelial cells was dependent on Shroom3 SD2 binding [5]. In order to test the above identified Rock SBD mutants for their capacity to colocalize with Shroom3, I recreated these mutants in a myc-tagged version of Rock spanning amino acids 681-942 in a pCS3 expression plasmid (Table 3). I cotransfected either wild type or hRock SBD mutants with Shroom3S into cos7 cells. Shroom3S is a naturally occurring short isoform of Shroom3 that contains both the SD1 and SD2 domain but lacks the N-terminal PDZ domain. Shroom3S can directly bind to F-actin and Rock and can induce apical constriction in polarized epithelial cells [11, 195, 234]. Shroom3 localizes to actin stress fibers and cortical actin in cos7 cells and Rock is usually cytoplasmic. Co-expression of Shroom3 with Rock results in Rock recruitment to actin stress fibers and cortical actin that colocalizes with Shroom3 (Figure 24A). However a Shroom3 variant lacking the SD2 domain fails to recruit Rock to actin stress fibers, showing that this interaction is SD2 dependent and it serves as the negative control. Similarly Rock SBD mutants that fail to bind Shroom also fail to get recruited to cortical actin or actin stress fibers and therefore were mostly cytoplasmic (Figure 24A) [327]. A color scatter plot indicating the codistribution of Shroom and Rock showed a significant decrease in the linear relationship for the mutants when compared to wild type Rock and Shroom (Figure 24B). All of the hRock SBD mutants tested ^{842}LQDQL^{846}, ^{842}L^{846}L^{855}L, ^{856}YKTQ^{859}, ^{855}LYKTQ^{859} were defective for colocalization with Shroom3, however with differing severity (Figure 24B). A colocalization plot using the fluorescent intensity of Shroom and Rock from a region of interest of wild type or each of the mutants, further confirmed our data (Figure 24C). These mutants were

generated in highly conserved amino acid residues that were predicted to be critical for either the Shroom-Rock binding or the Rock coiled-coil interactions. Of the four different Rock SBD mutants stated above, the ^{856}YKTQ^{859} and ^{855}LYKTQ^{859} were the most severe as they virtually eliminated recruitment to stress fibers, indicating that this region plays a critical role in Shroom-Rock interaction (Figure 24B, C). In contrast, the ^{842}LQDQL^{846} mutant is less severe in that it exhibits reduced recruitment of Rock to stress fibers, indicating that these residues are important but not essential for Shroom-Rock interaction in this assay. The triple Leucine mutant ^{842}L^{846}L^{855}L is also severely defective in colocalizing with Shroom, however, since this mutation is predicted to remove both surface exposed (^{855}Leu) and buried residues (^{842}L^{846}L) it might perturb both the Shroom binding interface and the coiled-coil interactions rendering Rock incapable of binding Shroom (Figure 24B, C) [327]. The colocalization data correlate well with the *in vitro* pull down results where I identified residues in Rock SBD important for Shroom SD2 binding. My data thus suggest that the Shroom-Rock interaction is essential for efficient Shroom3 and Rock colocalization *in vivo* and that Rock dimerization is probably required for Shroom binding and subsequent colocalization.

Table 3: hRock SBD mutants created to test for Shroom colocalization

Residue Number	Sequence	hRock template
842-846	LQDQL	681-942
842,846,855	3 Leu	681-942
856-859	YKTQ	681-942
855-859	LYKTQ	681-942

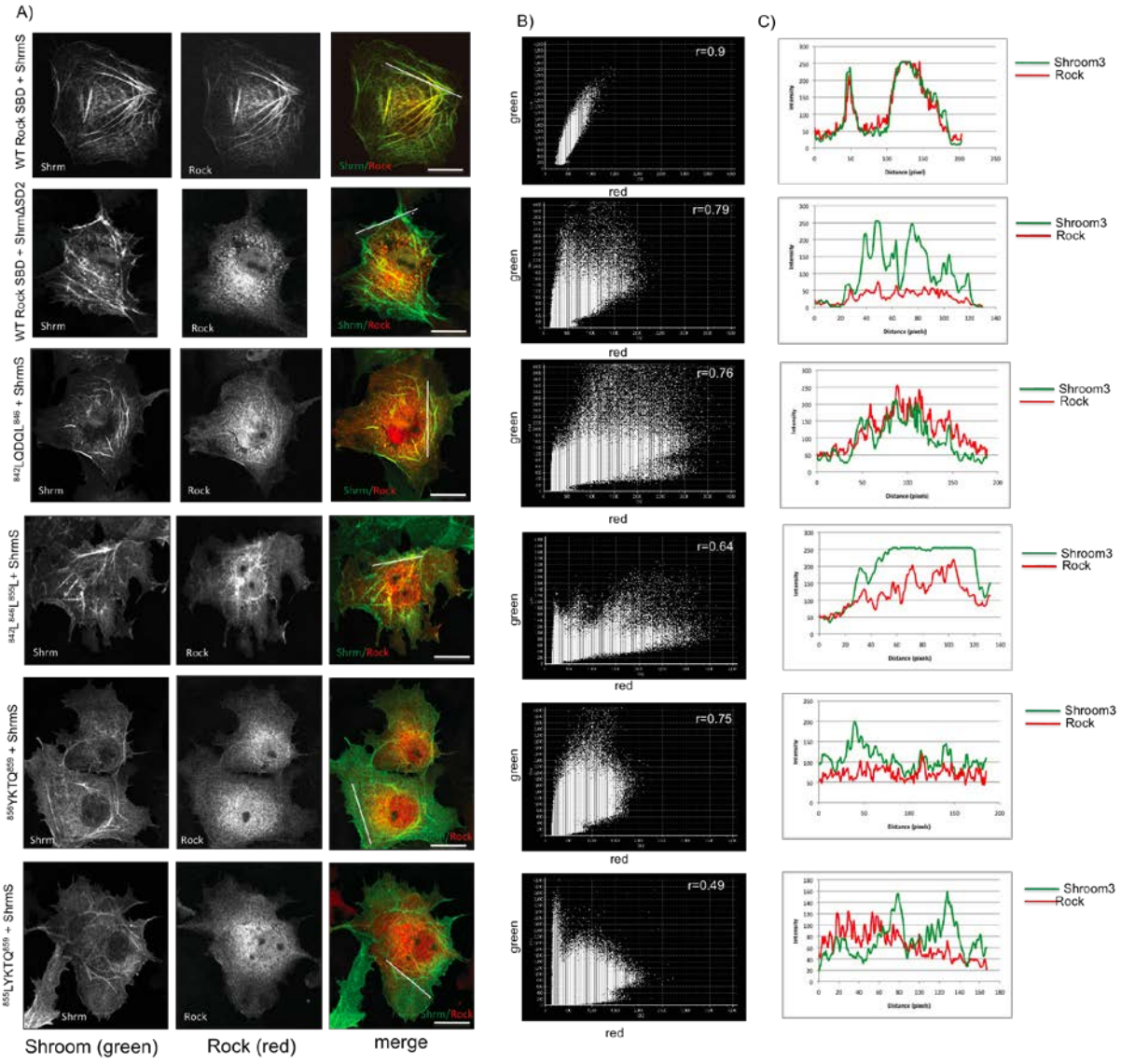

Figure 24: Shroom-Rock colocalization to actin stress fibers in cos 7 cells

A) Myc-tagged wild type or hRock1 SBD mutants (681-942) were co-expressed with wild type Shroom3S or a Shroom3 variant lacking SD2 in cos7 cells grown on fibronectin-coated coverslips and stained to detect Shroom3 (green) or the myc tagged Rock SBD (red). Scale bar 10μm.

B) The panels are colocalization plots and indicate the degree of overlap between Shroom3 and Rock-SBD with Pearson's r value indicated in each scatter plot.

C) Furthest right hand panels show the fluorescent intensity of Shroom3 (green) and Rock (red) at the position of the dotted line in the corresponding merge panels.

4.2.4 The Rock SBD is required for Shroom3 induced apical constriction

Results from the above experiments indicate which amino acid residues in the hRock SBD are important for binding to Shroom3. This highly conserved patch encompasses amino acids 855-859 situated in the N-terminal portion of the hRock 834-913 coiled-coil fragment. Previous work from our lab has shown that Shroom3 induced apical constriction in polarized MDCK cells is both Rock and myosinII dependent [4]. We hypothesize that Shroom binding triggers the kinase activity of Rock and therefore these hRock SBD mutants that fail to bind Shroom will be incapable of activating the constriction pathway in MDCK cells. In order to test this hypothesis we developed a knock-down/add back assay using specially engineered MDCK cells. These cells can express Shroom3 under the control of a Tet response element and the Tet transactivator [15]. We used T23 MDCK cells inducibly expressing a chimeric version of Shroom3 consisting of Endolyn and the C-terminus of Shroom3 containing the SD2 [4]. Endolyn is a trasmembrane protein that trafficks to the apical plasma membrane in MDCK cells and can be over expressed without altering cell morphology [371, 372]. It also increases the robustness of the apical constriction phenotype allowing easy identification of cells that are apically constricted. Upon induction of Endolyn-Shroom3 expression via removal of doxycyclin, cells exhibit robust apical constriction and disruption of tight junction organization as evidenced by ZO-1 staining (Figure 25A). To test whether this apical constriction phenotype is Rock dependent, we treated Endolyn-Shroom cells with siRNA specific to canine Rock1 and Rock2 and performed Western blot to

confirm their depletion (Figure 25B). Individual knockdown of Rock1 or Rock2 is unable to revert the apical constriction phenotype, whereas simultaneous knock down of both Rock1 and Rock2 effectively prevents the apical constriction phenotype, thereby suggesting that Rock1 and 2 function redundantly in Shroom3 induced apical constriction (Figure 25A). Importantly re-expression of full length wild type Rock in these siRNA treated cells effectively rescued apical constriction (Figure 25C) [327]. However, re-expression of a kinase dead version of Rock or Rock SBD mutant ^{855}LYKTQ^{859} failed to rescue apical constriction, thereby suggesting that the catalytic activity of Rock as well as its ability to bind Shroom is required to mediate Shroom-induced apical constriction (Figure 25C) [327]. Coexpression of Endolyn-Shroom and Rock in MDCK cells showed that the Rock SBD mutant ^{855}LYKTQ^{859} fails to get recruited to the apical surface of cells unlike wild type Rock (data not shown). Wild type Rock1 however, cannot elicit apical constriction or get apically localized in uninduced MDCK cells (data not shown). Taken together, the data suggest that the ability of Rock to mediate Shroom3 induced apical constriction is dependent on its ability to bind the Shroom SD2 [327].

Interestingly apical constriction is rescued with re-expression of a Rock RBD mutant (I1009A) that is defective in RhoA-GTP binding [280] but localizes apically in T23-Endolyn-Shroom cells similar to wild type Rock1 (Figure 25C) [327]. This suggests a unique Rock-dependent but Rho-independent mode of Shroom3-induced apical constriction, which is contrary to the prevailing models of Rock activation. However, we cannot overlook the fact that these are over-expression studies that can mask the need for active RhoA. Therefore, additional experiments designed to address the contribution of Rho-Rock and Shroom-Rock interactions during Shroom3 induced apical constriction will be necessary.

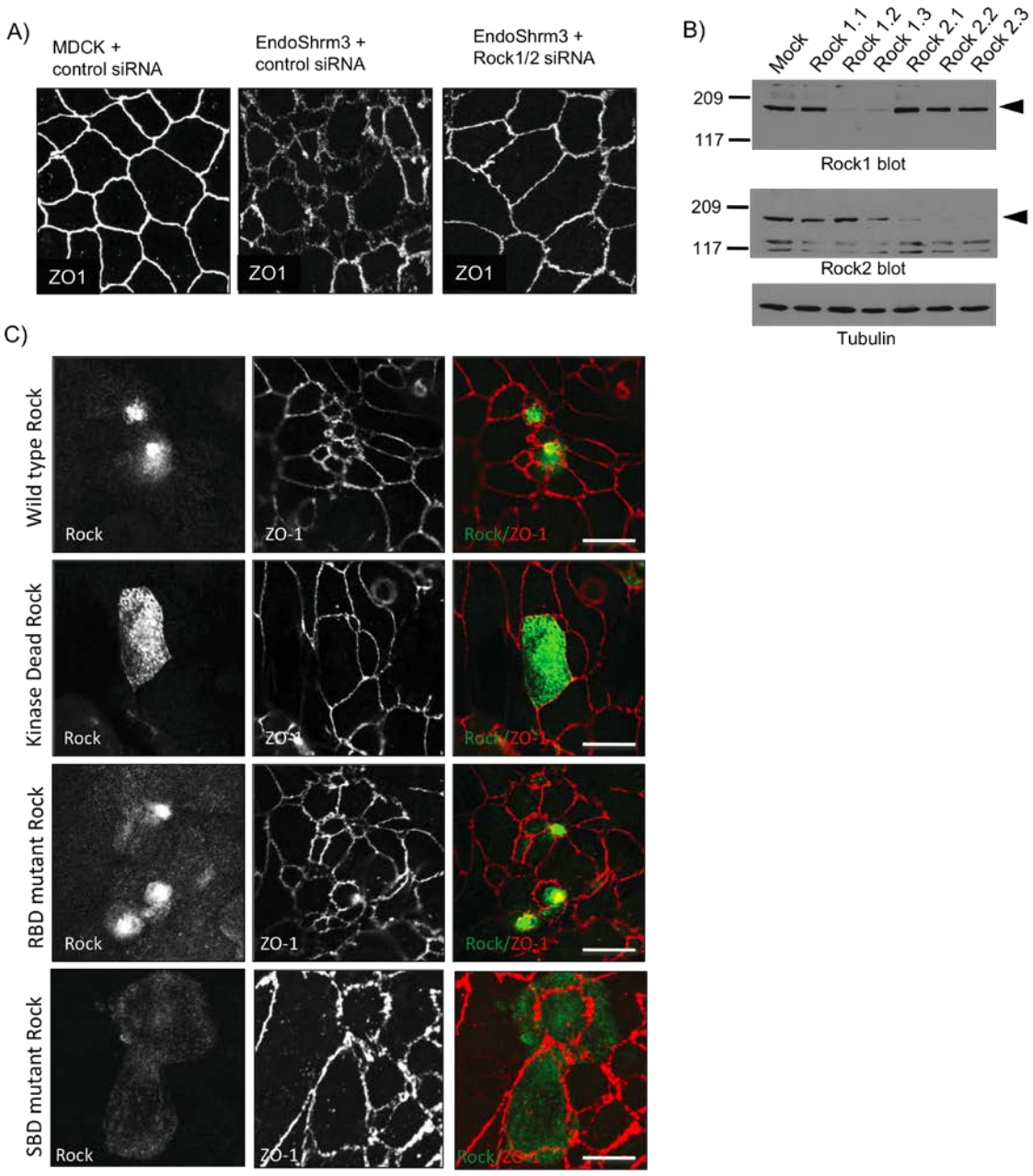

Figure 25: Key residues in hRock SBD are important for Shroom3-induced apical constriction

A) Parental or Endolyn-Shroom3 expressing T23 MDCK cells were treated with either control or Rock1 (1.2) and 2 (2.1) specific canine siRNAs and stained to detect ZO-1. siRNA mediated knock-down of Rock reverts apical constriction phenotype of cells.

B) Western blot analysis of Rock1 and Rock2 knockdown in MDCK cells. Three siRNAs specific for Rock1 (1.1, 1.2, 1.3) and Rock 2 (2.1, 2.2, 2.3) were tested for efficient knockdown via western blotting using rabbit anti-Rock antibodies.

C) T23 MDCK cells expressing Endolyn-Shroom3 treated with Rock1/2 (1.2 + 2.1) siRNA for 48 hours, transfected with the indicated hRock1 expression vectors, grown on transwell membranes for another 24 hours and stained to detect ZO-1 (red) and hRock1 (green). Scale bar 10μm.

4.3 DISCUSSION

Cellular morphogenesis is critical for normal embryonic development. Non-muscle cells undergo shape change such as apical constriction by spatially regulating the assembly and activation of myosinII. The activated myosinII, together with F-actin, forms a contractile actomyosin network that generates force to shrink the apical surface of cells. This motor activity of myosinII is triggered largely by the phosphorylation of its regulatory light chain. Several kinases that can directly phosphorylate and activate myosinII have been identified, including Calcium-calmodulin dependent Myosin Light Chain Kinase (MLCK) and Calcium-independent Rock. Rock is a prominent candidate that has been studied extensively for its role in regulating cytoskeletal dynamics in various cell processes. Rock is a Ser/Thr kinase with an N-terminal kinase domain that dimerizes in a head-to-head arrangement followed by a large extended central coiled-coil region and finally ending in a C-terminal PH domain. Structural studies of the Rock kinase, PH, RBD domain and parts of the central-coiled-coil region (including the SBD), has revealed a parallel coiled-coil homodimer structure [7, 267, 281, 282, 329-332]. However, information

regarding the region of Rock that can bind to Shroom and whether it forms a discrete binding site distinct from the other domains remains unknown. Since the Shroom-Rock signaling pathway is important in bringing about change in cell shape and behavior required during development of multiple tissues, it becomes important to understand the molecular mechanism of the Shroom-Rock interaction and its role in regulating cytoskeletal dynamics. In previous studies I have identified the Rock binding site in the Shroom SD2 and next wanted to map the SBD of Rock and identify residues that are critical for mediating this interaction. Guided by sequence conservation and structural studies I have successfully identified the minimal SBD and conserved surface residues critical for the Shroom-Rock interaction, Rock localization and Shroom3-induced apical constriction.

4.3.1 Key conserved patches at N-terminus of hRock SBD are important for Shroom binding

After examining the sequence conservation profile of Rock SBD across different species I predicted that the highly conserved or invariant amino acid residues in the SBD (834-913) probably are important for mediating the Shroom-Rock interaction. In order to test the hypothesis, I created numerous multi-residue hRock SBD alanine substitution mutants and tested the resulting substitution variants for their ability to bind Shroom. Alanine substitutions were selected to preserve the helical propensity of the coiled coil interface. I was able to identify six different SBD mutants that eliminated or reduced Shroom binding, thus helping me identify a region of the Rock SBD that is critical for SD2 binding. This highly conserved patch is in the N-terminus of the SBD, encompassing amino acids 839-860. Importantly two surface clusters, ^{850}QYF^{852} and ^{857}KTQ^{859}, seem particularly important in binding to Shroom [327]. The presence

of Leucines at characteristic coiled-coil heptad positions suggests a canonical leucine zipper motif in the coiled-coil SBD that is required for Rock-Rock or Rock-SD2 binding. The Rock SBD crystal structure revealed a parallel coiled-coil homodimer with canonical knobs into holes packing interactions at the coiled-coil interface. Results from our *in vitro* binding, colocalization, and apical constriction assays, along with the conservation profile and surface position of these residues, collectively suggests that the residues which are surface exposed on the Rock SBD structure form the Shroom binding site whereas the interiorly buried residues are probably required for Rock dimerization [327]. Mutants that were a combination of both surface exposed and buried residues might locally disrupt the dimerization interface that affected the binding site and combinatorially were defective in Shroom binding. This represents a previously unidentified binding surface on the coiled-coil region of Rock and it spans two highly conserved surface patches, the KTQ and QYF, which might constitute a portion of the binding interface between Shroom SD2 and Rock. The parallel coiled-coil homodimeric form of Rock SBD indicates the presence of an identical binding site on the opposite face of the coiled-coil dimer. Structural analysis of residues in this region reveals a protruded hydrophobic patch formed by the side chains of Y851, F852, L855 that might be important for mediating Shroom-Rock interaction [327].

However, our present analysis does not negate the prospect that the SBD is formed by residues from both chains of the dimer on account of an extended coiled-coil interface. Results from the mutational analysis cannot distinguish between these possibilities but we are confident of the presence of two identical binding sites on opposite faces of the Rock coiled-coil. Each binding site is thus individually occupied by an SD2 probably via its body segment. On account of the extended coiled-coil surface, presumably mutations in conserved residues that are

interiorly buried in the SBD homodimer can abrogate Shroom binding either by disrupting the overall structure of the dimer, thereby distorting the binding site, or by preventing coiled-coil strand interactions within Rock that prevent residues in both monomers from coming together to form a composite binding site. Our present data cannot distinguish between these possibilities. However, based on the previous work and structural and biochemical data obtained thus far regarding the Rock SBD and Shroom SD2 a couple of possible outcomes of Shroom-Rock interaction on Rock activation can be proposed.

Firstly, Shroom binding to Rock can localize it to cortical actin where it can be activated by other effector molecules like RhoA or lipids. This model therefore suggests that Shroom binds to an inactive conformation of Rock (Figure 26A). Secondly, Shroom can bind to pre-activated Rock and recruit it to actin stress fibers. In this model Shroom plays an exclusive localizing effect on Rock where RhoA or lipids have already activated it (Figure 26B). A third possibility is Shroom binding is sufficient to localize as well as activate Rock (Figure 26C). Growing evidence strongly supports the third model and we envision that binding of Shroom SD2 on each face of the Rock homodimer can open up the head to tail folded autoinhibitory conformation of Rock. In light of the Shroom SD2 structure each half dimer of Shroom SD2 contains the two surface patches required for Rock binding. Thus there can be two possibilities. Either each half of a Shroom SD2 dimer can form a half dimer and bind to opposite faces of the Rock SBD homodimer (Figure 26D) or each Shroom SD2 monomer can fold back on itself to form a half dimer that can bind to the Shroom binding site on the SBD homodimer (Figure 26E). This tetramer model would be in accordance with the Shroom-Rock binding stoichiometry of 1:1 and align with the conformational remodeling that is required for bringing the two surface clusters on SD2 to interact with the two Shroom binding site on opposite faces of the Rock

helices simultaneously (Figure 26D, E). Further experiments designed to directly assess the kinase activity of Rock before and after Shroom binding, in presence or absence of RhoA will be required to distinguish between these possibilities and conclusively prove our proposed model.

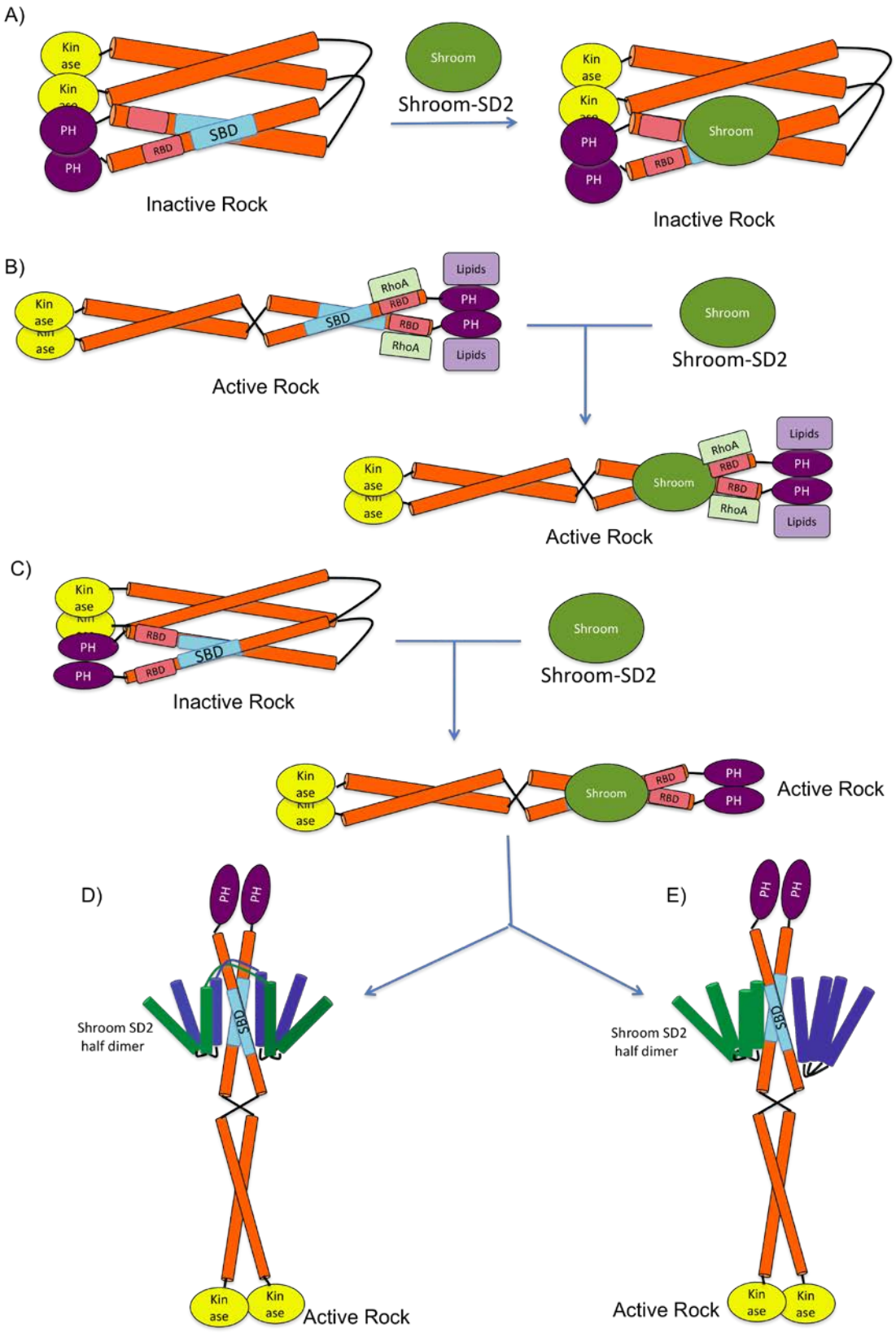
A)
Kin ase
Kin ase
PH
PH
RBD
SBD
Inactive Rock
Shroom
Shroom-SD2
Kin ase
Kin ase
PH
PH
RBD
Shroom
Inactive Rock
B)
Kin ase
Kin ase
SBD
RhoA
RBD
RBD
RhoA
Lipids
PH
PH
Lipids
Active Rock
Shroom
Shroom-SD2
Kin ase
Kin ase
Shroom
RhoA
RBD
RBD
RhoA
Lipids
PH
PH
Lipids
Active Rock
C)
Kin ase
Kin ase
PH
PH
RBD
RBD
SBD
Inactive Rock
Shroom
Shroom-SD2
Kin ase
Kin ase
Shroom
RBD
RBD
PH
PH
Active Rock
D)
PH
PH
SBD
Shroom SD2 half dimer
Kin ase
Kin ase
Active Rock
E)
PH
PH
SBD
Shroom SD2 half dimer
Active Rock
Kin ase
Kin ase

Figure 26: Different models of Shroom-Rock complex formation and Rock regulation

A) Shroom binding to Rock is required exclusively for Rock localization where it is activated by other effector molecules.

B) Shroom binding to Rock is required for Rock localization after it has been pre-activated by other effector molecules.

C) Shroom binding to Rock is necessary and sufficient for Rock localization and activation.

D) Half dimers from Shroom SD2 dimer binds to each binding site on opposite faces of Rock SBD homodimer.

E) Half dimers from Shroom SD2 monomer binds to each binding site on opposite faces of Rock SBD homodimer.

4.3.2 Shroom-Rock binding is important for Rock localization and apical constriction

Shroom3 binding to Rock via its SD2 domain recruits Rock to apical junctions of polarized epithelial cells [5]. Our data show that Rock SBD mutants that fail to bind Shroom also fail to colocalize with Shroom *in vivo*. Alanine substitution mutations at these critical residues abrogate Rock recruitment to the actin cytoskeleton. While all of the mutants tested are compromised in their ability to colocalize with Shroom, there is differing severity, suggesting absolute and accessory roles of these residues in Shroom-mediated Rock localization. Thus, our data reinforces the fact that Shroom-Rock binding is important for Shroom mediated recruitment of Rock to specific subcellular locales. In order to validate the role of these residues in Shroom3 mediated apical constriction, a rescue assay whereby over expression of wild type, kinase dead

or SBD mutant Rock was performed in siRNA treated cells expressing Shroom3. A failure to rescue apical constriction by the Rock SBD mutant clearly shows the importance of these residues in Shroom3 induced changes in cell morphology. These residues are moreover highly conserved across most vertebrate and invertebrate Rock proteins across different species thereby representing an evolutionarily conserved signaling module that regulates cell behavior during cell and tissue morphogenesis. Thus our *in vitro* binding results correlate with our *in vivo* data, thereby helping us to identify the important residues in Rock SBD that are essential for Shroom binding and colocalization.

4.3.3 Implications of a distinct SBD in close proximity of RBD

The presence of a distinct Shroom binding domain located in close proximity (50 amino acids away) to the Rho binding domain raises interesting possibilities of RhoA and Shroom binding to their respective domains and their involvement in Rock regulation. Previous work has shown that Shroom SD2 and active RhoA can simultaneously bind to Rock SBD *in vitro* and they do not outcompete each other [12]. Our *in vivo* results suggest a Rho-independent mode of Rock activation in mediating Shroom3 induced apical constriction. Thus we can conclude that Rock binds independently to both Shroom and RhoA and these interactions may have exclusive or combined roles in Rock regulation. However, in support of our model that Shroom-Rock interaction is necessary and sufficient for Rock activation, we predict that inputs from RhoA may modestly enhance Shroom induced cellular phenotype but is not absolutely required for the same. Our model directly contradicts previous models of Rho-dependent Shroom-induced apical constriction [242]. In the prevailing models, RhoA has been implicated in Shroom-Rock signaling but whether it is upstream or downstream of Shroom still needs to be determined.

RhoA can probably function upstream of Shroom3 in directing the assembly and organization of the actin cytoskeleton at the apical cell-cell adhesion sites that is required for proper Shroom3 localization. Upon apical localization, Shroom can bind to Rock and locally activate myosinII to bring about apical constriction. This is supported by evidence that basally targeted activated RhoA can redistribute ZO-1 and Shroom3 to the basal surface [242]. Recent work from the Zallen lab has shown exciting evidence that Shroom acts downstream of Rho in *Drosophila* where its localization requires RhoGTPase activity but not vice versa [373]. Though Rho does not bind directly to Shroom it can influence Shroom localization indirectly by modulating the actin cytoskeleton [373]. Thus RhoA can function upstream of Shroom3 localization and subsequent apical constriction just like N-cadherin which genetically interacts with Shroom3 to regulate cell shape during gut morphogenesis in mice [241]. More direct kinase assays to assess the catalytic activity of wild type and SBD mutants in presence or absence of Shroom and RhoA will help address this question better.

The identification of a distinct SBD in Rock separate from the other defined binding sites in the coiled-coil of Rock opens up a whole new area of research exploring the role of Shroom-Rock interaction in Rock function and regulation during various developmental processes. I have successfully been able to identify a conserved binding site for Shroom in the central coiled-coil region of Rock and have shown it to be important for Shroom-mediated Rock recruitment to specific subcellular locales and apical constriction in polarized epithelial cells. This novel Rho-independent mode of Rock activation may provide ways to regulate Rock activity in a spatially restricted manner to spatially regulate specific changes in cytoskeletal organization. Also this will provide ways for targeted modulation of Rock activity that would prove therapeutically beneficial in the development of treatment options for various human diseases.

5.0 DISCUSSION AND FUTURE DIRECTIONS

My project involved mapping the binding domains of the two interacting proteins Shroom and Rock, which are key regulators of the cytoskeleton. I have successfully identified the key amino acid residues in the interacting domains of each of the proteins, the SD2 of Shroom and SBD of Rock, and illustrated their role *in vivo*. I have also investigated the role of a single Arginine residue in SD2 in Shroom function *in vivo*. Though my work involved a streamlined investigation of only the interacting domains of Shroom and Rock, we cannot overlook the myriad other regulators of the cytoskeleton that also contribute to cellular and tissue morphogenesis by regulating the cytoskeletal dynamics. Localized activation and assembly of a contractile actomyosin network is the recurrent theme in altering cell behavior including cell shape, migration, adhesion, polarity and cell division. Hence understanding the signaling pathway that leads to the localized activation of this network is crucial for understanding how cells remodel their cytoskeletal architecture. This dissertation focuses only on Shroom and Rock and sections below will discuss the intricate implications of the Shroom-Rock interaction in regulating the cytoskeleton to alter cell shape and behavior.

5.1 DIFFERENTIAL ACTIN BINDING ABILITY AND LOCALIZATION OF SHROOM

An important question that awaits revelation is how actin-binding proteins can target specific populations of actin. Shroom is a class of actin-binding protein and it physically binds to F-actin for its subcellular localization. However, different Shroom family members bind to different populations of F-actin in cells and this probably contributes to their differential localization. Shroom2 and Shroom3 both contain a centrally located SD1 domain that physically interacts with F-actin, however they do so differently. In fibroblasts, Shroom3 can directly bind and bundle actin stress fibers, whereas Shroom2 localizes to cortical actin and fails to induce actin bundling. On the other hand Shroom4 localizes to cytoplasmic pools of F-actin and forms discrete cytoplasmic puncta in the cell [234]. The PDZ and SPR domains of Shroom2 are required for its localization however they are dispensable for Shroom3 localization. The SPR of Shroom2 has also been shown to directly bind to the tight junction protein ZO-1 however the requirement of this interaction for Shroom2 localization still remains unanswered [248]. POSH, a scaffolding protein, has also been shown to directly bind to the SPR domain of Shroom3 via its third SH3 domain to negatively regulate axon outgrowth by modulating the actin-myosin networks [14].

Shroom is a multidomain protein and there is evidence of other unique protein interactions outside of the SD1 and SD2 for both Shroom2 and Shroom3. Mena-Vasp family proteins are also known to regulate cytoskeletal dynamics and are involved in assembly of actin filament networks [345, 374]. It has been shown that mouse Mena/Vasp proteins facilitate localized apical assembly of actin filaments in neural epithelial cells undergoing active apical constriction during neurulation, formation of craniofacial features and during axon guidance

pathways during CNS and peripheral nervous system formation [375, 376]. Interestingly Mena/Vasp can bind to proteins that contain proline-rich consensus sequences via their EVH1 domain. These proline-rich sequences are often found in actin-associated cytoskeletal proteins, Shroom3 being one example. Though a direct physical interaction between Mena/Vasp proteins and Shroom3 has not yet been tested, cell based assays have shown the requirement of this proline-rich sequence in Shroom3 induced apical constriction in polarized MDCK cells and apical accumulation of Vasp. Further, dominant-negative Mena can block apical constriction both *in vivo* and *in vitro* [12]. Lulu or EPB4.1l5, another cytoskeleton associated protein promotes apical accumulation of Shroom3 and cooperates with Shroom3 to induce apical constriction during neural tube closure in *Xenopus* [226]. There are other examples of cytoskeleton associated proteins that are critical regulators of actomyosin contractility and are required during embryonic development especially during neural tube closure, with defects resembling Shroom3 null mutant mice. However interactions between these proteins and Shroom have not yet been established and it remains to be revealed whether Shroom can act as a scaffolding protein in bringing together all these components that can modulate the cell architecture by reorganizing the actomyosin networks. Recent work by the Zallen lab has shown RhoGTPase to be the upstream regulator of *Drosophila* Shroom, directing its localization to adherens junctions of cells [373]. Their work also suggests a role of Shroom in directing planar polarized actomyosin contractility during axis elongation. It will be interesting to elucidate the role of Shroom-Rock signaling in establishment and maintenance of this polarized actomyosin contractility during neural tube morphogenesis and convergent extension in mice.

It is still unknown whether Shroom exhibits an isoform specific binding to Rock or myosinII activation. It will be interesting to investigate whether selective binding of Shroom to

Rock1 and Rock2 as well as activation of myosinIIA, IIB or IIC, contributes to differential cellular outcomes. Thus it is probable that unique protein interactions outside of the known domains of Shroom can direct its differential subcellular localization. A structural insight into the SD1 domain from different Shroom family members will facilitate understanding of its ability to bind to different pools of actin to localize differentially in a cell and subsequently recruit Rock to these specific subcellular locales.

5.2 SHROOM REGULATION

Shroom is an actin-binding protein and it regulates cell shape and behavior by regulating F-actin and non-muscle myosinII both spatially and temporally. Thus, Shroom regulation proves critical for various developmental processes especially during neural tube morphogenesis, eye development, gut morphogenesis, neuronal architecture and function and many others. A few upstream transcriptional activators of Shroom have been identified, however post-transcriptional or post-translational modifications of Shroom, if any, remains unknown. Shroom protein is typically apically localized in polarized epithelial cells and previous work from our lab has shown actin binding of Shroom to be the critical spatial determinant in its function [234]. Though there is no precedence for an inactive and active form of Shroom, a question that remains unanswered is what regulates Shroom activity. The temporal regulation of Shroom, as to how it gets expressed at the right place and at the right time, whether it is constitutively expressed, and if there is a threshold level of protein expression that can mediate Shroom function still needs to be addressed. Since phosphorylation is a widely used mode of regulation employed by different multidomian proteins and most cytoskeleton binding proteins, it becomes

an interesting avenue to investigate for Shroom regulation. ExPASy phosphorylation prediction tool identifies numerous serine, threonine and tyrosine residues as putative sites for phosphorylation. Also, prediction of kinase specific phosphorylation sites in Shroom3 reveals quite a few kinases like PKC, PKA, PKB and cdk5 among others to have putative phosphorylation sites in Shroom3 with the highest score of 0.92 for PKC targeting Threonine at position 1088. It will be interesting to test for Shroom phosphorylation on incubation with PKC.

Rock can bind to lipids via its PH domain and since Rock is a binding partner for Shroom it might be interesting to investigate if Shroom is also a substrate for lipid membrane kinases. Lipid phosphorylation by PI3K can orchestrate complex cell behaviors like cell motility, migration, growth and survival all of which contributes to cancer. Various signaling proteins like serine threonine kinases, Rho effector molecules have specific domains to interact with these phosphorylated lipids. These interactions promote apical accumulation of these signal transducers and assembly of signaling complexes to initiate local responses like actin polymerization and assembly, or triggering phosphorylation cascades. Investigating the role of Shroom and Rock in acting as a scaffolding protein to assemble signaling complexes that can in turn phosphorylate Shroom in a feedback loop will shed some light on Shroom regulation. Other post translational modifications like acetylation and glycosylation which also play a role in regulating protein function are not detected by ExPASy for Shroom protein, however a direct investigation of the phosphorylation status of Shroom and its implications in Shroom activity need to be undertaken.

5.3 ROLE OF SHROOM-ROCK INTERACTION IN ROCK ACTIVATION AND CELL MORPHOLOGY

An important aspect of the Shroom-Rock-MyosinII signaling pathway is the mechanism of Rock activation. Rock remains in a folded autoinhibitory conformation via intramolecular interactions between the N-terminal kinase domain and the C-terminal region. It is thought that relief of this intramolecular inhibition is brought about by RhoA-GTP binding, lipid binding or caspase cleavage of the C-terminus. RhoA-GTP binding modestly enhances the catalytic activity of Rock *in vitro* [6, 263] and there is no direct evidence that RhoA is the exclusive upstream activator of Rock. There is growing evidence of a Rho-independent mode of Rock activation and work from our lab and others have shown that inhibiting RhoA does not abrogate Shroom3-induced apical constriction in MDCK cells or *Xenopus* embryos. Also Shroom, Rock and Rho can form a trimeric complex *in vitro* despite the physical proximity of the Shroom binding and Rho binding domains in Rock, establishing a non-competitive simultaneous binding of Shroom and Rho to Rock [242]. A RhoA-Rock complex is however not detected *in vivo*. Also siRNA mediated knockdown and rescue assays have shown the requirement of Shroom-Rock binding and not Rho-Rock binding in eliciting apical constriction in polarized epithelial cells.

We propose that Shroom-Rock interaction is sufficient for Rock activation. There can be two possibilities, one being that Shroom binding to Rock is required for its subcellular localization whereas Rock activation is brought about by other effector molecules like RhoA-GTP. The other possibility being Shroom binding is necessary and sufficient for Rock localization and activation. My data on Shroom SD2 has shown the requirement of Shroom-Rock binding in activation of Rock-MyosinII pathway. Using indirect immunofluoresence we have already shown the Shroom SD2 mutants that fail to bind Rock, fail to cause apical constriction

and apical enrichment of activated myosinII. An alternative way to test this will be to perform Western blotting using antibodies specific to the phosphorylated form of Rock substrates, mainly RMLC and MYPT, in cells that express Shroom3 or Shroom3 SD2 mutants to determine if Shroom3 can increase the phosphorylation levels of Rock targets. A direct estimation of the catalytic activity of Rock via kinase assays using WT Rock or SBD or RBD mutants, immunoprecipitated from cells in the presence or absence of Shroom SD2, towards a known substrate, will help us accurately determine the role of Shroom in Rock activation. Perhaps, switching to a baculovirus expression system for purification of a functional form of the kinase and utilizing it in direct kinase assays may prove helpful.

Cell adhesion maintains tissue integrity as well as transduces signals from extracellular matrix and adjoining cell neighbors. Shroom localizes to the adherens junctions of epithelial cells by directly binding to actin. Therefore cell adhesion seems to be important for proper localization and function of Shroom. Previous work from our lab has shown that Shroom-mediated apical constriction in polarized MDCK cells is Rock and MyosinII dependent. We can assess Shroom3-induced apical constriction in cells treated with siRNAs against RhoA, MyosinII and E-cadherin (an adherens junction protein). A Rho-independent mode of Rock activation would still cause apical constriction in RhoA siRNA treated cells whereas myosinII siRNA treated cells would fail to undergo apical constriction. I am in the process of creating stable MDCK cell lines expressing Shroom3 or Shroom3 SD2 mutants under an inducible promoter to assess the phosphorylation status of RMLC which will serve as a direct readout of activated myosinII and substantiate the role of Shroom-Rock signaling in activation of Rock-myosinII pathway to bring about apical constriction in polarized epithelial cells. However, these are all over expression systems and variable results regarding Rho-dependent or independent mode of

Rock activation can be attributed to the differences in models where it has been tested like chick, *Xenopus*, mice and MDCK cells. Thus *in vitro* biochemical approaches combined with *in vivo* results could provide a more convincing and accurate picture of the Shroom-Rock-MyosinII pathway operating in cells undergoing morphogenesis during development. To that end generating a Shroom-Rock compound heterozygous mouse will be helpful. Alternatively, conditionally knocking-out Rock1/2 in Shroom3 heterozygous mice will probably help elucidate the role of Shroom-Rock binding in cell and tissue morphogenesis. This *in vivo* model would also facilitate understanding of the role of Shroom in Rock activation and the consequences of simultaneous depletion of both Shroom and Rock on the downstream targets of this signaling pathway.

Though data from our lab directly contradicts the canonical mode of Rock activation via RhoAGTP, the present body of data cannot determine if RhoA functions upstream or downstream of Shroom or Rock. Work from other labs have shown that apically targeted, activated RhoA can direct Shroom subcellular localization at the apical surface of cells. Basally targeted activated RhoA can also induce basal constriction and promote basal localization of Shroom3 with redistribution of ZO-1 at the basal surface [242]. Thus, it is probable that RhoA activity is required for reorganizing the actin cytoskeleton associated with apical cell-cell junctions, which is essential for proper Shroom3 localization. In fact recent work has shown evidence of RhoGTPase signaling upstream of Shroom in *Drosophila* to direct its subcellular localization to the adherens junctions of cells [373]. There is evidence of other adhesion proteins like N-cadherin that can genetically interact with Shroom3 to modulate the cytoskeleton machinery to drive apical constriction and cell elongation during embryonic gut development [13], thus further confirming an accessory and not an obligate role of RhoA in Shroom mediated

apical constriction. Conversely, both RhoA and Shroom binding may be required individually or combinatorially for regulating Rock activity in distinct biological processes that conforms a Rho-dependent mode of Rock activation. In order to clearly dissect the contributions of RhoA and Shroom in regulating Rock localization and activity, experiments designed to directly measure the catalytic activity of Rock in presence of various combinations of RhoA and Shroom will be required.

All the Shroom proteins tested to date can either bind to F-actin directly or can colocalize with actin [11, 15, 234, 235, 238, 248, 377, 378]. This Shroom-Actin interaction is mediated by the centrally located SD1 in Shroom2, Shroom3 and dShroom and a less conserved centrally located region in Shroom4. Aditionally Shroom proteins have the ability to regulate higher order architecture of actin filaments. Both Shroom3 and dShroom can cause actin bundling both in vivo and in vitro whereas Shroom2 and Shroom4 can induce ectopic actin structures when expressed in fibroblasts, endothelial or epithelial cells [11, 234, 235, 238]. This partially explains the two different phenotypes that we observe when we overexpress Shroom in MDCK cells or Cos7 cells. Shroom3 elicits apical constriction in polarized epithelial MDCK cells, whereas it localizes to actin stress fibers and cortical actin in fibroblast like Cos7 cells. We think that Shroom3 binds to a specific population of actin at the apical domain of MDCK cells to induce contractility. However, it binds to cortical actin and actin stress fibers in Cos7 cells to reorganize actin into higher order structures. Therefore the cell specific effects that we observe are probably due to Shroom localizing to different populations of actin in a cell.

Also, our collaborator, the VanDemark lab, is currently extending efforts to solve the structure of the Shroom-Rock complex and the conformational changes that are involved in this interaction. The structure of Shroom-Rock complex along with information gleaned from the

structure of the Shroom SD2 and Rock SBD will provide structural insights into the protein conformational rearrangement during Shroom-Rock binding and facilitate understanding of its influence on Rock activity, as well as the precise stoichiometry of Shroom-Rock interaction.

5.4 CLINICAL IMPLICATIONS OF SHROOM-ROCK-MYOSIN II PATHWAY

Rock has been implicated in many debilitating diseases like cancer, pulmonary hypertension, diabetes, CNS disorders, cardiovascular diseases, atherosclerosis, obesity and many others [357-359, 379-388]. In all of these examples, Rock imparts pathophysiologic effects by modulating the cytoskeletal architecture of the cell. Rock positively regulates myosinII and negatively regulates myosin phosphatase targeting subunit by phosphorylating Serine and Threonine residues of these downstream targets. This leads to the activation of myosinII ATPase activity and assembly of a contractile actomyosin network. Thus phosphorylation of RMLC or MYPT is considered as a direct readout of Rock activity and activated myosinII. Shroom3, a binding partner for Rock has also been shown to cause apical enrichment of activated myosinII during apical constriction. My previous work on Shroom SD2 and Shroom ENU mutants has shown the essentiality of Shroom-Rock binding in activating the Rock-myosinII pathway and bringing about apical constriction in polarized MDCK cells. Previous work has established the clinical importance of Shroom family of proteins in vertebrate embryonic development especially during neural tube closure, gut morphogenesis, eye development, kidney development, vascular development, neuronal development and function [5, 8-15, 195, 231, 232, 237, 243, 244]. By knowing the role of Shroom and Rock individually in vertebrate development, it becomes important to understand the implications of the Shroom-Rock-myosinII pathway for assessing

the clinical significance of this signaling module and establishing a paradigm for cellular and tissue morphogenesis.

The kinase activity of Rock is central to cytoskeletal reorganization. The autoinhibited conformation of Rock adds another layer of complexity to Rock regulation. Lack of conclusive proof regarding a Rho-dependent or independent mode of Rock activation has opened up new vistas of research. Rock is a direct downstream target of Rho family of GTPases specifically RhoA and this interaction is thought to relieve the intramoelcular inhibition between the kinase domain and C-terminal domain of Rock rendering it catalytically active. Work from our lab has provided evidence of a Rho-independent mode of Rock activation. We therefore propose a model whereby Shroom-Rock interaction is necessary and sufficient for Rock subcellular localization and activation. Rock's involvement in a multitude of cell processes like cell migration, adhesion, division, polarity, epithelial morphogenesis and neurite retraction and its involvement in a variety of different diseases makes it an interesting therapeutic target for drug development. This has indeed proven to be a daunting task since blocking or increasing Rock activity without causing global perturbations in the cell has been impossible [382, 385, 389-396]. A clear understanding of the molecular mechanism of the Shroom-Rock-myosinII pathway fills in this void and would prove beneficial for selective modulation of Rock activity by targeting Rock localization and activation. It will facilitate understanding of the spatial and functional regulation of Rock activity via Shroom and would help us to target defined aspects of Rock activity leaving others untouched. Additionally, Rock1 and 2 exhibit unique roles as well as functional redundancy. To dissect the contributions of each isoform in vertebrate development and disease, knowing the critical residues in Rock that mediate dimerization, protein binding and kinase activity, may elucidate targets for an isoform specific inhibitor of Rock. Future experiments

ultilizing isoform specific siRNAs will also be able to address the differential roles of Rock1 and Rock2 in altering cell morphology. Since Shroom, Rock, Rho and myosinII are involved in myriad different processes we predict that a clear understanding of the molecular mechanism of Shroom-Rock interaction will provide insights into how different signaling network and pathways are integrated. Also, understanding this signaling module will provide a paradigm as to how cell morphology is controlled during normal development and how lesions in this pathway can lead to disease development. This will further help in the designing of pharmaco-therapeutic inhibitors or drugs as treatment options for these diseases.

6.0 MATERIALS AND METHODS

6.1 MUTAGENESIS OF SHROOM SD2 AND ROCK SBD PROTEINS

Mouse Shroom SD2 mutants (SC and HD mutations) were made using the QuickChange Site-Directed Mutagenesis kit. Mutagenesis was performed on mShroom3 in pCS2-Endolyn-Shroom3 expression plasmid spanning amino acids 1372-1986. For *in vitro* expression of mShroom3 SD2 mutant proteins the mutated sequence encoding amino acids 1562-1986 was cloned from the Endolyn-Shroom3 vector into pGex-2TK for expression in *E.coli* CodonPlus (RIPL) cells. Shroom SD2 mutants (R1844A, R1844C in mouse Shroom3 and R1474A and R1474C in *Drosophila*) were made using the QuikChange Site-Directed Mutagenesis Kit (Stratagene, Santa Clara, CA). mShroom3 mutagenesis was performed on the pCS2 vector harboring ShroomS (amino acids 286-1986) [11]. The mutated Shroom SD2 sequences were further cloned from pCS2 into pGEX-3X vector for various biochemical assays and *in vitro* expression in *E.coli* CodonPlus RIPL cells. The dShroom mutants were created in a pET151-D/TOPO vector (Invitrogen, Carlsbad, CA) harboring the dShroom SD2 coding sequence for amino acids 1393-1576. Recombinant proteins were expressed in codon plus BL-21(DE3) *E.coli* cells and purified as described [9, 327, 328]. Human Rock SBD mutants were made using the QuickChange Site-Directed Mutagenesis Kit (Stratagene, Santa Clara, CA). hRock1 mutagenesis was performed on pET151D/TOPO vector harboring either hRock1 amino acids 707-946 or amino acids 834-913.

hRock SBD mutants that were tested for colocalization assays were made in pCS3-myc tag vector harboring hRock1 amino acids 681-942.

6.2 PROTEIN EXPRESSION AND PURIFICATION

Large-scale protein expression of His-tagged SD2 and Rock SBD proteins was performed in BL21(DE3) *Escherichia coli* cells using ZY autoinduction media as described [9, 344]. The Shroom3 and Rock proteins were concentrated to 0.78 mg/ml (WT Shroom) and 1.43 mg/ml (R1838A) and 1.7 mg/ml (R1838C) and 1mg/ml (WT Rock) in 20 mM Tris, pH 8.0, 0.5 M NaCl, 8% glycerol, and 5 mM dithiothreitol (DTT). For purification of GST-Shroom3 SD2 or small-scale (<50 ml) expression of His-tagged hRock SBD proteins, BL21 cells or RIPL cells harboring the relevant plasmids were induced with 0.5 mM isopropyl β-D-1-thioglactopyranoside(IPTG) for 2 hours and collected by centrifugation. Cells were lysed by sonication in NETN buffer (for GST-fusion proteins; 20mM Tris, pH 8.0, 0.1 M NaCl, 1mM EDTA, 0.5% NP-40) or His-lysis buffer (for His-fusion proteins; 20mM Tris, pH 8.0, 0.5 M NaCl, 8% glycerol, 5mM β-mercaptoethanol) supplemented with Protease inhibitor cocktail and soluble proteins were purified using either glutathione-sepharose resin or Ni-NTA beads. Beads were washed in lysis buffer and the proteins eluted with either free glutathione or imidazole in the respective lysis buffers. Protein expression of dShroom SD2 proteins was performed in BL21(DE3) *Escherichia coli* cells using ZY autoinduction media as described in Mohan etal, 2012 [328]. The dShroom proteins were concentrated to 2 mg/ml (WT and R1474A) and

10mg/ml (R1474C) in 20 mM Tris, pH 8.0, 0.5 M NaCl, 8% glycerol, and 5 mM dithiothreitol (DTT).

6.3 IN VITRO PULL DOWN ASSAYS

GST-pull down assays was performed with either wild type GST-mShroom3 SD2 or SC and HD mutants spanning amino acids 1562-1986 bound to glutathione beads and mixed with soluble hRock1 (residues 707-946). Complexes were washed with NETN, resuspended in SDS-PAGE sample buffer, resolved on 12% SDS-PAGE and detected using Coomassie Blue. GST pull-down assays were also performed using either wild type GST-Shrm3 SD2 or R1844A and R1844C mutant versions (spanning amino acids 1562-1986) bound to Glutathione beads (GE Healthcare) and mixed with soluble, His tagged hRock1 SBD (residues 707-946). The binding reaction was incubated for 2 hours at room temperature. Complexes were washed with NETN, resuspended in SDS-PAGE sample buffer, resolved on 12% SDS-PAGE, and detected using Coomassie Blue. His-tagged versions of hRock1 SBD wild type or mutant proteins harboring either amino acids 707-946 or 834-913 were bound to Ni-resin and mixed with untagged mShroom3 SD2 (residues 1642-1951), incubated for 2 hours at room temperature. Complexes were washed with Lysis Buffer, resuspended in SDS-PAGE sample buffer, resolved on 12% SDS-PAGE and detected using Coomassie Blue.

6.4 COMPLEX FORMATION

For native gel electrophoresis, a fixed concentration (5 µM) of hRock SBD spanning amino acids 707-946 was mixed with increasing concentration of purified Shroom3 SD2 spanning amino acids 1642-1951 (0.25-5µM) and incubated for 2 hours at 4^0C. Samples were then loaded on 8% PAGE gels, resolved by electrophoresis at 4^O C and proteins detected with Coomassie blue. For solution binding and native gel electrophoresis, a fixed concentration (5 µM) of dRock 724-938 was mixed with increasing concentration of dShrmSD2 (1-10 µM) and incubated overnight at 4^0C. Samples were then loaded on 8% PAGE gels, resolved by electrophoresis at 4^O C and proteins detected with Coomassie blue.

6.5 CELL CULTURE AND IN VIVO ANALYSIS

T23 MDCK cells were grown in EMEM supplemented with 10% FBS (Hyclone), pen/strep, and L-Glutamine at 37^0C and 5% CO_2. Cos7 cells were grown in DMEM supplemented with 10% FBS (Hyclone), pen/strep, and L-Glutamine under similar conditions. Cells were removed from the plates using Trypsin-EDTA and passaged every 2-3 days. For transient transfection of cells on transwell filters, cells were plated at a density of $8x10^5$ cells (MDCK) or $6x10^5$ cells per well (Cos7) and grown for 24 hours. Cells were transfected with the DNA of interest (1µg) using Lipofectamine 2000 (Invitrogen) and grown for 24 hours prior to processing. For immunofluorescent analysis, cells were fixed using either –20°C methanol for 5 minutes or 4% paraformaldehyde (PFA) in PBS for 15 minutes. Fixed cells were stained with primary antibody

for 1 hour at RT, washed in PBT three times for 5 minutes at room temperature, stained with secondary antibody for 1 hour at room temperature, washed as above and mounted using VectaShield (Vector Labs) or Immuno-fluore Mounting medium (MP Biomedicals).

Shroom3-induced apical constriction using expression plasmids pCS2-Endolyn-Shroom3(WT) or the SC and HD mutants, pCS2-Shroom3, pCS2-Shroom3 R1838A, pCS2-Shroom3 R1838C was performed and imaged as described previously [15]. Transfected cells were stained with primary antibodies UPT132 (1:100, rabbit anti-Shrm3) [15] and Rat anti-ZO1 (1:100, Chemicon) and Alexa-488 or 568 conjugated goat anti-rabbit or goat anti-rat secondary antibodies conjugated to (1:400, Invitrogen). Apical constriction was quantified by measuring the apical area of either parental or transfected cells, as determined by ZO1 staining, in ImageJ. To determine colocalizaton of Shroom3, Rock SBD, and pRLC, MDCK cells or Cos7 cells expressing Shroom3 variants and/or myc-tagged, wild type hRock1 SBD (spanning amino acids 681-942) were plated on either transwell membranes or fibronectin (Sigma Life Sciences) coated coverslips, respectively, for 24 hours. Cells were stained with UPT132 (1:100, rabbit anti-Shrm3, Hildebrand, 2005), 9E10 (1:100, mouse anti-myc, a gift from Dr. Ora Weisz), and mouse anti-pS19 myosin RLC (Cell Signaling). Primary antibodies were detected using Alexa-488 or 568 conjugated secondary antibodies goat anti-rabbit or goat anti-mouse (1:400, Invitrogen) and imaged as described above. To determine the degree of colocalization in Cos7 cells, ImageJ plug-ins Colocalization Finder and Mander's Coefficients were used to analyze individual channels from merged confocal images. To analyze the co-distribution of Shroom3 and pRLC, fluorescent intensities along line segments drawn on individual channels were measured and plotted using Excel. Images were acquired using a Biorad Radiance 2000 Laser Scanning System

mounted on a Nikon E800 microscope or Olympus Fluoview FV1000 Confocal microscope (FV10-ASW) with 40X oil objectives and processed using either ImageJ or Photoshop.

6.6 LIMITED PROTEOLYSIS

This assay was performed by Jenna Zalewski and Swarna Mohan from the VanDemark lab. 50μM of wild-type and mutant Shroom3 SD2 proteins were treated with 40μg of the protease Subtilisin A for the indicated times and samples taken at each time point were resolved via SDS-PAGE.

6.7 SIZE-EXCLUSION CHROMATOGRAPHY

This assay was performed by Jenna Zalewski from the VanDemark lab. Purified WT and mutant proteins were concentrated to 1mg/mL in buffer containing 2% glycerol, 250mM NaCl, 20mM Tris pH 8.0, and 1mM β-mercaptoethanol. 500uL were run over a Sephacryl S-200 gel filtration column, and traces were generated using Unicorn 6.3.2.89 Control Software.

6.8 CHEMICAL CROSSLINKING

This assay was performed by Jenna Zalewski and Swarna Mohan from the VanDemark lab. dShrm SD2 mutants and wild type protein was incubated with the indicated concentration of glutaraldehyde in a reaction buffer containing 25 mM HEPES pH 7.5, 8% Glycerol, 500 mM NaCl and 5 mM β-ME, with a final dShrm SD2 concentration of 16μM. At each time point, 20μl of the crosslinking reaction was removed and the reaction stopped with 2 μl of 1.0 M Tris at pH 8.0 and the sample subjected to SDS-PAGE and visualized using Coomassie blue staining.

APPENDIX A

PROTEIN PURIFICATION

A.1 HUMAN ROCK1 SBD MUTANT PROTEINS PURIFICATION

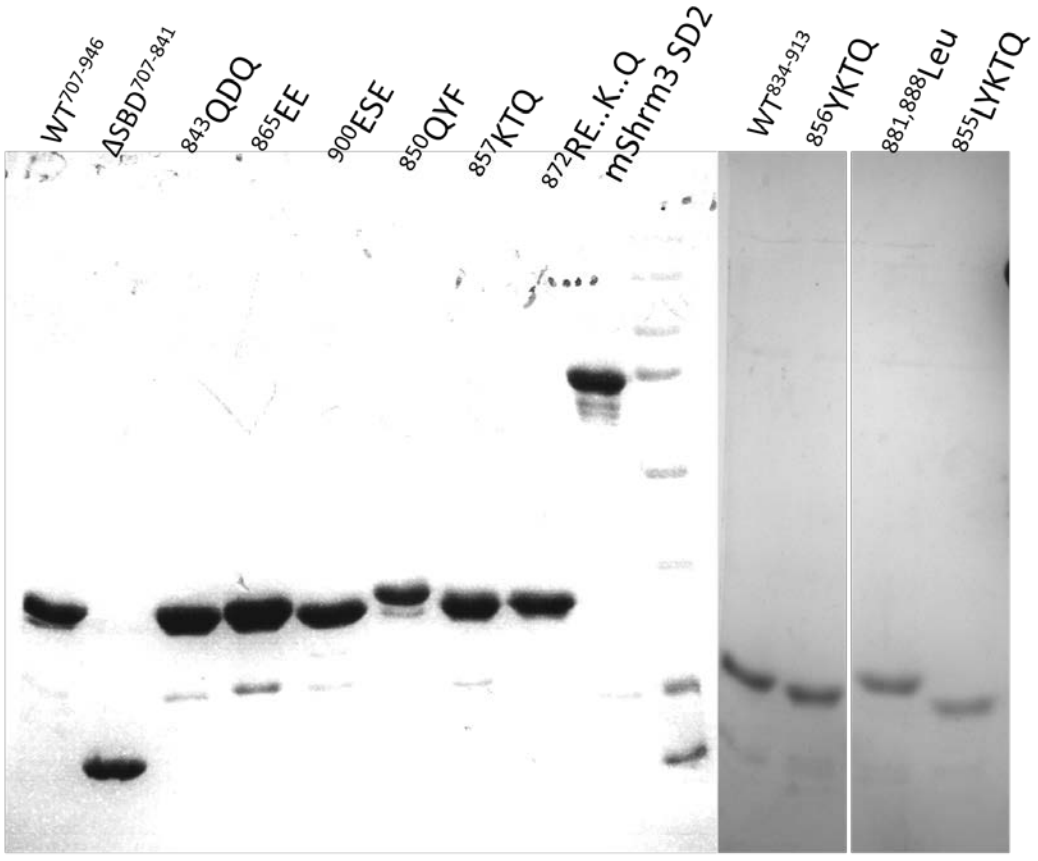

Figure 27: hRock1 SBD mutant proteins expression and purification

pET151D/TOPO expression plasmid harboring hRock1 SBD (amino acids 707-946 or 834-913) was used as a template to create the different SBD mutants via Site-Directed mutagenesis. Correct clones were selected after sequencing and transformed into RIPL cells. Protein expression was induced using IPTG and purified from a 50ml culture using Ni-NTA beads. 10ul of 10uM purified His-tagged protein was run on a 12% SDS-PAGE to assess for expression levels and purity.

A.2 HUMAN ROCK1 RBD PROTEINS PURIFICATION AND PULL DOWN

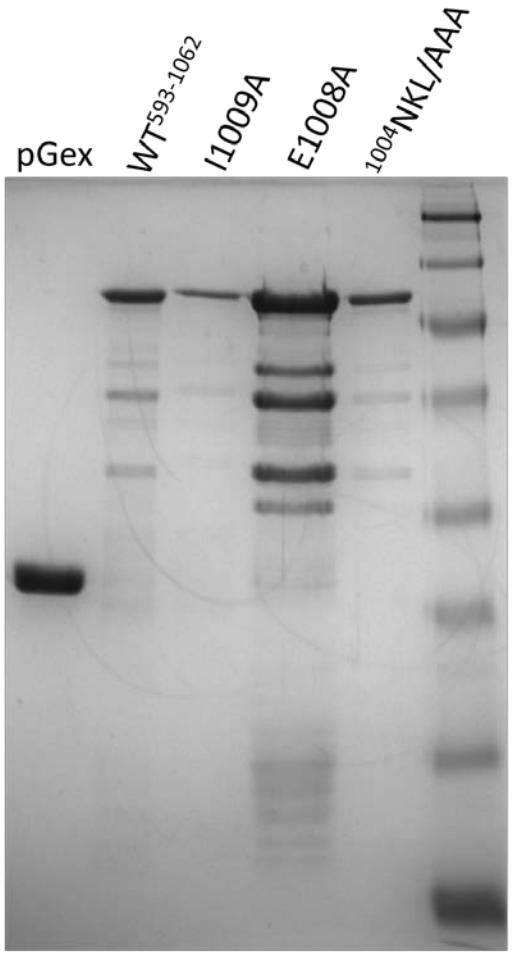

Figure 28: hRock1 RBD mutant proteins expression and purification

pGEX expression plasmid containing hRock1, spannig amino acids 593-1062, was used as a template to generate the RBD mutants I1009A, E1008A and ^{1004}NKL^{1006}/AAA via Site-directed mutagenesis. Correct clones were selected after sequencing and transformed into RIPL cells. Protein expression was induced using IPTG and purified using Glutathione beads. 10 ul of purified GST-tagged hRock1 RBD proteins were run on a 12% SDS-PAGE and stained with Coomassie Blue to assess for expression and purity.

APPENDIX B

OLIGONUCLEOTIDE SEQUENCES

B.1 SHROOM SD2 OLIGONUCLEOTIDES

^{1766}KKAEL^{1770}/^{1766}AKARA^{1770}

(F) 5’ GAG GAT GTC TAT GAG GCT AAG GCT CGC GCT ATC GGA AGC CTC ACC 3’

(R) 5’ GGT GAG GCT TCC GAT AGC GCG AGC CTT AGC CTC ATA GAC ATC CTC 3’

^{1840}SLSGRLA^{1846}/^{1840}ALEADLE^{1846}

(F) 5’ GTC AAC CTG CTG CTG GCT CTG GAG GCT GAC CTG GAG CGC GTG GAG AAC GTC 3’

(R) 5’ GAC GTT CTC CAC GCG CTC CAG GTC AGC CTC CAG AGC CAG CAG CAG GTT GAC 3’

^{1878}LKENLDRR^{1885}/^{1878}AAENLDDA^{1885}

(F) 5’ GAG GAC GCA CGG GAG GCT GCT GAG AAC CTG GAC GAC GCT GAG CGC GTG GTG CTG 3’

(R) 5’ CAG CAC CAC GCG CTC AGC GTC GTC CAG GTT CTC AGC AGC CTC CCG TGC GTC CTC 3’

^{1832}LLSL^{1835}/^{1832}AASA^{1835}

(F) 5’ AAG GTG GTC AAC CTG GCT GCT TCC GCT TCT GGA CGC CTG GCC 3’

(R) 5’ GGC CAG GCG TCC AGA AGC GGA AGC AGC CAG GTT GAC CAC CTT 3’

^{1915}LLIEQRKL^{1922}/^{1915}ALIEQAKA^{1922}

(F) 5’ AAG ATG AAG TCC ACA GCT CTC ATT GAG CAG GCT AAG GCT GAT GAC AAG AAG ATA AAG 3’

(R) 5’ CTT TAT CTT GTC ATC AGC CTT AGC CTG CTC AAT GAG AGC TGT GGA CTT CAT CTT 3’

^{1840}SLSGRLA^{1846}/^{1840}SLSGALA^{1846} (mouse)

(F) 5’ CTG TCC CTG TCT GGA GCC CTG GCC CGC GTG GAG 3’

(R) 5’ CTC CAC GCG GGC CAG GGC TCC AGA CAG GGA CAG 3’

^{1840}SLSGRLA^{1846}/^{1840}SLSGCLA^{1846} (mouse)

(F) 5’ CTG TCC CTG TCT GGA TGC CTG GCC CGC GTG GAG 3’

(R) 5’ CTC CAC GCG GGC CAG GCA TCC AGA CAG GGA CAG 3

^{1470}SLSERLA^{1476}/^{1470}SLSEALA^{1476} (Drosophila)

(F) 5’ CTG TCG CTT TCC GAG GCC TTG GCC CAA ACC GAA 3’

(R) 5’ TTC GGT TTG GGC CAA GGC CTC GGA AAG CGA CAG 3’

^{1470}SLSERLA^{1476}/^{1470}SLSECLA^{1476} (Drosophila)

(F) 5’ CTG TCG CTT TCC GAG TGT TTG GCC CAA ACC GAA 3’

(R) 5’ TTC GGT TTG GGC CAA ACA CTC GGA AAG CGA CAG 3’

B.2 ROCK SBD OLIGONUCLEOTIDES

^{843}QDQ^{845}/^{843}AAA^{845}

(F) 5’ CAG ATG CGG GAG CTA GCT GCT GCT CTT GAA GCT GAG CAA 3’

(R) 5’ TTG CTC AGC TTC AAG AGC AGC AGC TAG CTC CCG CAT CTG 3’

^{865}EE^{866}/^{865}AA^{866}

(F) 5’ GTA AAG GAA CTT AAA GCT GCT ATT GAA GAA AAA AAC 3’

(R) 5’ GTT TTT TTC TTC AAT AGC AGC TTT AAG TTC CTT TAC 3’

^{900}ESE^{902}/^{900}AAA^{902}

(F) 5’ GCA GAA ACA AAA GCT GCT GCT GCT CAG TTG GCG CGA GGC 3’

(R) 5’ GCC TCG CGC CAA CTG AGC AGC AGC AGC CTT TTG TTT CTG 3’

^{850}QYF^{852}/^{850}AAA^{852}

(F) 5’ CAA GAT CAG CTT GAA GCT GAG GCA GCT GCC TCG ACA CTT TAT AAA ACC C 3’

(R) 5’ GGG TTT TAT AAA GTG TCG AGG CAG CTG CCT CAG CTT CAA GCT GAT CTT G 3’

^{857}KTQ^{859}/^{857}AAA^{859}

(F) 5’ GAG CAA TAT TTC TCG ACA CTT TAT GCA GCC GCG GTA AAG GAA CTT AAA GAA G 3’

(R) 5’ CTT CTT TAA GTT CCT TTA CCG CGG CTG CAT AAA GTG TCG AGA AAT AAT ATT GCT C 3’

^{872,873,876,879}RE..K..Q/^{872,873,876,879}AA..A..A

(F) 5’ GAA GAA ATT GAA GAA AAA AAC GCA GCA AAT TTA GCG AAA ATA GCG GAA CTA CAA AAT GAA 3’

(R) 5’ TTC ATT TTG TAG TTC CGC TAT TTT CGC TAA ATT TGC TGC GTT TTT TTC TTC AAT TTC TTC 3’

^{842,846}Leu/^{842,846}Ala

(F) 5’ GAA GGA CAG ATG CGG GAG GCA CAA GAT CAG GCT GAA GCT GAG CAA TAT TTC 3’

(R) 5’ GAA ATA TTG CTC AGC TTC AGC CTG ATC TTG TGC CTC CCG CAT CTG TCC TTC 3’

^{860,863}V..L/^{860,863}A..A

(F) 5’ GAC ACT TTA TAA AAC CCA GGC AAA GGA AGC TAA AGA AGA AAT TGA AG 3’

(R) 5’ CTT CAA TTT CTT CTT TAG CTT CCT TTG CCT GGG TTT TAT AAA GTG TC 3’

^{849}EQYF^{852}/^{849}AAAA^{852}

(F) 5’ GAT CAG CTT GAA GCT GCT GCT GCT GCT TCG ACA CTT TAT AAA 3’

(R) 5’ TTT ATA AAG TGT CGA AGC AGC AGC AGC AGC TTC AAG CTG ATC 3’

^{900}ESEQLAR^{906}/^{900}AAAAAAA^{906}

(F) 5’ GCA GAA ACA AAA GCT GCT GCT GCT GCT GCT GCT GCT GGC CTT CTG GAA GAA 3’

(R) 5’ TTC TTC CAG AAG GCC AGC AGC AGC AGC AGC AGC AGC AGC TTT TGT TTC TGC 3’

^{842,846,855}Leu/ ^{842,846,855}Ala

(F) 5’ ATG CGG GAG GCT CAA GAT CAG GCT GAA GCT GAG CAA TAT TTC TCG ACA GCT TAT AAA ACC 3’

(R) 5’ GGT TTT ATA AGC TGT CGA GAA ATA TTG CTC AGC TTC AGC CTG ATC TTG AGC CTC CCG CAT 3’

^{856}YKTQ^{859}/^{856}AAAA^{859}

(F) 5’ TAT TTC TCG ACA CTT GCT GCT GCT GCT GTA AAG GAA CTT AAA 3’

(R) 5’ TTT AAG TTC CTT TAC AGC AGC AGC AGC AAG TGT CGA GAA ATA 3’

^{855}LYKTQ^{859}/^{855}AAAAA^{859}

(F) 5’ CAA TAT TTC TCG ACA GCG GCC GCT GCT GCT GTA AAG GAA CTT AAA 3’

(R) 5’ TTT AAG TTC CTT TAC AGC AGC AGC GGC CGC TGT CGA GAA ATA TTG 3’

^{881,888}Leu/ ^{881,888}Ala

(F) 5’ AAG AAA ATA CAG GAA GCT CAA AAT GAA AAA GAA ACT GCT GCT ACT CAG TTG GAT 3’

(R) 5’ ATC CAA CTG AGT AGC AGC AGT TTC TTT TTC ATT TTG AGC TTC CTG TAT TTT CTT 3’

^{842}LQDQL^{846}/^{842}AAAAA^{846}

(F) 5’ GGA CAG ATG CGG GAG GCT GCT GCT GCT GCT GAA GCT GAG CAA TAT 3’

(R) 5’ ATA TTG CTC AGC TTC AGC AGC AGC AGC AGC CTC CCG CAT CTG TCC 3’

B.3 ROCK RBD OLIGONUCLEOTIDES

^{1009}I/^{1009}A

(F) 5’ AAC AAA TTG GCA GAA GCT ATG AAT CGA AAA GAT 3’

(R) 5’ ATC TTT TCG ATT CAT AGC TTC TGC CAA TTT GTT 3’

^{1008}E/^{1008}A

(F) 5’ GTT AAC TTG GCA GCT ATA ATG AAT CGA AAA 3’

(R) 5’ TTT TCG ATT CAT TAT AGC TGC CAA TTT GTT AAC 3’

^{1004}NKL^{1006}/^{1004}AAA^{1006}

(F) 5’ AAA ACA CAG GCT GTT GCT GCT GCT GCA GAA ATA ATG AAT 3’

(R) 5’ ATT CAT TAT TTC TGC AGC AGC AGC AAC AGC CTG TGT TTT 3’

BIBLIOGRAPHY

1. Sawyer, J.K., et al., *A contractile actomyosin network linked to adherens junctions by Canoe/afadin helps drive convergent extension.* Mol Biol Cell, 2011. **22**(14): p. 2491-508.
2. Sawyer, J.M., et al., *Apical constriction: a cell shape change that can drive morphogenesis.* Dev Biol, 2010. **341**(1): p. 5-19.
3. Jordan, P. and R. Karess, *Myosin light chain-activating phosphorylation sites are required for oogenesis in Drosophila.* J Cell Biol, 1997. **139**(7): p. 1805-19.
4. Amano, M., et al., *Phosphorylation and activation of myosin by Rho-associated kinase (Rho-kinase).* J Biol Chem, 1996. **271**(34): p. 20246-9.
5. Nishimura, T. and M. Takeichi, *Shroom3-mediated recruitment of Rho kinases to the apical cell junctions regulates epithelial and neuroepithelial planar remodeling.* Development, 2008. **135**(8): p. 1493-502.
6. Matsui, T., et al., *Rho-associated kinase, a novel serine/threonine kinase, as a putative target for small GTP binding protein Rho.* EMBO J, 1996. **15**(9): p. 2208-16.
7. Wen, W., et al., *Structure basis and unconventional lipid membrane binding properties of the PH-C1 tandem of rho kinases.* J Biol Chem, 2008. **283**(38): p. 26263-73.
8. Fairbank, P.D., et al., *Shroom2 (APXL) regulates melanosome biogenesis and localization in the retinal pigment epithelium.* Development, 2006. **133**(20): p. 4109-18.
9. Farber, M.J., R. Rizaldy, and J.D. Hildebrand, *Shroom2 regulates contractility to control endothelial morphogenesis.* Mol Biol Cell. **22**(6): p. 795-805.
10. Grosse, A.S., et al., *Cell dynamics in fetal intestinal epithelium: implications for intestinal growth and morphogenesis.* Development. **138**(20): p. 4423-32.
11. Hildebrand, J.D. and P. Soriano, *Shroom, a PDZ domain-containing actin-binding protein, is required for neural tube morphogenesis in mice.* Cell, 1999. **99**(5): p. 485-97.
12. Plageman, T.F., Jr., et al., *Pax6-dependent Shroom3 expression regulates apical constriction during lens placode invagination.* Development. **137**(3): p. 405-15.
13. Plageman, T.F., Jr., et al., *Shroom3 and a Pitx2-N-cadherin pathway function cooperatively to generate asymmetric cell shape changes during gut morphogenesis.* Dev Biol. **357**(1): p. 227-34.
14. Taylor, J., et al., *The scaffold protein POSH regulates axon outgrowth.* Mol Biol Cell, 2008. **19**(12): p. 5181-92.
15. Hildebrand, J.D., *Shroom regulates epithelial cell shape via the apical positioning of an actomyosin network.* J Cell Sci, 2005. **118**(Pt 22): p. 5191-203.
16. Quintin, S., C. Gally, and M. Labouesse, *Epithelial morphogenesis in embryos: asymmetries, motors and brakes.* Trends Genet, 2008. **24**(5): p. 221-30.

17. Straub, F.B. and G. Feuer, *[Adenosine triphosphate, the functional group of actin]*. Kiserl Orvostud, 1950. **2**(2): p. 141-51.
18. Niederman, R. and T.D. Pollard, *Human platelet myosin. II. In vitro assembly and structure of myosin filaments.* J Cell Biol, 1975. **67**(1): p. 72-92.
19. Ruegg, C., et al., *Molecular motors: force and movement generated by single myosin II molecules.* News Physiol Sci, 2002. **17**: p. 213-8.
20. Wendt, T., et al., *Three-dimensional image reconstruction of dephosphorylated smooth muscle heavy meromyosin reveals asymmetry in the interaction between myosin heads and placement of subfragment 2.* Proc Natl Acad Sci U S A, 2001. **98**(8): p. 4361-6.
21. Somlyo, A.P. and A.V. Somlyo, *Ca2+ sensitivity of smooth muscle and nonmuscle myosin II: modulated by G proteins, kinases, and myosin phosphatase.* Physiol Rev, 2003. **83**(4): p. 1325-58.
22. Ikebe, M., J. Koretz, and D.J. Hartshorne, *Effects of phosphorylation of light chain residues threonine 18 and serine 19 on the properties and conformation of smooth muscle myosin.* J Biol Chem, 1988. **263**(13): p. 6432-7.
23. Kottgen, A., et al., *Multiple loci associated with indices of renal function and chronic kidney disease.* Nat Genet, 2009. **41**(6): p. 712-7.
24. Hartshorne, D.J., M. Ito, and F. Erdodi, *Role of protein phosphatase type 1 in contractile functions: myosin phosphatase.* J Biol Chem, 2004. **279**(36): p. 37211-4.
25. Komatsu, S. and M. Ikebe, *ZIP kinase is responsible for the phosphorylation of myosin II and necessary for cell motility in mammalian fibroblasts.* J Cell Biol, 2004. **165**(2): p. 243-54.
26. Leung, T., et al., *Myotonic dystrophy kinase-related Cdc42-binding kinase acts as a Cdc42 effector in promoting cytoskeletal reorganization.* Mol Cell Biol, 1998. **18**(1): p. 130-40.
27. Matsumura, F., et al., *Role of myosin light chain phosphorylation in the regulation of cytokinesis.* Cell Struct Funct, 2001. **26**(6): p. 639-44.
28. Shohat, G., et al., *The DAP-kinase family of proteins: study of a novel group of calcium-regulated death-promoting kinases.* Biochim Biophys Acta, 2002. **1600**(1-2): p. 45-50.
29. Matsumura, F., *Regulation of myosin II during cytokinesis in higher eukaryotes.* Trends Cell Biol, 2005. **15**(7): p. 371-7.
30. Murata-Hori, M., et al., *ZIP kinase identified as a novel myosin regulatory light chain kinase in HeLa cells.* FEBS Lett, 1999. **451**(1): p. 81-4.
31. Tan, I., et al., *A tripartite complex containing MRCK modulates lamellar actomyosin retrograde flow.* Cell, 2008. **135**(1): p. 123-36.
32. Totsukawa, G., et al., *Distinct roles of ROCK (Rho-kinase) and MLCK in spatial regulation of MLC phosphorylation for assembly of stress fibers and focal adhesions in 3T3 fibroblasts.* J Cell Biol, 2000. **150**(4): p. 797-806.
33. Kim, K.Y., et al., *Disease-associated mutations and alternative splicing alter the enzymatic and motile activity of nonmuscle myosins II-B and II-C.* J Biol Chem, 2005. **280**(24): p. 22769-75.
34. Wang, F., et al., *Kinetic mechanism of non-muscle myosin IIB: functional adaptations for tension generation and maintenance.* J Biol Chem, 2003. **278**(30): p. 27439-48.
35. Burridge, K., et al., *Focal adhesions: transmembrane junctions between the extracellular matrix and the cytoskeleton.* Annu Rev Cell Biol, 1988. **4**: p. 487-525.

36. Byers, H.R., G.E. White, and K. Fujiwara, *Organization and function of stress fibers in cells in vitro and in situ. A review.* Cell Muscle Motil, 1984. **5**: p. 83-137.
37. Otto, J.J., *Detection of vinculin-binding proteins with an 125I-vinculin gel overlay technique.* J Cell Biol, 1983. **97**(4): p. 1283-7.
38. Amano, M., et al., *Formation of actin stress fibers and focal adhesions enhanced by Rho-kinase.* Science, 1997. **275**(5304): p. 1308-11.
39. Ridley, A.J. and A. Hall, *The small GTP-binding protein rho regulates the assembly of focal adhesions and actin stress fibers in response to growth factors.* Cell, 1992. **70**(3): p. 389-99.
40. Watanabe, N., et al., *Cooperation between mDia1 and ROCK in Rho-induced actin reorganization.* Nat Cell Biol, 1999. **1**(3): p. 136-43.
41. Leung, T., et al., *The p160 RhoA-binding kinase ROK alpha is a member of a kinase family and is involved in the reorganization of the cytoskeleton.* Mol Cell Biol, 1996. **16**(10): p. 5313-27.
42. Ishizaki, T., et al., *p160ROCK, a Rho-associated coiled-coil forming protein kinase, works downstream of Rho and induces focal adhesions.* FEBS Lett, 1997. **404**(2-3): p. 118-24.
43. Hall, A., *Rho GTPases and the actin cytoskeleton.* Science, 1998. **279**(5350): p. 509-14.
44. Butler, B., et al., *Purified integrin adhesion complexes exhibit actin-polymerization activity.* Curr Biol, 2006. **16**(3): p. 242-51.
45. Riento, K., et al., *RhoE binds to ROCK I and inhibits downstream signaling.* Mol Cell Biol, 2003. **23**(12): p. 4219-29.
46. Ward, Y., et al., *The GTP binding proteins Gem and Rad are negative regulators of the Rho-Rho kinase pathway.* J Cell Biol, 2002. **157**(2): p. 291-302.
47. Riento, K., et al., *RhoE function is regulated by ROCK I-mediated phosphorylation.* EMBO J, 2005. **24**(6): p. 1170-80.
48. Nakano, K., et al., *Distinct actions and cooperative roles of ROCK and mDia in Rho small G protein-induced reorganization of the actin cytoskeleton in Madin-Darby canine kidney cells.* Mol Biol Cell, 1999. **10**(8): p. 2481-91.
49. Franke, R.P., et al., *Induction of human vascular endothelial stress fibres by fluid shear stress.* Nature, 1984. **307**(5952): p. 648-9.
50. Chrzanowska-Wodnicka, M. and K. Burridge, *Rho-stimulated contractility drives the formation of stress fibers and focal adhesions.* J Cell Biol, 1996. **133**(6): p. 1403-15.
51. Lauffenburger, D.A. and A.F. Horwitz, *Cell migration: a physically integrated molecular process.* Cell, 1996. **84**(3): p. 359-69.
52. Theriot, J.A. and T.J. Mitchison, *Actin microfilament dynamics in locomoting cells.* Nature, 1991. **352**(6331): p. 126-31.
53. Ding, Z., Y.H. Bae, and P. Roy, *Molecular insights on context-specific role of profilin-1 in cell migration.* Cell Adh Migr, 2012. **6**(5): p. 442-9.
54. Ponti, A., et al., *Two distinct actin networks drive the protrusion of migrating cells.* Science, 2004. **305**(5691): p. 1782-6.
55. Witke, W., *The role of profilin complexes in cell motility and other cellular processes.* Trends Cell Biol, 2004. **14**(8): p. 461-9.
56. Wilson, A.K., et al., *An increase or a decrease in myosin II phosphorylation inhibits macrophage motility.* J Cell Biol, 1991. **114**(2): p. 277-83.

57. Lin, C.H. and P. Forscher, *Growth cone advance is inversely proportional to retrograde F-actin flow.* Neuron, 1995. **14**(4): p. 763-71.
58. Choi, C.K., et al., *Actin and alpha-actinin orchestrate the assembly and maturation of nascent adhesions in a myosin II motor-independent manner.* Nat Cell Biol, 2008. **10**(9): p. 1039-50.
59. del Rio, A., et al., *Stretching single talin rod molecules activates vinculin binding.* Science, 2009. **323**(5914): p. 638-41.
60. Humphries, J.D., et al., *Vinculin controls focal adhesion formation by direct interactions with talin and actin.* J Cell Biol, 2007. **179**(5): p. 1043-57.
61. Discher, D.E., P. Janmey, and Y.L. Wang, *Tissue cells feel and respond to the stiffness of their substrate.* Science, 2005. **310**(5751): p. 1139-43.
62. Vicente-Manzanares, M., et al., *Segregation and activation of myosin IIB creates a rear in migrating cells.* J Cell Biol, 2008. **183**(3): p. 543-54.
63. Vicente-Manzanares, M., et al., *Regulation of protrusion, adhesion dynamics, and polarity by myosins IIA and IIB in migrating cells.* J Cell Biol, 2007. **176**(5): p. 573-80.
64. Worthylake, R.A., et al., *RhoA is required for monocyte tail retraction during transendothelial migration.* J Cell Biol, 2001. **154**(1): p. 147-60.
65. Conti, M.A., et al., *Defects in cell adhesion and the visceral endoderm following ablation of nonmuscle myosin heavy chain II-A in mice.* J Biol Chem, 2004. **279**(40): p. 41263-6.
66. Takeda, K., et al., *Ablation and mutation of nonmuscle myosin heavy chain II-B results in a defect in cardiac myocyte cytokinesis.* Circ Res, 2003. **93**(4): p. 330-7.
67. Bao, J., et al., *Replacement of nonmuscle myosin II-B with II-A rescues brain but not cardiac defects in mice.* J Biol Chem, 2007. **282**(30): p. 22102-11.
68. Wang, A., et al., *Nonmuscle myosin II isoform and domain specificity during early mouse development.* Proc Natl Acad Sci U S A, 2010. **107**(33): p. 14645-50.
69. Golomb, E., et al., *Identification and characterization of nonmuscle myosin II-C, a new member of the myosin II family.* J Biol Chem, 2004. **279**(4): p. 2800-8.
70. Kolega, J., *The role of myosin II motor activity in distributing myosin asymmetrically and coupling protrusive activity to cell translocation.* Mol Biol Cell, 2006. **17**(10): p. 4435-45.
71. Krendel, M. and M.S. Mooseker, *Myosins: tails (and heads) of functional diversity.* Physiology (Bethesda), 2005. **20**: p. 239-51.
72. Sandquist, J.C., et al., *Rho kinase differentially regulates phosphorylation of nonmuscle myosin II isoforms A and B during cell rounding and migration.* J Biol Chem, 2006. **281**(47): p. 35873-83.
73. Straussman, R., L. Even, and S. Ravid, *Myosin II heavy chain isoforms are phosphorylated in an EGF-dependent manner: involvement of protein kinase C.* J Cell Sci, 2001. **114**(Pt 16): p. 3047-57.
74. Heissler, S.M. and D.J. Manstein, *Nonmuscle myosin-2: mix and match.* Cell Mol Life Sci, 2013. **70**(1): p. 1-21.
75. De Lozanne, A. and J.A. Spudich, *Disruption of the Dictyostelium myosin heavy chain gene by homologous recombination.* Science, 1987. **236**(4805): p. 1086-91.
76. Mabuchi, I. and M. Okuno, *The effect of myosin antibody on the division of starfish blastomeres.* J Cell Biol, 1977. **74**(1): p. 251-63.

77. Moussavi, R.S., C.A. Kelley, and R.S. Adelstein, *Phosphorylation of vertebrate nonmuscle and smooth muscle myosin heavy chains and light chains.* Mol Cell Biochem, 1993. **127-128**: p. 219-27.
78. Ikebe, M., et al., *Correlation of conformation and phosphorylation and dephosphorylation of smooth muscle myosin.* J Biol Chem, 1988. **263**(22): p. 10698-704.
79. Scholey, J.M., K.A. Taylor, and J. Kendrick-Jones, *Regulation of non-muscle myosin assembly by calmodulin-dependent light chain kinase.* Nature, 1980. **287**(5779): p. 233-5.
80. Komatsu, S., et al., *Effects of the regulatory light chain phosphorylation of myosin II on mitosis and cytokinesis of mammalian cells.* J Biol Chem, 2000. **275**(44): p. 34512-20.
81. Matsumura, F., et al., *Specific localization of serine 19 phosphorylated myosin II during cell locomotion and mitosis of cultured cells.* J Cell Biol, 1998. **140**(1): p. 119-29.
82. Kamm, K.E. and J.T. Stull, *Dedicated myosin light chain kinases with diverse cellular functions.* J Biol Chem, 2001. **276**(7): p. 4527-30.
83. Mege, R.M., J. Gavard, and M. Lambert, *Regulation of cell-cell junctions by the cytoskeleton.* Curr Opin Cell Biol, 2006. **18**(5): p. 541-8.
84. Revenu, C., et al., *The co-workers of actin filaments: from cell structures to signals.* Nat Rev Mol Cell Biol, 2004. **5**(8): p. 635-46.
85. Kobielak, A. and E. Fuchs, *Alpha-catenin: at the junction of intercellular adhesion and actin dynamics.* Nat Rev Mol Cell Biol, 2004. **5**(8): p. 614-25.
86. Kobielak, A., H.A. Pasolli, and E. Fuchs, *Mammalian formin-1 participates in adherens junctions and polymerization of linear actin cables.* Nat Cell Biol, 2004. **6**(1): p. 21-30.
87. Kovacs, E.M., et al., *E-cadherin homophilic ligation directly signals through Rac and phosphatidylinositol 3-kinase to regulate adhesive contacts.* J Biol Chem, 2002. **277**(8): p. 6708-18.
88. Vasioukhin, V., et al., *Directed actin polymerization is the driving force for epithelial cell-cell adhesion.* Cell, 2000. **100**(2): p. 209-19.
89. Yamanaka, T., et al., *PAR-6 regulates aPKC activity in a novel way and mediates cell-cell contact-induced formation of the epithelial junctional complex.* Genes Cells, 2001. **6**(8): p. 721-31.
90. Sahai, E. and C.J. Marshall, *ROCK and Dia have opposing effects on adherens junctions downstream of Rho.* Nat Cell Biol, 2002. **4**(6): p. 408-15.
91. Smutny, M., et al., *Myosin II isoforms identify distinct functional modules that support integrity of the epithelial zonula adherens.* Nat Cell Biol, 2010. **12**(7): p. 696-702.
92. le Duc, Q., et al., *Vinculin potentiates E-cadherin mechanosensing and is recruited to actin-anchored sites within adherens junctions in a myosin II-dependent manner.* J Cell Biol, 2010. **189**(7): p. 1107-15.
93. Yonemura, S., et al., *alpha-Catenin as a tension transducer that induces adherens junction development.* Nat Cell Biol, 2010. **12**(6): p. 533-42.
94. Assemat, E., et al., *Polarity complex proteins.* Biochim Biophys Acta, 2008. **1778**(3): p. 614-30.
95. Dow, L.E., et al., *The tumour-suppressor Scribble dictates cell polarity during directed epithelial migration: regulation of Rho GTPase recruitment to the leading edge.* Oncogene, 2007. **26**(16): p. 2272-82.
96. Humbert, P.O., L.E. Dow, and S.M. Russell, *The Scribble and Par complexes in polarity and migration: friends or foes?* Trends Cell Biol, 2006. **16**(12): p. 622-30.

97. Joberty, G., et al., *The cell-polarity protein Par6 links Par3 and atypical protein kinase C to Cdc42.* Nat Cell Biol, 2000. **2**(8): p. 531-9.
98. Lin, D., et al., *A mammalian PAR-3-PAR-6 complex implicated in Cdc42/Rac1 and aPKC signalling and cell polarity.* Nat Cell Biol, 2000. **2**(8): p. 540-7.
99. Axelrod, J.D., et al., *Differential recruitment of Dishevelled provides signaling specificity in the planar cell polarity and Wingless signaling pathways.* Genes Dev, 1998. **12**(16): p. 2610-22.
100. Klingensmith, J., R. Nusse, and N. Perrimon, *The Drosophila segment polarity gene dishevelled encodes a novel protein required for response to the wingless signal.* Genes Dev, 1994. **8**(1): p. 118-30.
101. Krasnow, R.E. and P.N. Adler, *A single frizzled protein has a dual function in tissue polarity.* Development, 1994. **120**(7): p. 1883-93.
102. Mlodzik, M., *Planar polarity in the Drosophila eye: a multifaceted view of signaling specificity and cross-talk.* EMBO J, 1999. **18**(24): p. 6873-9.
103. Noordermeer, J., et al., *dishevelled and armadillo act in the wingless signalling pathway in Drosophila.* Nature, 1994. **367**(6458): p. 80-3.
104. Shulman, J.M., N. Perrimon, and J.D. Axelrod, *Frizzled signaling and the developmental control of cell polarity.* Trends Genet, 1998. **14**(11): p. 452-8.
105. Theisen, H., et al., *dishevelled is required during wingless signaling to establish both cell polarity and cell identity.* Development, 1994. **120**(2): p. 347-60.
106. Vinson, C.R., S. Conover, and P.N. Adler, *A Drosophila tissue polarity locus encodes a protein containing seven potential transmembrane domains.* Nature, 1989. **338**(6212): p. 263-4.
107. Wodarz, A. and R. Nusse, *Mechanisms of Wnt signaling in development.* Annu Rev Cell Dev Biol, 1998. **14**: p. 59-88.
108. Etienne-Manneville, S., *Cdc42--the centre of polarity.* J Cell Sci, 2004. **117**(Pt 8): p. 1291-300.
109. Fukata, M., M. Nakagawa, and K. Kaibuchi, *Roles of Rho-family GTPases in cell polarisation and directional migration.* Curr Opin Cell Biol, 2003. **15**(5): p. 590-7.
110. Jaffe, A.B. and A. Hall, *Rho GTPases: biochemistry and biology.* Annu Rev Cell Dev Biol, 2005. **21**: p. 247-69.
111. Van Aelst, L. and M. Symons, *Role of Rho family GTPases in epithelial morphogenesis.* Genes Dev, 2002. **16**(9): p. 1032-54.
112. Friedl, P. and D. Gilmour, *Collective cell migration in morphogenesis, regeneration and cancer.* Nat Rev Mol Cell Biol, 2009. **10**(7): p. 445-57.
113. Lecuit, T. and P.F. Lenne, *Cell surface mechanics and the control of cell shape, tissue patterns and morphogenesis.* Nat Rev Mol Cell Biol, 2007. **8**(8): p. 633-44.
114. Leptin, M., *Gastrulation movements: the logic and the nuts and bolts.* Dev Cell, 2005. **8**(3): p. 305-20.
115. Verkhovsky, A.B. and G.G. Borisy, *Non-sarcomeric mode of myosin II organization in the fibroblast lamellum.* J Cell Biol, 1993. **123**(3): p. 637-52.
116. Schroeder, T.E., *Neurulation in Xenopus laevis. An analysis and model based upon light and electron microscopy.* J Embryol Exp Morphol, 1970. **23**(2): p. 427-62.
117. Sweeton, D., et al., *Gastrulation in Drosophila: the formation of the ventral furrow and posterior midgut invaginations.* Development, 1991. **112**(3): p. 775-89.

118. Viamontes, G.I. and D.L. Kirk, *Cell shape changes and the mechanism of inversion in Volvox.* J Cell Biol, 1977. **75**(3): p. 719-30.
119. Brun, R.B. and J.A. Garson, *Neurulation in the Mexican salamander (Ambystoma mexicanum): a drug study and cell shape analysis of the epidermis and the neural plate.* J Embryol Exp Morphol, 1983. **74**: p. 275-95.
120. Karfunkel, P., *The role of microtubules and microfilaments in neurulation in Xenopus.* Dev Biol, 1971. **25**(1): p. 30-56.
121. Messier, P.E., *Microtubules, interkinetic nuclear migration and neurulation.* Experientia, 1978. **34**(3): p. 289-96.
122. Bement, W.M., P. Forscher, and M.S. Mooseker, *A novel cytoskeletal structure involved in purse string wound closure and cell polarity maintenance.* J Cell Biol, 1993. **121**(3): p. 565-78.
123. Martin, P. and J. Lewis, *Actin cables and epidermal movement in embryonic wound healing.* Nature, 1992. **360**(6400): p. 179-83.
124. Tamada, M., et al., *Two distinct modes of myosin assembly and dynamics during epithelial wound closure.* J Cell Biol, 2007. **176**(1): p. 27-33.
125. Du, D., et al., *The tight junction protein, occludin, regulates the directional migration of epithelial cells.* Dev Cell, 2010. **18**(1): p. 52-63.
126. Wu, X., et al., *Myosin V associates with melanosomes in mouse melanocytes: evidence that myosin V is an organelle motor.* J Cell Sci, 1997. **110 (Pt 7)**: p. 847-59.
127. Apodaca, G., *Endocytic traffic in polarized epithelial cells: role of the actin and microtubule cytoskeleton.* Traffic, 2001. **2**(3): p. 149-59.
128. Smythe, E. and K.R. Ayscough, *Actin regulation in endocytosis.* J Cell Sci, 2006. **119**(Pt 22): p. 4589-98.
129. Thompson, R.F. and G.M. Langford, *Myosin superfamily evolutionary history.* Anat Rec, 2002. **268**(3): p. 276-89.
130. Lister, I., et al., *Myosin VI: a multifunctional motor.* Biochem Soc Trans, 2004. **32**(Pt 5): p. 685-8.
131. Roberts, R., et al., *Myosin VI: cellular functions and motor properties.* Philos Trans R Soc Lond B Biol Sci, 2004. **359**(1452): p. 1931-44.
132. Ridley, A.J., *Rho GTPases and actin dynamics in membrane protrusions and vesicle trafficking.* Trends Cell Biol, 2006. **16**(10): p. 522-9.
133. Carter, S.B., *Effects of cytochalasins on mammalian cells.* Nature, 1967. **213**(5073): p. 261-4.
134. Morriss-Kay, G. and F. Tuckett, *The role of microfilaments in cranial neurulation in rat embryos: effects of short-term exposure to cytochalasin D.* J Embryol Exp Morphol, 1985. **88**: p. 333-48.
135. Ybot-Gonzalez, P. and A.J. Copp, *Bending of the neural plate during mouse spinal neurulation is independent of actin microfilaments.* Dev Dyn, 1999. **215**(3): p. 273-83.
136. Shimizu, Y., et al., *ROCK-I regulates closure of the eyelids and ventral body wall by inducing assembly of actomyosin bundles.* J Cell Biol, 2005. **168**(6): p. 941-53.
137. Thumkeo, D., et al., *ROCK-I and ROCK-II cooperatively regulate closure of eyelid and ventral body wall in mouse embryo.* Genes Cells, 2005. **10**(8): p. 825-34.
138. Reed, R.A., et al., *Morphogenesis of the primitive gut tube is generated by Rho/ROCK/myosin II-mediated endoderm rearrangements.* Dev Dyn, 2009. **238**(12): p. 3111-25.

139. Flynn, K.C., *The cytoskeleton and neurite initiation.* Bioarchitecture, 2013. **3**(4).
140. Shirao, T. and C. Gonzalez-Billault, *Actin filaments and microtubules in dendritic spines.* J Neurochem, 2013. **126**(2): p. 155-64.
141. Vicente-Manzanares, M., J. Hodges, and A.R. Horwitz, *Dendritic Spines: Similarities with Protrusions and Adhesions in Migrating Cells.* Open Neurosci J, 2009. **3**: p. 87-96.
142. Lagrue, K., et al., *The central role of the cytoskeleton in mechanisms and functions of the NK cell immune synapse.* Immunol Rev, 2013. **256**(1): p. 203-21.
143. Marin-Padilla, M., *Early vascularization of the embryonic cerebral cortex: Golgi and electron microscopic studies.* J Comp Neurol, 1985. **241**(2): p. 237-49.
144. Lamalice, L., et al., *Phosphorylation of tyrosine 1214 on VEGFR2 is required for VEGF-induced activation of Cdc42 upstream of SAPK2/p38.* Oncogene, 2004. **23**(2): p. 434-45.
145. Tan, W., et al., *An essential role for Rac1 in endothelial cell function and vascular development.* FASEB J, 2008. **22**(6): p. 1829-38.
146. Hoang, M.V., M.C. Whelan, and D.R. Senger, *Rho activity critically and selectively regulates endothelial cell organization during angiogenesis.* Proc Natl Acad Sci U S A, 2004. **101**(7): p. 1874-9.
147. van Nieuw Amerongen, G.P., et al., *Involvement of RhoA/Rho kinase signaling in VEGF-induced endothelial cell migration and angiogenesis in vitro.* Arterioscler Thromb Vasc Biol, 2003. **23**(2): p. 211-7.
148. Fischer, R.S., et al., *Local cortical tension by myosin II guides 3D endothelial cell branching.* Curr Biol, 2009. **19**(3): p. 260-5.
149. Bi, J., et al., *Myosin 1e is a component of the glomerular slit diaphragm complex that regulates actin reorganization during cell-cell contact formation in podocytes.* Am J Physiol Renal Physiol, 2013. **305**(4): p. F532-44.
150. Boute, N., et al., *NPHS2, encoding the glomerular protein podocin, is mutated in autosomal recessive steroid-resistant nephrotic syndrome.* Nat Genet, 2000. **24**(4): p. 349-54.
151. Kestila, M., et al., *Positionally cloned gene for a novel glomerular protein--nephrin--is mutated in congenital nephrotic syndrome.* Mol Cell, 1998. **1**(4): p. 575-82.
152. Weins, A., et al., *Mutational and Biological Analysis of alpha-actinin-4 in focal segmental glomerulosclerosis.* J Am Soc Nephrol, 2005. **16**(12): p. 3694-701.
153. Franke, J.D., R.A. Montague, and D.P. Kiehart, *Nonmuscle myosin II generates forces that transmit tension and drive contraction in multiple tissues during dorsal closure.* Curr Biol, 2005. **15**(24): p. 2208-21.
154. Landsberg, K.P., et al., *Increased cell bond tension governs cell sorting at the Drosophila anteroposterior compartment boundary.* Curr Biol, 2009. **19**(22): p. 1950-5.
155. Ojelade, S.A., S.F. Acevedo, and A. Rothenfluh, *The role of the actin cytoskeleton in regulating Drosophila behavior.* Rev Neurosci, 2013. **24**(5): p. 471-84.
156. Bourne, H.R., D.A. Sanders, and F. McCormick, *The GTPase superfamily: conserved structure and molecular mechanism.* Nature, 1991. **349**(6305): p. 117-27.
157. Van Aelst, L. and C. D'Souza-Schorey, *Rho GTPases and signaling networks.* Genes Dev, 1997. **11**(18): p. 2295-322.
158. Gibbs, J.B., et al., *Modulation of guanine nucleotides bound to Ras in NIH3T3 cells by oncogenes, growth factors, and the GTPase activating protein (GAP).* J Biol Chem, 1990. **265**(33): p. 20437-42.

159. Rossman, K.L., C.J. Der, and J. Sondek, *GEF means go: turning on RHO GTPases with guanine nucleotide-exchange factors.* Nat Rev Mol Cell Biol, 2005. **6**(2): p. 167-80.
160. Fujisawa, K., et al., *Different regions of Rho determine Rho-selective binding of different classes of Rho target molecules.* J Biol Chem, 1998. **273**(30): p. 18943-9.
161. Hart, M.J., et al., *A GDP dissociation inhibitor that serves as a GTPase inhibitor for the Ras-like protein CDC42Hs.* Science, 1992. **258**(5083): p. 812-5.
162. Nobes, C.D. and A. Hall, *Rho, rac and cdc42 GTPases: regulators of actin structures, cell adhesion and motility.* Biochem Soc Trans, 1995. **23**(3): p. 456-9.
163. Nobes, C.D. and A. Hall, *Rho, rac, and cdc42 GTPases regulate the assembly of multimolecular focal complexes associated with actin stress fibers, lamellipodia, and filopodia.* Cell, 1995. **81**(1): p. 53-62.
164. Ridley, A.J., et al., *The small GTP-binding protein rac regulates growth factor-induced membrane ruffling.* Cell, 1992. **70**(3): p. 401-10.
165. Narumiya, S., T. Ishizaki, and N. Watanabe, *Rho effectors and reorganization of actin cytoskeleton.* FEBS Lett, 1997. **410**(1): p. 68-72.
166. Braga, V.M., *Cell-cell adhesion and signalling.* Curr Opin Cell Biol, 2002. **14**(5): p. 546-56.
167. Burridge, K. and K. Wennerberg, *Rho and Rac take center stage.* Cell, 2004. **116**(2): p. 167-79.
168. DeMali, K.A., K. Wennerberg, and K. Burridge, *Integrin signaling to the actin cytoskeleton.* Curr Opin Cell Biol, 2003. **15**(5): p. 572-82.
169. Machesky, L.M. and R.H. Insall, *Scar1 and the related Wiskott-Aldrich syndrome protein, WASP, regulate the actin cytoskeleton through the Arp2/3 complex.* Curr Biol, 1998. **8**(25): p. 1347-56.
170. Miki, H., S. Suetsugu, and T. Takenawa, *WAVE, a novel WASP-family protein involved in actin reorganization induced by Rac.* EMBO J, 1998. **17**(23): p. 6932-41.
171. Nakagawa, H., et al., *N-WASP, WAVE and Mena play different roles in the organization of actin cytoskeleton in lamellipodia.* J Cell Sci, 2001. **114**(Pt 8): p. 1555-65.
172. Nakanishi, O., et al., *Effect of WAVE2 phosphorylation on activation of the Arp2/3 complex.* J Biochem, 2007. **141**(3): p. 319-25.
173. Ridley, A.J., P.M. Comoglio, and A. Hall, *Regulation of scatter factor/hepatocyte growth factor responses by Ras, Rac, and Rho in MDCK cells.* Mol Cell Biol, 1995. **15**(2): p. 1110-22.
174. Stowers, L., et al., *Regulation of the polarization of T cells toward antigen-presenting cells by Ras-related GTPase CDC42.* Proc Natl Acad Sci U S A, 1995. **92**(11): p. 5027-31.
175. Drechsel, D.N., et al., *A requirement for Rho and Cdc42 during cytokinesis in Xenopus embryos.* Curr Biol, 1997. **7**(1): p. 12-23.
176. Dutartre, H., et al., *Cytokinesis arrest and redistribution of actin-cytoskeleton regulatory components in cells expressing the Rho GTPase CDC42Hs.* J Cell Sci, 1996. **109 (Pt 2)**: p. 367-77.
177. Qiu, R.G., et al., *Cdc42 regulates anchorage-independent growth and is necessary for Ras transformation.* Mol Cell Biol, 1997. **17**(6): p. 3449-58.
178. Qiu, R.G., et al., *An essential role for Rac in Ras transformation.* Nature, 1995. **374**(6521): p. 457-9.

179. Qiu, R.G., et al., *A role for Rho in Ras transformation.* Proc Natl Acad Sci U S A, 1995. **92**(25): p. 11781-5.
180. Aspenstrom, P., U. Lindberg, and A. Hall, *Two GTPases, Cdc42 and Rac, bind directly to a protein implicated in the immunodeficiency disorder Wiskott-Aldrich syndrome.* Curr Biol, 1996. **6**(1): p. 70-5.
181. Symons, M., et al., *Wiskott-Aldrich syndrome protein, a novel effector for the GTPase CDC42Hs, is implicated in actin polymerization.* Cell, 1996. **84**(5): p. 723-34.
182. Martin, A.C., *Pulsation and stabilization: contractile forces that underlie morphogenesis.* Dev Biol, 2010. **341**(1): p. 114-25.
183. Martin, A.C., M. Kaschube, and E.F. Wieschaus, *Pulsed contractions of an actin-myosin network drive apical constriction.* Nature, 2009. **457**(7228): p. 495-9.
184. Rauzi, M., P.F. Lenne, and T. Lecuit, *Planar polarized actomyosin contractile flows control epithelial junction remodelling.* Nature, 2010. **468**(7327): p. 1110-4.
185. Lee, J.Y. and B. Goldstein, *Mechanisms of cell positioning during C. elegans gastrulation.* Development, 2003. **130**(2): p. 307-20.
186. Kimberly, E.L. and J. Hardin, *Bottle cells are required for the initiation of primary invagination in the sea urchin embryo.* Dev Biol, 1998. **204**(1): p. 235-50.
187. Hardin, J. and R. Keller, *The behaviour and function of bottle cells during gastrulation of Xenopus laevis.* Development, 1988. **103**(1): p. 211-30.
188. Lee, J.Y. and R.M. Harland, *Actomyosin contractility and microtubules drive apical constriction in Xenopus bottle cells.* Dev Biol, 2007. **311**(1): p. 40-52.
189. Young, P.E., T.C. Pesacreta, and D.P. Kiehart, *Dynamic changes in the distribution of cytoplasmic myosin during Drosophila embryogenesis.* Development, 1991. **111**(1): p. 1-14.
190. Costa, M., E.T. Wilson, and E. Wieschaus, *A putative cell signal encoded by the folded gastrulation gene coordinates cell shape changes during Drosophila gastrulation.* Cell, 1994. **76**(6): p. 1075-89.
191. Leptin, M. and B. Grunewald, *Cell shape changes during gastrulation in Drosophila.* Development, 1990. **110**(1): p. 73-84.
192. Solon, J., et al., *Pulsed forces timed by a ratchet-like mechanism drive directed tissue movement during dorsal closure.* Cell, 2009. **137**(7): p. 1331-42.
193. Tomlinson, A., *The cellular dynamics of pattern formation in the eye of Drosophila.* J Embryol Exp Morphol, 1985. **89**: p. 313-31.
194. Burnside, B., *Microtubules and microfilaments in newt neuralation.* Dev Biol, 1971. **26**(3): p. 416-41.
195. Haigo, S.L., et al., *Shroom induces apical constriction and is required for hingepoint formation during neural tube closure.* Curr Biol, 2003. **13**(24): p. 2125-37.
196. Jacobson, A.G., et al., *Neurulation and the cortical tractor model for epithelial folding.* J Embryol Exp Morphol, 1986. **96**: p. 19-49.
197. Solursh, M. and J.P. Revel, *A scanning electron microscope study of cell shape and cell appendages in the primitive streak region of the rat and chick embryo.* Differentiation, 1978. **11**(3): p. 185-90.
198. Barrett, K., M. Leptin, and J. Settleman, *The Rho GTPase and a putative RhoGEF mediate a signaling pathway for the cell shape changes in Drosophila gastrulation.* Cell, 1997. **91**(7): p. 905-15.

199. Brodu, V. and J. Casanova, *The RhoGAP crossveinless-c links trachealess and EGFR signaling to cell shape remodeling in Drosophila tracheal invagination.* Genes Dev, 2006. **20**(13): p. 1817-28.
200. Homem, C.C. and M. Peifer, *Diaphanous regulates myosin and adherens junctions to control cell contractility and protrusive behavior during morphogenesis.* Development, 2008. **135**(6): p. 1005-18.
201. Beane, W.S., J.M. Gross, and D.R. McClay, *RhoA regulates initiation of invagination, but not convergent extension, during sea urchin gastrulation.* Dev Biol, 2006. **292**(1): p. 213-25.
202. Corrigall, D., et al., *Hedgehog signaling is a principal inducer of Myosin-II-driven cell ingression in Drosophila epithelia.* Dev Cell, 2007. **13**(5): p. 730-42.
203. Escudero, L.M., M. Bischoff, and M. Freeman, *Myosin II regulates complex cellular arrangement and epithelial architecture in Drosophila.* Dev Cell, 2007. **13**(5): p. 717-29.
204. Kolsch, V., et al., *Control of Drosophila gastrulation by apical localization of adherens junctions and RhoGEF2.* Science, 2007. **315**(5810): p. 384-6.
205. Xu, N., B. Keung, and M.M. Myat, *Rho GTPase controls invagination and cohesive migration of the Drosophila salivary gland through Crumbs and Rho-kinase.* Dev Biol, 2008. **321**(1): p. 88-100.
206. Campbell, L.R., D.H. Dayton, and G.S. Sohal, *Neural tube defects: a review of human and animal studies on the etiology of neural tube defects.* Teratology, 1986. **34**(2): p. 171-87.
207. Copp, A.J., et al., *The embryonic development of mammalian neural tube defects.* Prog Neurobiol, 1990. **35**(5): p. 363-403.
208. Greene, N.D. and A.J. Copp, *Development of the vertebrate central nervous system: formation of the neural tube.* Prenat Diagn, 2009. **29**(4): p. 303-11.
209. Greene, N.D., V. Massa, and A.J. Copp, *Understanding the causes and prevention of neural tube defects: Insights from the splotch mouse model.* Birth Defects Res A Clin Mol Teratol, 2009. **85**(4): p. 322-30.
210. Greene, N.D., P. Stanier, and A.J. Copp, *Genetics of human neural tube defects.* Hum Mol Genet, 2009. **18**(R2): p. R113-29.
211. Wallingford, J.B., *Neural tube closure and neural tube defects: studies in animal models reveal known knowns and known unknowns.* Am J Med Genet C Semin Med Genet, 2005. **135C**(1): p. 59-68.
212. Copp, A.J., N.D. Greene, and J.N. Murdoch, *The genetic basis of mammalian neurulation.* Nat Rev Genet, 2003. **4**(10): p. 784-93.
213. Baker, P.C. and T.E. Schroeder, *Cytoplasmic filaments and morphogenetic movement in the amphibian neural tube.* Dev Biol, 1967. **15**(5): p. 432-50.
214. Karfunkel, P., *The mechanisms of neural tube formation.* Int Rev Cytol, 1974. **38**(0): p. 245-71.
215. Lee, H.Y. and R.G. Nagele, *Studies on the mechanisms of neurulation in the chick: interrelationship of contractile proteins, microfilaments, and the shape of neuroepithelial cells.* J Exp Zool, 1985. **235**(2): p. 205-15.
216. Sadler, T.W., et al., *Actin distribution patterns in the mouse neural tube during neurulation.* Science, 1982. **215**(4529): p. 172-4.
217. Schoenwolf, G.C., D. Folsom, and A. Moe, *A reexamination of the role of microfilaments in neurulation in the chick embryo.* Anat Rec, 1988. **220**(1): p. 87-102.

218. Wiley, M.J., *The effects of cytochalasins on the ultrastructure of neurulating hamster embryos in vivo.* Teratology, 1980. **22**(1): p. 59-69.
219. Rakeman, A.S. and K.V. Anderson, *Axis specification and morphogenesis in the mouse embryo require Nap1, a regulator of WAVE-mediated actin branching.* Development, 2006. **133**(16): p. 3075-83.
220. Koleske, A.J., et al., *Essential roles for the Abl and Arg tyrosine kinases in neurulation.* Neuron, 1998. **21**(6): p. 1259-72.
221. Brouns, M.R., et al., *The adhesion signaling molecule p190 RhoGAP is required for morphogenetic processes in neural development.* Development, 2000. **127**(22): p. 4891-903.
222. Lanier, L.M., et al., *Mena is required for neurulation and commissure formation.* Neuron, 1999. **22**(2): p. 313-25.
223. Xu, W., H. Baribault, and E.D. Adamson, *Vinculin knockout results in heart and brain defects during embryonic development.* Development, 1998. **125**(2): p. 327-37.
224. Lakkis, M.M., et al., *Neurofibromin deficiency in mice causes exencephaly and is a modifier for Splotch neural tube defects.* Dev Biol, 1999. **212**(1): p. 80-92.
225. Roffers-Agarwal, J., K.J. Hutt, and L.S. Gammill, *Paladin is an antiphosphatase that regulates neural crest cell formation and migration.* Dev Biol, 2012. **371**(2): p. 180-90.
226. Chu, C.W., et al., *Lulu Regulates Shroom-Induced Apical Constriction during Neural Tube Closure.* PLoS One, 2013. **8**(11): p. e81854.
227. Lee, C., H.M. Scherr, and J.B. Wallingford, *Shroom family proteins regulate gamma-tubulin distribution and microtubule architecture during epithelial cell shape change.* Development, 2007. **134**(7): p. 1431-41.
228. Stumpo, D.J., et al., *MARCKS deficiency in mice leads to abnormal brain development and perinatal death.* Proc Natl Acad Sci U S A, 1995. **92**(4): p. 944-8.
229. Staub, O., et al., *Primary structure of an apical protein from Xenopus laevis that participates in amiloride-sensitive sodium channel activity.* J Cell Biol, 1992. **119**(6): p. 1497-506.
230. Schiaffino, M.V., et al., *Cloning of a human homologue of the Xenopus laevis APX gene from the ocular albinism type 1 critical region.* Hum Mol Genet, 1995. **4**(3): p. 373-82.
231. Hagens, O., et al., *Disruptions of the novel KIAA1202 gene are associated with X-linked mental retardation.* Hum Genet, 2006. **118**(5): p. 578-90.
232. Hagens, O., et al., *A new standard nomenclature for proteins related to Apx and Shroom.* BMC Cell Biol, 2006. **7**: p. 18.
233. Lee, C., M.P. Le, and J.B. Wallingford, *The shroom family proteins play broad roles in the morphogenesis of thickened epithelial sheets.* Dev Dyn, 2009. **238**(6): p. 1480-91.
234. Dietz, M.L., et al., *Differential actin-dependent localization modulates the evolutionarily conserved activity of Shroom family proteins.* J Biol Chem, 2006. **281**(29): p. 20542-54.
235. Bolinger, C., et al., *Specific isoforms of drosophila shroom define spatial requirements for the induction of apical constriction.* Dev Dyn. **239**(7): p. 2078-93.
236. Ernst, S., et al., *Shroom3 is required downstream of FGF signalling to mediate proneuromast assembly in zebrafish.* Development, 2012. **139**(24): p. 4571-81.
237. Plageman, T.F., Jr., et al., *A Trio-RhoA-Shroom3 pathway is required for apical constriction and epithelial invagination.* Development. **138**(23): p. 5177-88.
238. Yoder, M. and J.D. Hildebrand, *Shroom4 (Kiaa1202) is an actin-associated protein implicated in cytoskeletal organization.* Cell Motil Cytoskeleton, 2007. **64**(1): p. 49-63.

239. Job, D., O. Valiron, and B. Oakley, *Microtubule nucleation.* Curr Opin Cell Biol, 2003. **15**(1): p. 111-7.
240. Chung, M.I., et al., *Direct activation of Shroom3 transcription by Pitx proteins drives epithelial morphogenesis in the developing gut.* Development. **137**(8): p. 1339-49.
241. Plageman, T.F., Jr., et al., *Shroom3 and a Pitx2-N-cadherin pathway function cooperatively to generate asymmetric cell shape changes during gut morphogenesis.* Dev Biol, 2011. **357**(1): p. 227-34.
242. Plageman, T.F., Jr., et al., *A Trio-RhoA-Shroom3 pathway is required for apical constriction and epithelial invagination.* Development, 2011. **138**(23): p. 5177-88.
243. Sevilla-Perez, J., et al., *Shroom expression is attenuated in pulmonary arterial hypertension.* Eur Respir J, 2008. **32**(4): p. 871-80.
244. Tariq, M., et al., *SHROOM3 is a novel candidate for heterotaxy identified by whole exome sequencing.* Genome Biol. **12**(9): p. R91.
245. Oetting, W.S. and R.A. King, *Molecular basis of albinism: mutations and polymorphisms of pigmentation genes associated with albinism.* Hum Mutat, 1999. **13**(2): p. 99-115.
246. Marmorstein, A.D., *The polarity of the retinal pigment epithelium.* Traffic, 2001. **2**(12): p. 867-72.
247. Marks, M.S. and M.C. Seabra, *The melanosome: membrane dynamics in black and white.* Nat Rev Mol Cell Biol, 2001. **2**(10): p. 738-48.
248. Etournay, R., et al., *Shroom2, a myosin-VIIa- and actin-binding protein, directly interacts with ZO-1 at tight junctions.* J Cell Sci, 2007. **120**(Pt 16): p. 2838-50.
249. Tak, W.J., et al., *Ocular albinism with sensorineural deafness.* Int J Dermatol, 2004. **43**(4): p. 290-2.
250. Winship, I.M., M. Babaya, and R.S. Ramesar, *X-linked ocular albinism and sensorineural deafness: linkage to Xp22.3.* Genomics, 1993. **18**(2): p. 444-5.
251. El-Amraoui, A. and C. Petit, *Usher I syndrome: unravelling the mechanisms that underlie the cohesion of the growing hair bundle in inner ear sensory cells.* J Cell Sci, 2005. **118**(Pt 20): p. 4593-603.
252. Weil, D., et al., *Defective myosin VIIA gene responsible for Usher syndrome type 1B.* Nature, 1995. **374**(6517): p. 60-1.
253. Gibson, F., et al., *A type VII myosin encoded by the mouse deafness gene shaker-1.* Nature, 1995. **374**(6517): p. 62-4.
254. Etournay, R., et al., *Cochlear outer hair cells undergo an apical circumference remodeling constrained by the hair bundle shape.* Development, 2010. **137**(8): p. 1373-83.
255. Sahly, I., et al., *Expression of myosin VIIA during mouse embryogenesis.* Anat Embryol (Berl), 1997. **196**(2): p. 159-70.
256. Abraham, S., et al., *VE-Cadherin-mediated cell-cell interaction suppresses sprouting via signaling to MLC2 phosphorylation.* Curr Biol, 2009. **19**(8): p. 668-74.
257. Kroll, J., et al., *Inhibition of Rho-dependent kinases ROCK I/II activates VEGF-driven retinal neovascularization and sprouting angiogenesis.* Am J Physiol Heart Circ Physiol, 2009. **296**(3): p. H893-9.
258. Mavria, G., et al., *ERK-MAPK signaling opposes Rho-kinase to promote endothelial cell survival and sprouting during angiogenesis.* Cancer Cell, 2006. **9**(1): p. 33-44.
259. Ropers, H.H., *X-linked mental retardation: many genes for a complex disorder.* Curr Opin Genet Dev, 2006. **16**(3): p. 260-9.

260. Ropers, H.H. and B.C. Hamel, *X-linked mental retardation.* Nat Rev Genet, 2005. **6**(1): p. 46-57.
261. Assef, Y.A., et al., *ENaC channels in oocytes from Xenopus laevis and their regulation by xShroom1 protein.* Cell Physiol Biochem, 2011. **28**(2): p. 259-66.
262. Dye, D.E., et al., *hShroom1 links a membrane bound protein to the actin cytoskeleton.* Cell Mol Life Sci, 2009. **66**(4): p. 681-96.
263. Ishizaki, T., et al., *The small GTP-binding protein Rho binds to and activates a 160 kDa Ser/Thr protein kinase homologous to myotonic dystrophy kinase.* EMBO J, 1996. **15**(8): p. 1885-93.
264. Leung, T., et al., *A novel serine/threonine kinase binding the Ras-related RhoA GTPase which translocates the kinase to peripheral membranes.* J Biol Chem, 1995. **270**(49): p. 29051-4.
265. Dawes-Hoang, R.E., et al., *folded gastrulation, cell shape change and the control of myosin localization.* Development, 2005. **132**(18): p. 4165-78.
266. Chen, X.Q., et al., *Characterization of RhoA-binding kinase ROKalpha implication of the pleckstrin homology domain in ROKalpha function using region-specific antibodies.* J Biol Chem, 2002. **277**(15): p. 12680-8.
267. Jacobs, M., et al., *The structure of dimeric ROCK I reveals the mechanism for ligand selectivity.* J Biol Chem, 2006. **281**(1): p. 260-8.
268. Nakagawa, O., et al., *ROCK-I and ROCK-II, two isoforms of Rho-associated coiled-coil forming protein serine/threonine kinase in mice.* FEBS Lett, 1996. **392**(2): p. 189-93.
269. Yoneda, A., H.A. Multhaupt, and J.R. Couchman, *The Rho kinases I and II regulate different aspects of myosin II activity.* J Cell Biol, 2005. **170**(3): p. 443-53.
270. Amano, M., et al., *The COOH terminus of Rho-kinase negatively regulates rho-kinase activity.* J Biol Chem, 1999. **274**(45): p. 32418-24.
271. Sebbagh, M., et al., *Direct cleavage of ROCK II by granzyme B induces target cell membrane blebbing in a caspase-independent manner.* J Exp Med, 2005. **201**(3): p. 465-71.
272. Sebbagh, M., et al., *Caspase-3-mediated cleavage of ROCK I induces MLC phosphorylation and apoptotic membrane blebbing.* Nat Cell Biol, 2001. **3**(4): p. 346-52.
273. Thumkeo, D., et al., *Targeted disruption of the mouse rho-associated kinase 2 gene results in intrauterine growth retardation and fetal death.* Mol Cell Biol, 2003. **23**(14): p. 5043-55.
274. Kamijo, H., et al., *Impaired vascular remodeling in the yolk sac of embryos deficient in ROCK-I and ROCK-II.* Genes Cells, 2011. **16**(10): p. 1012-21.
275. Mizuno, T., et al., *Identification and characterization of Drosophila homolog of Rho-kinase.* Gene, 1999. **238**(2): p. 437-44.
276. Winter, C.G., et al., *Drosophila Rho-associated kinase (Drok) links Frizzled-mediated planar cell polarity signaling to the actin cytoskeleton.* Cell, 2001. **105**(1): p. 81-91.
277. Verdier, V., et al., *Drosophila Rho-kinase (DRok) is required for tissue morphogenesis in diverse compartments of the egg chamber during oogenesis.* Dev Biol, 2006. **297**(2): p. 417-32.
278. Verdier, V., C. Guang Chao, and J. Settleman, *Rho-kinase regulates tissue morphogenesis via non-muscle myosin and LIM-kinase during Drosophila development.* BMC Dev Biol, 2006. **6**: p. 38.

279. Zheng, J., et al., *Crystal structure of the catalytic subunit of cAMP-dependent protein kinase complexed with MgATP and peptide inhibitor.* Biochemistry, 1993. **32**(9): p. 2154-61.
280. Fujisawa, K., et al., *Identification of the Rho-binding domain of p160ROCK, a Rho-associated coiled-coil containing protein kinase.* J Biol Chem, 1996. **271**(38): p. 23022-8.
281. Dvorsky, R., et al., *Structural insights into the interaction of ROCKI with the switch regions of RhoA.* J Biol Chem, 2004. **279**(8): p. 7098-104.
282. Shimizu, T., et al., *Parallel coiled-coil association of the RhoA-binding domain in Rho-kinase.* J Biol Chem, 2003. **278**(46): p. 46046-51.
283. Lei, M., et al., *Structure of PAK1 in an autoinhibited conformation reveals a multistage activation switch.* Cell, 2000. **102**(3): p. 387-97.
284. Morreale, A., et al., *Structure of Cdc42 bound to the GTPase binding domain of PAK.* Nat Struct Biol, 2000. **7**(5): p. 384-8.
285. Feng, J., et al., *Rho-associated kinase of chicken gizzard smooth muscle.* J Biol Chem, 1999. **274**(6): p. 3744-52.
286. Tan, I., et al., *Intermolecular and intramolecular interactions regulate catalytic activity of myotonic dystrophy kinase-related Cdc42-binding kinase alpha.* Mol Cell Biol, 2001. **21**(8): p. 2767-78.
287. Araki, S., et al., *Arachidonic acid-induced Ca2+ sensitization of smooth muscle contraction through activation of Rho-kinase.* Pflugers Arch, 2001. **441**(5): p. 596-603.
288. Tumusiime, S., et al., *Regulation of ROCKII by localization to membrane compartments and binding to DynaminI.* Biochem Biophys Res Commun, 2009. **381**(3): p. 393-6.
289. Kimura, K., et al., *Regulation of myosin phosphatase by Rho and Rho-associated kinase (Rho-kinase).* Science, 1996. **273**(5272): p. 245-8.
290. Riento, K., et al., *Function and regulation of RhoE.* Biochem Soc Trans, 2005. **33**(Pt 4): p. 649-51.
291. Amano, M., et al., *Myosin II activation promotes neurite retraction during the action of Rho and Rho-kinase.* Genes Cells, 1998. **3**(3): p. 177-88.
292. Chevrier, V., et al., *The Rho-associated protein kinase p160ROCK is required for centrosome positioning.* J Cell Biol, 2002. **157**(5): p. 807-17.
293. Fukata, Y., et al., *Phosphorylation of adducin by Rho-kinase plays a crucial role in cell motility.* J Cell Biol, 1999. **145**(2): p. 347-61.
294. Goto, H., et al., *Phosphorylation of vimentin by Rho-associated kinase at a unique amino-terminal site that is specifically phosphorylated during cytokinesis.* J Biol Chem, 1998. **273**(19): p. 11728-36.
295. Hirose, M., et al., *Molecular dissection of the Rho-associated protein kinase (p160ROCK)-regulated neurite remodeling in neuroblastoma N1E-115 cells.* J Cell Biol, 1998. **141**(7): p. 1625-36.
296. Kosako, H., et al., *Phosphorylation of glial fibrillary acidic protein at the same sites by cleavage furrow kinase and Rho-associated kinase.* J Biol Chem, 1997. **272**(16): p. 10333-6.
297. Kureishi, Y., et al., *Rho-associated kinase directly induces smooth muscle contraction through myosin light chain phosphorylation.* J Biol Chem, 1997. **272**(19): p. 12257-60.
298. Oshiro, N., Y. Fukata, and K. Kaibuchi, *Phosphorylation of moesin by rho-associated kinase (Rho-kinase) plays a crucial role in the formation of microvilli-like structures.* J Biol Chem, 1998. **273**(52): p. 34663-6.

299. Chisholm, A.A. and P. Cohen, *The myosin-bound form of protein phosphatase 1 (PP-1M) is the enzyme that dephosphorylates native myosin in skeletal and cardiac muscles.* Biochim Biophys Acta, 1988. **971**(2): p. 163-9.
300. Feng, J., et al., *Dephosphorylation of distinct sites on the 20 kDa myosin light chain by smooth muscle myosin phosphatase.* FEBS Lett, 1999. **448**(1): p. 101-4.
301. Ito, M., et al., *Myosin phosphatase: structure, regulation and function.* Mol Cell Biochem, 2004. **259**(1-2): p. 197-209.
302. Feng, J., et al., *Inhibitory phosphorylation site for Rho-associated kinase on smooth muscle myosin phosphatase.* J Biol Chem, 1999. **274**(52): p. 37385-90.
303. Ichikawa, K., M. Ito, and D.J. Hartshorne, *Phosphorylation of the large subunit of myosin phosphatase and inhibition of phosphatase activity.* J Biol Chem, 1996. **271**(9): p. 4733-40.
304. Kawano, Y., et al., *Phosphorylation of myosin-binding subunit (MBS) of myosin phosphatase by Rho-kinase in vivo.* J Cell Biol, 1999. **147**(5): p. 1023-38.
305. Maekawa, M., et al., *Signaling from Rho to the actin cytoskeleton through protein kinases ROCK and LIM-kinase.* Science, 1999. **285**(5429): p. 895-8.
306. Arber, S., et al., *Regulation of actin dynamics through phosphorylation of cofilin by LIM-kinase.* Nature, 1998. **393**(6687): p. 805-9.
307. Lappalainen, P. and D.G. Drubin, *Cofilin promotes rapid actin filament turnover in vivo.* Nature, 1997. **388**(6637): p. 78-82.
308. Moon, A. and D.G. Drubin, *The ADF/cofilin proteins: stimulus-responsive modulators of actin dynamics.* Mol Biol Cell, 1995. **6**(11): p. 1423-31.
309. Bretscher, A., *Regulation of cortical structure by the ezrin-radixin-moesin protein family.* Curr Opin Cell Biol, 1999. **11**(1): p. 109-16.
310. Matsui, T., et al., *Rho-kinase phosphorylates COOH-terminal threonines of ezrin/radixin/moesin (ERM) proteins and regulates their head-to-tail association.* J Cell Biol, 1998. **140**(3): p. 647-57.
311. Tsukita, S., S. Yonemura, and S. Tsukita, *ERM proteins: head-to-tail regulation of actin-plasma membrane interaction.* Trends Biochem Sci, 1997. **22**(2): p. 53-8.
312. Denker, S.P., et al., *Direct binding of the Na--H exchanger NHE1 to ERM proteins regulates the cortical cytoskeleton and cell shape independently of H(+) translocation.* Mol Cell, 2000. **6**(6): p. 1425-36.
313. Tominaga, T. and D.L. Barber, *Na-H exchange acts downstream of RhoA to regulate integrin-induced cell adhesion and spreading.* Mol Biol Cell, 1998. **9**(8): p. 2287-303.
314. Tominaga, T., et al., *p160ROCK mediates RhoA activation of Na-H exchange.* EMBO J, 1998. **17**(16): p. 4712-22.
315. Kimura, K., et al., *Regulation of the association of adducin with actin filaments by Rho-associated kinase (Rho-kinase) and myosin phosphatase.* J Biol Chem, 1998. **273**(10): p. 5542-8.
316. Hashimoto, R., et al., *Domain- and site-specific phosphorylation of bovine NF-L by Rho-associated kinase.* Biochem Biophys Res Commun, 1998. **245**(2): p. 407-11.
317. Izawa, T., et al., *Elongation factor-1 alpha is a novel substrate of rho-associated kinase.* Biochem Biophys Res Commun, 2000. **278**(1): p. 72-8.
318. Kaneko, T., et al., *Identification of calponin as a novel substrate of Rho-kinase.* Biochem Biophys Res Commun, 2000. **273**(1): p. 110-6.

319. Nagumo, H., et al., *Rho-associated kinase phosphorylates MARCKS in human neuronal cells.* Biochem Biophys Res Commun, 2001. **280**(3): p. 605-9.
320. Winder, S.J. and M.P. Walsh, *Smooth muscle calponin. Inhibition of actomyosin MgATPase and regulation by phosphorylation.* J Biol Chem, 1990. **265**(17): p. 10148-55.
321. Arimura, N., et al., *Phosphorylation of collapsin response mediator protein-2 by Rho-kinase. Evidence for two separate signaling pathways for growth cone collapse.* J Biol Chem, 2000. **275**(31): p. 23973-80.
322. Bourguignon, L.Y., et al., *Rho-kinase (ROK) promotes CD44v(3,8-10)-ankyrin interaction and tumor cell migration in metastatic breast cancer cells.* Cell Motil Cytoskeleton, 1999. **43**(4): p. 269-87.
323. Goshima, Y., et al., *Collapsin-induced growth cone collapse mediated by an intracellular protein related to UNC-33.* Nature, 1995. **376**(6540): p. 509-14.
324. Inagaki, N., et al., *CRMP-2 induces axons in cultured hippocampal neurons.* Nat Neurosci, 2001. **4**(8): p. 781-2.
325. Leung, T., et al., *p80 ROKalpha binding protein is a novel splice variant of CRMP-1 which associates with CRMP-2 and modulates RhoA-induced neuronal morphology.* FEBS Lett, 2002. **532**(3): p. 445-9.
326. Singleton, P.A. and L.Y. Bourguignon, *CD44v10 interaction with Rho-kinase (ROK) activates inositol 1,4,5-triphosphate (IP3) receptor-mediated Ca2+ signaling during hyaluronan (HA)-induced endothelial cell migration.* Cell Motil Cytoskeleton, 2002. **53**(4): p. 293-316.
327. Mohan, S., et al., *Structure of a highly conserved domain of rock1 required for shroom-mediated regulation of cell morphology.* PLoS One, 2013. **8**(12): p. e81075.
328. Mohan, S., et al., *Structure of Shroom domain 2 reveals a three-segmented coiled-coil required for dimerization, Rock binding, and apical constriction.* Mol Biol Cell, 2012. **23**(11): p. 2131-42.
329. Tu, D., et al., *Crystal structure of a coiled-coil domain from human ROCK I.* PLoS One, 2011. **6**(3): p. e18080.
330. Komander, D., et al., *Mechanism of multi-site phosphorylation from a ROCK-I:RhoE complex structure.* EMBO J, 2008. **27**(23): p. 3175-85.
331. Yamaguchi, H., et al., *Molecular mechanism for the regulation of rho-kinase by dimerization and its inhibition by fasudil.* Structure, 2006. **14**(3): p. 589-600.
332. Yamaguchi, H., et al., *Structural basis for induced-fit binding of Rho-kinase to the inhibitor Y-27632.* J Biochem, 2006. **140**(3): p. 305-11.
333. Allard, J. and A. Mogilner, *Traveling waves in actin dynamics and cell motility.* Curr Opin Cell Biol, 2013. **25**(1): p. 107-15.
334. Babbin, B.A., et al., *Non-muscle myosin IIA differentially regulates intestinal epithelial cell restitution and matrix invasion.* Am J Pathol, 2009. **174**(2): p. 436-48.
335. Etienne-Manneville, S., *Microtubules in cell migration.* Annu Rev Cell Dev Biol, 2013. **29**: p. 471-99.
336. Luo, W., et al., *Analysis of the local organization and dynamics of cellular actin networks.* J Cell Biol, 2013. **202**(7): p. 1057-73.
337. Provenzano, P.P., K.W. Eliceiri, and P.J. Keely, *Shining new light on 3D cell motility and the metastatic process.* Trends Cell Biol, 2009. **19**(11): p. 638-48.
338. Provenzano, P.P. and P.J. Keely, *The role of focal adhesion kinase in tumor initiation and progression.* Cell Adh Migr, 2009. **3**(4): p. 347-50.

339. Vicente-Manzanares, M., C.K. Choi, and A.R. Horwitz, *Integrins in cell migration--the actin connection.* J Cell Sci, 2009. **122**(Pt 2): p. 199-206.
340. Vicente-Manzanares, M., et al., *Non-muscle myosin II takes centre stage in cell adhesion and migration.* Nat Rev Mol Cell Biol, 2009. **10**(11): p. 778-90.
341. Assef, Y.A., et al., *ENaC channels in oocytes from Xenopus laevis and their regulation by xShroom1 protein.* Cell Physiol Biochem. **28**(2): p. 259-66.
342. Marean, A., et al., *Folic acid supplementation can adversely affect murine neural tube closure and embryonic survival.* Hum Mol Genet. **20**(18): p. 3678-83.
343. Zohn, I.E., K.V. Anderson, and L. Niswander, *Using genomewide mutagenesis screens to identify the genes required for neural tube closure in the mouse.* Birth Defects Res A Clin Mol Teratol, 2005. **73**(9): p. 583-90.
344. Mohan, S., et al., *Structure of Shroom domain 2 reveals a three-segmented coiled-coil required for dimerization, Rock binding, and apical constriction.* Mol Biol Cell. **23**(11): p. 2131-42.
345. Roffers-Agarwal, J., et al., *Enabled (Xena) regulates neural plate morphogenesis, apical constriction, and cellular adhesion required for neural tube closure in Xenopus.* Dev Biol, 2008. **314**(2): p. 393-403.
346. Nikolaidou, K.K. and K. Barrett, *A Rho GTPase signaling pathway is used reiteratively in epithelial folding and potentially selects the outcome of Rho activation.* Curr Biol, 2004. **14**(20): p. 1822-6.
347. Bertet, C., L. Sulak, and T. Lecuit, *Myosin-dependent junction remodelling controls planar cell intercalation and axis elongation.* Nature, 2004. **429**(6992): p. 667-71.
348. Zallen, J.A. and E. Wieschaus, *Patterned gene expression directs bipolar planar polarity in Drosophila.* Dev Cell, 2004. **6**(3): p. 343-55.
349. Blankenship, J.T., et al., *Multicellular rosette formation links planar cell polarity to tissue morphogenesis.* Dev Cell, 2006. **11**(4): p. 459-70.
350. Simoes, S., et al., *Compartmentalisation of Rho regulators directs cell invagination during tissue morphogenesis.* Development, 2006. **133**(21): p. 4257-67.
351. Kolesnikov, T. and S.K. Beckendorf, *18 wheeler regulates apical constriction of salivary gland cells via the Rho-GTPase-signaling pathway.* Dev Biol, 2007. **307**(1): p. 53-61.
352. Mulinari, S., M.P. Barmchi, and U. Hacker, *DRhoGEF2 and diaphanous regulate contractile force during segmental groove morphogenesis in the Drosophila embryo.* Mol Biol Cell, 2008. **19**(5): p. 1883-92.
353. Coleman, M.L., et al., *Membrane blebbing during apoptosis results from caspase-mediated activation of ROCK I.* Nat Cell Biol, 2001. **3**(4): p. 339-45.
354. Fukata, Y., M. Amano, and K. Kaibuchi, *Rho-Rho-kinase pathway in smooth muscle contraction and cytoskeletal reorganization of non-muscle cells.* Trends Pharmacol Sci, 2001. **22**(1): p. 32-9.
355. Wei, L., et al., *Rho kinases play an obligatory role in vertebrate embryonic organogenesis.* Development, 2001. **128**(15): p. 2953-62.
356. Kamijo, H., et al., *Impaired vascular remodeling in the yolk sac of embryos deficient in ROCK-I and ROCK-II.* Genes Cells. **16**(10): p. 1012-21.
357. Kuzelova, K. and Z. Hrkal, *Rho-signaling pathways in chronic myelogenous leukemia.* Cardiovasc Hematol Disord Drug Targets, 2008. **8**(4): p. 261-7.
358. Narumiya, S., M. Tanji, and T. Ishizaki, *Rho signaling, ROCK and mDia1, in transformation, metastasis and invasion.* Cancer Metastasis Rev, 2009. **28**(1-2): p. 65-76.

359. Itoh, K., et al., *An essential part for Rho-associated kinase in the transcellular invasion of tumor cells.* Nat Med, 1999. **5**(2): p. 221-5.
360. Liu, X., et al., *ROCK1 as a potential therapeutic target in osteosarcoma.* J Orthop Res. **29**(8): p. 1259-66.
361. Tokuyama, H., et al., *Role of mineralocorticoid receptor/Rho/Rho-kinase pathway in obesity-related renal injury.* Int J Obes (Lond). **36**(8): p. 1062-71.
362. Washida, N., et al., *Rho-kinase inhibition ameliorates peritoneal fibrosis and angiogenesis in a rat model of peritoneal sclerosis.* Nephrol Dial Transplant. **26**(9): p. 2770-9.
363. Hara, Y., et al., *Rho and Rho-kinase activity in adipocytes contributes to a vicious cycle in obesity that may involve mechanical stretch.* Sci Signal. **4**(157): p. ra3.
364. Biswas, P.S., et al., *Aberrant ROCK activation promotes the development of type I diabetes in NOD mice.* Cell Immunol. **266**(2): p. 111-5.
365. Connolly, M.J. and P.I. Aaronson, *Key role of the RhoA/Rho kinase system in pulmonary hypertension.* Pulm Pharmacol Ther. **24**(1): p. 1-14.
366. Zhou, Q., C. Gensch, and J.K. Liao, *Rho-associated coiled-coil-forming kinases (ROCKs): potential targets for the treatment of atherosclerosis and vascular disease.* Trends Pharmacol Sci. **32**(3): p. 167-73.
367. Dong, M., et al., *Rho-kinase inhibition: a novel therapeutic target for the treatment of cardiovascular diseases.* Drug Discov Today. **15**(15-16): p. 622-9.
368. Amano, M., M. Nakayama, and K. Kaibuchi, *Rho-kinase/ROCK: A key regulator of the cytoskeleton and cell polarity.* Cytoskeleton (Hoboken), 2010. **67**(9): p. 545-54.
369. Riento, K. and A.J. Ridley, *Rocks: multifunctional kinases in cell behaviour.* Nat Rev Mol Cell Biol, 2003. **4**(6): p. 446-56.
370. Schmandke, A., A. Schmandke, and S.M. Strittmatter, *ROCK and Rho: biochemistry and neuronal functions of Rho-associated protein kinases.* Neuroscientist, 2007. **13**(5): p. 454-69.
371. Ihrke, G., et al., *Competing sorting signals guide endolyn along a novel route to lysosomes in MDCK cells.* EMBO J, 2001. **20**(22): p. 6256-64.
372. Ihrke, G., S.R. Gray, and J.P. Luzio, *Endolyn is a mucin-like type I membrane protein targeted to lysosomes by its cytoplasmic tail.* Biochem J, 2000. **345 Pt 2**: p. 287-96.
373. Simoes Sde, M., A. Mainieri, and J.A. Zallen, *Rho GTPase and Shroom direct planar polarized actomyosin contractility during convergent extension.* J Cell Biol, 2014. **204**(4): p. 575-89.
374. Krause, M., et al., *Ena/VASP proteins: regulators of the actin cytoskeleton and cell migration.* Annu Rev Cell Dev Biol, 2003. **19**: p. 541-64.
375. Kwiatkowski, A.V., et al., *Ena/VASP Is Required for neuritogenesis in the developing cortex.* Neuron, 2007. **56**(3): p. 441-55.
376. Menzies, A.S., et al., *Mena and vasodilator-stimulated phosphoprotein are required for multiple actin-dependent processes that shape the vertebrate nervous system.* J Neurosci, 2004. **24**(37): p. 8029-38.
377. Prat, A.G., et al., *Renal epithelial protein (Apx) is an actin cytoskeleton-regulated Na+ channel.* J Biol Chem, 1996. **271**(30): p. 18045-53.
378. Zuckerman, J.B., et al., *Association of the epithelial sodium channel with Apx and alpha-spectrin in A6 renal epithelial cells.* J Biol Chem, 1999. **274**(33): p. 23286-95.

379. Biswas, P.S., et al., *Aberrant ROCK activation promotes the development of type I diabetes in NOD mice.* Cell Immunol, 2011. **266**(2): p. 111-5.
380. Connolly, M.J. and P.I. Aaronson, *Key role of the RhoA/Rho kinase system in pulmonary hypertension.* Pulm Pharmacol Ther, 2011. **24**(1): p. 1-14.
381. Hara, Y., et al., *Rho and Rho-kinase activity in adipocytes contributes to a vicious cycle in obesity that may involve mechanical stretch.* Sci Signal, 2011. **4**(157): p. ra3.
382. Kubo, T., et al., *The therapeutic effects of Rho-ROCK inhibitors on CNS disorders.* Ther Clin Risk Manag, 2008. **4**(3): p. 605-15.
383. Liu, X., et al., *ROCK1 as a potential therapeutic target in osteosarcoma.* J Orthop Res, 2011. **29**(8): p. 1259-66.
384. Loirand, G., P. Guerin, and P. Pacaud, *Rho kinases in cardiovascular physiology and pathophysiology.* Circ Res, 2006. **98**(3): p. 322-34.
385. Rath, N. and M.F. Olson, *Rho-associated kinases in tumorigenesis: re-considering ROCK inhibition for cancer therapy.* EMBO Rep, 2012. **13**(10): p. 900-8.
386. Shi, J., L. Zhang, and L. Wei, *Rho-kinase in development and heart failure: insights from genetic models.* Pediatr Cardiol, 2011. **32**(3): p. 297-304.
387. Surma, M., L. Wei, and J. Shi, *Rho kinase as a therapeutic target in cardiovascular disease.* Future Cardiol, 2011. **7**(5): p. 657-71.
388. Washida, N., et al., *Rho-kinase inhibition ameliorates peritoneal fibrosis and angiogenesis in a rat model of peritoneal sclerosis.* Nephrol Dial Transplant, 2011. **26**(9): p. 2770-9.
389. Hahmann, C. and T. Schroeter, *Rho-kinase inhibitors as therapeutics: from pan inhibition to isoform selectivity.* Cell Mol Life Sci, 2010. **67**(2): p. 171-7.
390. Liao, J.K., M. Seto, and K. Noma, *Rho kinase (ROCK) inhibitors.* J Cardiovasc Pharmacol, 2007. **50**(1): p. 17-24.
391. McLean, G.W., et al., *The role of focal-adhesion kinase in cancer - a new therapeutic opportunity.* Nat Rev Cancer, 2005. **5**(7): p. 505-15.
392. Mueller, B.K., H. Mack, and N. Teusch, *Rho kinase, a promising drug target for neurological disorders.* Nat Rev Drug Discov, 2005. **4**(5): p. 387-98.
393. Olson, M.F., *Applications for ROCK kinase inhibition.* Curr Opin Cell Biol, 2008. **20**(2): p. 242-8.
394. Saitoh, A., et al., *ROCK inhibition produces anxiety-related behaviors in mice.* Psychopharmacology (Berl), 2006. **188**(1): p. 1-11.
395. Tokushige, H., et al., *Effects of topical administration of y-39983, a selective rho-associated protein kinase inhibitor, on ocular tissues in rabbits and monkeys.* Invest Ophthalmol Vis Sci, 2007. **48**(7): p. 3216-22.
396. van Nimwegen, M.J. and B. van de Water, *Focal adhesion kinase: a potential target in cancer therapy.* Biochem Pharmacol, 2007. **73**(5): p. 597-609.